Delineating multiple salinization processes in a coastal plain aquifer, northern China: hydrochemical and isotopic evidence

Han Dongmei[a,b], Matthew Currell[c]

a Key Laboratory of Water Cycle & Related Land Surface Processes, Institute of Geographic Sciences and Natural Resources Research, Chinese Academy of Sciences, Beijing, 100101, China

b College of Resources and Environment, University of Chinese Academy of Sciences, Beijing 100049, China

c School of Engineering, RMIT University, Melbourne VIC 3000, Australia.

Abstract

Groundwater is an important water resource for agricultural irrigation, urban and industrial utilization in the coastal regions of northern China. In the past five decades, coastal groundwater salinization in the Yang-Dai River plain has become increasingly serious under the influence of anthropogenic activities and climatic change. It is pivotal for the scientific management of coastal water resources to accurately understand groundwater salinization processes and their causative factors. Hydrochemical (major ion and trace element) and stable isotopic ($\delta^{18}O$ and $\delta^{2}H$) analysis of different water bodies (surface water, groundwater, geothermal water, and seawater) were conducted to improve understanding of groundwater salinization processes in the plain's Quaternary aquifer. Saltwater intrusion due to intensive groundwater pumping is a major process, either by vertical infiltration along riverbeds which convey saline surface water inland, and/or direct subsurface lateral inflow. Trends in salinity with depth indicate that the former may be more important than previously assumed. The proportion of seawater in groundwater is estimated to have reached up to 13% in shallow groundwater of a local well field. End-member mixing calculations also indicate that highly mineralized geothermal water (TDS of up to 10.6 g/L) with depleted stable isotope compositions and elevated strontium concentrations (>10 mg/L) also locally mixes with water in the overlying Quaternary aquifers. This is particularly evident in samples with elevated Sr/Cl ratios (>0.005 mass ratio). Deterioration of groundwater quality by salinization is also clearly exacerbated by anthropogenic pollution. Nitrate contamination via intrusion of heavily polluted marine water is evident locally (e.g. in the Zaoyuan well field); however, more widespread nitrate contamination due to other local sources such as fertilizers and/or domestic wastewater is evident on the basis of NO_3/Cl ratios. This study provides an example of how multiple geochemical indicators can delineate different salinization processes and guide future water management practices in a densely populated water-stressed coastal region.

Key words: Groundwater salinization; Stable isotopes; Coastal aquifers, Water quality

1. Introduction

Coastal regions are key areas for the world’s social and economic development. Approximately 40% of the world’s population lives within 100 kilometers of the coast (UN Atlas, 2010). Worldwide, these areas have become increasingly urbanized, with 14 of the world's 17 largest cities located along coasts (Creel, 2003). China has 18,000 km of continental coastline, and around 164 million people (approximately 12% of the total population) living in 14 coastal provinces; nearly 80% of these people inhabit three coastal ‘economic zones’, namely Beijing-Tianjin-Hebei, the Yangtze River delta and the Pearl River delta (Shi, 2012). The rapid economic development and growing population in these regions have greatly increased demand for fresh water. Meanwhile, they are also confronted with increased sewage and other wastewater discharge into coastal environments.

Groundwater resources play crucial roles in the social, economic and ecologic function of global coastal systems (IPCC, 2007). Coastal aquifers connect with the ocean and with continental hydro-ecological systems (Moore, 1996; Ferguson and Gleeson, 2012). As an important freshwater resource, groundwater may be over-extracted during periods of high demand, which are often periods of low recharge and/or surface water availability (Post, 2005). Over-exploitation of groundwater can therefore result in seawater intrusion, as well as related environmental issues such as land subsidence. Seawater intrusion has become a global issue and related studies can be found from coastal aquifers around the world, including Israel (Sivan et al., 2005;Yechieli et al., 2009; Mazi et al., 2014), Spain (Price and Herman, 1991; Pulido-Leboeuf, 2004; Garing et al., 2013), France (Barbecot et al., 2000; de Montety et al., 2008), Italy (Giambastiani et al., 2007; Ghiglieri et al., 2012), Morocco (Bouchaou et al., 2008; El Yaouti et al., 2009), USA (Gingerich and Voss, 2002; Masterson, 2004; Langevin et al., 2010), Australia (Zhang et al., 2004; Narayan et al., 2007; Werner, 2010), China (Xue et al., 2000; Han et al., 2011, 2015), Vietnam (An et al., 2014), Indonesia (Rahmawati et al., 2013), India (Radhakrishna, 2001; Bobba, 2002) and Brazil (Montenegro et al., 2006; Cary et al., 2015). Werner et al. (2013) provides a comprehensive review of seawater intrusion processes, investigation and management.

Seawater/saltwater intrusion is a complicated hydrogeological process, due to the impact of aquifer properties, anthropogenic activities (e.g., intensive groundwater pumping, irrigation practices), recharge rates, variable density flow, tidal activity and effects relating to global climate change, such as sea level rise (Ghassemi et al., 1993; Robinson et al., 1998; Smith and Turner, 2001; Simpson and Clement, 2004; Narayan et al., 2007; Werner and Simmons, 2009; Wang et al., 2015). Understanding the complex interactions between groundwater, surface water, and seawater is thus essential for effective management of coastal water resources (Mondal et al., 2010). Very different salinization patterns may arise as a result of diverse interactions in coastal settings (Sherif and Singh, 1999; Bobba, 2002; Westbrook et al., 2005). Modeling has shown that generally, seawater intrusion is more sensitive to groundwater pumping and recharge rates in comparison to tidal fluctuation and sea level rise (Narayan et al., 2007; Ferguson and Gleeson, 2012). However, most models of seawater intrusion require simplification of the coastal interface zone. Relatively few studies have focused on delineating complex interactions among the surface-ground-sea-water continuum in estuarine environments, including the effects of vertical infiltration of seawater into aquifers through river channels, as compared to sub-surface lateral landward migration of the freshwater-saltwater interface. Recent data indicate that such processes may be more important in causing historical salinization of coastal groundwater than previously appreciated (e.g. Cary et al., 2015; Lee et al., 2016; Larsen et al., 2017).

Additionally, groundwater in coastal aquifers may be affected by other salinization processes, such as input of anthropogenic contaminants or induced mixing with saline water from deeper or adjacent formations, which may include mineralized geothermal water or brines emplaced in the coastal zone over geologic history. The data from China's marine environment bulletin released on March 2015 by the State Oceanic Administration showed that the major bays, including Bohai Bay, Liaodong Bay and Hangzhou Bay, are seriously polluted, with inorganic nitrogen and active phosphate being the major pollutants (SOA, 2015). Seawater intrusion in China is most serious in the Circum-Bohai-Sea region (Han et al., 2011, 2016a); and due to the heavy marine pollution, the impacts of anthropogenic activities on groundwater quality in future may not simply be a case of simple salt-water intrusion. This region is also characterized by deep brines and geothermal waters (e.g. Han et al., 2014), which may migrate and mix with fresher groundwater under due to intensive water extraction. Depending on the specific processes involved, additional contaminants may mix with fresh groundwater resources in parallel with seawater intrusion, and it is thus likely to be more difficult to mitigate and remediate groundwater pollution.

A variety of approaches can be used to investigate and differentiate seawater intrusion and other salinization processes, including time-series water level and salinity measurements, geophysical methods, conceptual and mathematical modeling as well as geochemical methods (see reviews by Jones et al., 1999; Werner et al., 2013). Geochemical techniques are particularly valuable in areas where the dynamics of saline intrusion are complicated and may involve long-term processes pre-dating accurate water level records, or where multiple salinization processes may be occurring simultaneously. These techniques typically employ the use of major ion ratios such as Cl/Br and Cl/Na, which are indicative of solute origins (Edmunds, 1996; Jones et al., 1999). Other ionic ratios, involving Mg, Ca, Na, HCO_3 and SO_4, and characterization of water ‘types’ can also be useful in determining the geochemical evolution of coastal groundwater, for example, indicating freshening or salinization, due to commonly associated ion exchange and redox reactions (Anderson et al., 2005; Walraevens, 2007). Trace elements such as strontium, lithium and boron can provide additional valuable information about sources of salinity and mixing between various end-members, as particular waters can have distinctive concentrations (and/or isotopic compositions) of these elements (e.g., Vengosh et al., 1999). Stable isotopes of water ($\delta^{18}O$ and $\delta^{2}H$) are also commonly used in such studies, as they are sensitive indicators of water and salinity sources, allowing seawater to be distinguished from other salt sources (e.g., Currell et al., 2015).

This study examines the Yang-Dai River coastal plain in Qinhuangdao City, Hebei province, north China, specifically focusing on salinization of fresh groundwater caused by groundwater exploitation in the Zaoyuan well field and surrounding areas. The study investigates groundwater salinization processes and interactions among surface water, seawater and geothermal groundwater in a dynamic environment, with significant pressure on water resources. Qinhuangdao is an important port and tourist city of northern China. In the past 30 years, many studies have investigated seawater intrusion and its influencing factors in the region using hydrochemical analysis (Xu, 1986; Yang et al., 1994, 2008; Chen and Ma, 2002; Sun and Yang, 2007; Zhang, 2012) and numerical simulations (Han, 1990; Bao, 2005; Zuo, 2009). However, these studies have yet to provide clear resolution of the different mechanisms contributing to salinization, and have typically ignored the role of anthropogenic pollution and groundwater-surface water interaction. This study is thus a continuation of previous investigations of the region, using a range of hydrochemical and stable isotopic data to delineate the major processes responsible for increasing groundwater salinity, including lateral sub-surface sea-water intrusion, vertical leakage of marine-influenced surface water, induced mixing of saline geothermal water, and anthropogenic pollution. The goal is to obtain a more robust conceptual model of the interconnections between the various water sources under the impact of groundwater exploitation. The results provide significant new information to assist water resources management in the coastal plain of Bohai Bay, and other similar coastal areas globally.

2. Study area

The Yang-Dai River coastal plain (Fig. 1) covers approximately 200km^2 of the west side of Beidaihe District of Qinhuangdao City, northeastern Hebei Province. It is surrounded by the Yanshan Mountains to the north and west, and the southern boundary of the study area is the Bohai Sea. The plain declines in topographic elevation (with an average slope of 0.008) from approximately 390m above sea-level in the northwest to 1-25m in the southeast, forming a fan-shaped distribution of incised piedmont-alluvial plain sediments. Zaoyuan well field, located in the southern edge of the alluvial fan, approximately 4.3km from the Yang River estuary, was built in 1959 (Xu, 1986) as a major water supply for the region (Fig. 1).

2.1 Climate and hydrology

The study area is in a warm and semi-humid monsoon climate. On the basis of a 56-year record in Qinhuangdao, the mean annual rainfall is approximately 640 mm, the average annual temperature approximately 11^{o}C, and mean potential evaporation 1469 mm. 75% of the total annual rainfall falls in July-September (Zuo, 2006), during the East Asian Summer Monsoon. The average annual tide level is 0.86m (meters above Yellow Sea base level), while the high and low tides are approximately 2.48m and -1.43m.

The Yanghe River and Daihe River, originating from the Yanshan Mountains, are the major surface water bodies in the area, flowing southward into the Bohai Sea (Fig. 1). The Yang River is approximately 100 km long with a catchment area of 1029 km^2 and average annual runoff of 1.11×10^8 m^3/a (Han, 1988). Dai River has a length of 35 km and catchment area of 290 km^2, with annual runoff of 0.27×10^8 m^3/a. The rivers become full during intense rain events, and revert to minimal flow during the dry season – in part this is related to impoundment of flow in upstream reservoirs.

2.2 Geological and hydrogeological setting

Groundwater in the area includes water in Quaternary porous sediment as well as fractured bedrock in the northern platform area. Fractured rock groundwater volume mainly depends on the degree of weathering and the nature and regularity of fault zones (Fig. 1). The strata outcropping in the west, north and eastern edge of the plain include Archean, Proterozoic and Jurassic aged metamorphic and igneous rocks, which also underlie the Quaternary sediments of the plain (from which most samples in this study were collected). The basement faults under Quaternary cover are mainly NE-trending and NW-trending (Fig. 1); these structures control the development and thickness of the overlying sediments, as well as the distribution of hot springs and geothermal anomalies. Fault zones are thought to be the main channel for transport of thermal water from deeper to shallower depths.

The Quaternary sediments are widely distributed in the area, with the thickness ranging from approximately 5-80 m (mostly 20-40 m), up to more than 100 m immediately adjacent to the coastline. The bottom of the Holocene (Q_4) unit in most areas consists of clay, making the groundwater in the coastal zone confined or semi-confined, although there are no regional, continuous aquitards between several layers of aquifer-forming sediments (Fig. 1b). The aquifer is mainly composed of medium sand, coarse sand and gravel layers with a water table depth of 1-4 m in the phreatic aquifer, and deeper semi-confined groundwater (where present and hydraulically separated from the phreatic aquifer) hosted in similar deposits with a potentiometric surface 1-5 m below topographic elevation (Zuo, 2006).

The general flow direction of groundwater is from northwest to south, according to the topography. The main sources of recharge are from infiltration of rainfall, river water and irrigation return-flow, as well as lateral subsurface inflow from the piedmont area. Naturally, groundwater discharges into the rivers and the Bohai Sea. Apart from phreatic water evaporation, groundwater pumping for agricultural, industrial and domestic usage (including seasonal tourism) are currently the main pathways of groundwater discharge.

Geothermal water discharges into shallow Quaternary sediments near the fault zones, evident as geothermal anomalies (Hui, 2009). The temperature of thermal water ranges from 27-57^{o}C in this low-to-medium temperature geothermal field (Zeng, 1991). Deeper thermal water is stored in the Archaeozoic granite and metamorphic rocks; major fracture zones provide pathways into the overlying Quaternary sediments (Pan, 1990; Shen et al., 1993; Yang, 2011).

2.3 Groundwater usage and seawater intrusion history

Shallow groundwater pumped from the Quaternary aquifer occupies 94% of total groundwater exploitation, and is used for agricultural irrigation (52% of total groundwater use), industrial (32%) and domestic water (16%) (Meng, 2004). Many large and medium-sized reservoirs were built in the 1960s and 1970s meaning that the surface water was intercepted and downstream runoff dropped sharply, even causing rivers to dry up in drought years. With the intensification of human socio-economic activities and growing urbanization, coupled with extended drought years (severe drought during 1976-1989 in north China) (Wilhite,1993; Han et al., 2015), increased groundwater exploitation to meet the ever-growing fresh water demand resulted in groundwater level declines and seawater intrusion (SWI) in the aquifers.

The pumping rate in the Zaoyuan well field gradually increased from 1.25 million m^3/a in the early 1960s to 3.5 million m^3/a in the late 1970s, and beyond 10 million m^3/a in the 1980s. During 1966-1989, planting of paddy fields became common, resulting in significant agricultural water consumption. This caused formation of a cone of depression in the Quaternary aquifer system. Groundwater pumping in this region mainly occurs in spring and early summer, with typical pumping rates of 7~80,000 m^3/d. Pumping from the Zaoyuan well-field occurs in wells approximately 15 to 20m deep. Groundwater levels decline sharply and reach their lowest level during May, before the summer rains begin, and recover to their yearly high in January-February (Fig. 2). In May 1986, the groundwater level in the depression center, which is located in Zaoyuan-Jiangying (Figure S1), decreased to -2 m.a.s.l.(meters above sea level) and the area with groundwater levels below sea level covered 28.2 km^2. The local government commenced reduction in groundwater exploitation in this area after 1992, and groundwater levels began to decrease more slowly after 1995, even showing recovery in some wells. However, during an extreme drought year (1999), increased water demand resulted in renewed groundwater level declines in the region (Fig. 2). Since 2000, the groundwater levels have responded seasonally to water demand peaks and recharge (Fig. 2; Fig. S1).

From 1990, the rapid development of township enterprises (mainly paper mills), also began to cause groundwater over-exploitation in the western area of the plain. The groundwater pumping rate for paper mills reached 55,000 m^3/d in 2002, resulting in groundwater level depressions around Liushouying and Fangezhuang (Fig. 1). The groundwater level in the western depression associated with this pumping reached -11.6 m.a.s.l. in 1991 and -17.4 in 2002. After the implementation of "Transfering Qing River water to Qinhuangdao" project in 1992, the intensity of groundwater pumping generally reduced, and the groundwater level in the depression center recovered to -4.3 m.a.s.l. in July 2006.

Overall, the depression area (groundwater levels below mean sea level) was recorded as 132.3km^2 in May 2004 and the shape of the depression has generally been elliptical with the major axis aligned E-W. In addition to groundwater over-exploitation, climate change-induced recharge reduction has also likely contributed to groundwater level declines and hence seawater intrusion (Fig. S2). The annual average rainfall declined from 639.7 mm between 1954 - 1979 to 594.2 mm between 1980-2010; a significant decrease over the last 30 years (Zhang, 2012). As indicated in Figure S2, the severity of seawater intrusion (indicated by changes in Cl concentration, and the total area impacted by SWI, as defined by the 250mg/L Cl contour) correlates with periods of below average rainfall – indicated by monthly cumulative rainfall departure (CRD, Weber and Stewart, 2004).

Groundwater quality of the area gradually became more saline from the early 1980s, with chloride concentrations increasing year by year. As early as 1979, seawater intrusion was recorded in the Zaoyuan well field. The intrusion area with groundwater chloride concentration greater than 250 mg/L was 21.8 km^2 in 1984, 32.4 km^2 in 1991, 52.6 km^2 in 2004 and 57.3 km^2 in 2007 (Zuo, 2006; Zang et al., 2010). The chloride concentration of groundwater pumped from the a monitored well-field well (depth of 18 m, G10 in Fig. 1) changed from 90 mg/L in 1963 to 218 mg/L in 1978, 567 mg/L in 1986, 459 mg/L in 1995, and 1367 mg/L in 2002 (Zuo, 2006), reducing to 812 mg/L in July 2007. The distance of estimated seawater intrusion into the inland area from the coastline had reached 6.5 km in 1991, and 8.75 km in 2008 (Zang et al., 2010). In the early 1990s, 16 of 21 pumping wells in the well field were abandoned due to the saline water quality (Liang et al., 2010). Additionally, 370 of 520 pumping wells were abandoned in the wider Yang-Dai River coastal plain during 1982-1991 (Zuo, 2006).

3. Methods

In total, 80 water samples were collected from the Yang-Dai River coastal plain, including 58 groundwater samples, 19 river water samples (from 12 sites) and 3 seawater samples, during three sampling campaigns (June 2008, September 2009 and August 2010). Groundwater samples were pumped from 28 production wells with depths between 6 and 110m, including 7 deep wells with depths greater than 60m (Fig. 1). While ideally, sampling for geochemical parameters would be conducted on monitoring wells, due to an absence of these, production wells were utilised. In most cases, the screened interval of these wells encompasses aquifer thicknesses of approximately 5 to 15m above the depths indicated in Table 1.

In this study, sampling focused predominantly on low temperature groundwater; however, geothermal water from around Danihe was also considered a potentially important ongoing source of groundwater salinity. As such, while geothermal water samples were not accessible during our sampling campaigns (as the area is now protected), data reported by Zeng (1991) were compiled and analyzed in conjunction with the sampled wells.

Measurements of physico-chemical parameters (pH, temperature, and electrical conductivity (EC)) were conducted in situ using a portable meter (WTW Multi 3500i). All water samples were filtered with 0.45μm membrane filters before analysis of hydrochemical composition. Two aliquots in polyethylene 100mL bottles at each site were collected for major cation and anion analysis, respectively. Samples for cation analysis (Na^+, K^+, Mg^{2+} and Ca^{2+}) were treated with 6N HNO_3 to prevent precipitation. Water samples were sealed and stored at 4°C until analysis. Bicarbonate was determined by titration within 12 hours of sampling. Concentrations of cations and some trace elements (B, Sr, Li) were analyzed by inductively coupled plasma-optical emission spectrometry (ICP-OES) in the chemical laboratory of the Institute of Geographic Sciences and Natural Resources Research (IGSNRR), Chinese Academy Sciences (CAS). Only the Sr data are reported here, as the other trace elements were not relevant to the interpretations discussed (Table 1). The detection limits for analysis of Na^+, K^+, Mg^{2+} and Ca^{2+} are 0.03, 0.05, 0.009, and 0.02 mg/L. Concentrations of major anions (i.e. Cl^-, SO_4^{2-}, NO_3^- and F^-) were analyzed using a High Performance Ion Chromatograph (SHIMADZU, LC-10ADvp) at the IGSNRR, CAS. The detection limits for analysis of Cl^-, SO_4^{2-}, NO_3^- and F^- are 0.007, 0.018, 0.016, and 0.006 mg/L. The testing precision the cation and anion analysis is 0.1-5.0%. Charge balance errors were less than 8%. Stable isotopes ($\delta^{18}O$ and δ^2H) of water samples were measured using a Finnigan MAT 253 mass spectrometer after on-line pyrolysis with a Thermo Finnigan TC/EA in the Stable Isotope Laboratory of the IGSNRR, CAS. The results are expressed in ‰ relative to international standards (V-SMOW (Vienna Standard Mean Ocean Water)) and resulting $\delta^{18}O$ and δ^2H values are shown in Table 1. The analytical precision for δ^2H is ±2‰ and for $\delta^{18}O$ is ±0.5‰. All hydrochemical, physico-chemical and isotope data are reported in Table 1.

Mixing calculations were also conducted on the basis of Cl^- concentrations of the samples under a conservative freshwater-seawater mixing system (Fidelibus et al., 1993; Appelo, 1994). The seawater contribution for each sample is expressed as a fraction of seawater (f_{sw}), using (Appelo and Postma, 2005):

$$f_{sw} = \frac{C_{Cl,sam} - C_{Cl,f}}{C_{Cl,sw} - C_{Cl,f}} \tag{1}$$

where $C_{Cl,sam}$, $C_{Cl,f}$, and $C_{Cl,sw}$ refer to the Cl^- concentration in the sample, freshwater, and seawater, respectively.

4. Results

4.1 Water stable isotopes (δ^2H and $\delta^{18}O$)

The local meteoric water line (LMWL, δ^2H=6.6 $\delta^{18}O$+0.3, n=64, r^2=0.88) is based on δ^2H and $\delta^{18}O$ mean monthly rainfall values between 1985 and 2003 from Tianjin station some 120 km SW of Qinhuangdao City (IAEA/WMO, 2006). Due to similar climate and position relative to the coast, this can be regarded as representative of the study area. Surface water samples collected from Yang River and Dai River (n = 19) have $\delta^{18}O$ and δ^2H values ranging from -10.1 to -0.6‰ (mean= -5.4‰) and -71 to-11‰

(mean = -43‰), respectively. Stable isotope compositions for surface water appear to exhibit significant seasonal variation (Fig. S3); for Yang River samples from the relatively dry season (June 2008, n = 3) had mean $\delta^{18}O$ and $\delta^{2}H$ values of -3.0‰ -31‰, respectively; samples from the wet season (August 2009 and September 2010, n = 6) had mean $\delta^{18}O$ and $\delta^{2}H$ values of -6.6‰ -48‰, respectively. Dai River samples showed similar results; the dry season mean $\delta^{18}O$ and $\delta^{2}H$ values (n = 3) were -2.6‰ and -32‰, respectively; wet season samples (n = 7), had mean $\delta^{18}O$ and $\delta^{2}H$ values of -6.6‰ and -49‰, respectively (Fig. 3).

The 56 groundwater samples were characterized by $\delta^{18}O$ and $\delta^{2}H$ values ranging from -11.0 to -4.2‰ (mean= -6.5‰) and -76 to -39‰ (mean = -50‰), respectively. Among these, shallow and deep groundwater samples showed similar mean values, although deep groundwater samples (n = 13) showed relatively narrow overall ranges (-7.8 to -5.1‰ and mean = -6.3‰ for $\delta^{18}O$; -58 to -43‰ and mean = -50‰ for $\delta^{2}H$; Fig. 3). Slight seasonal variation was evident in the groundwater isotope compositions; shallow groundwater from the dry season (n = 12) showed $\delta^{18}O$ and $\delta^{2}H$ values from -7.2 to -4.2‰ (mean = -5.7‰) and $\delta^{2}H$ values from -56 to -39‰ (mean = -48‰); while during the wet season (n = 31) $\delta^{18}O$ and $\delta^{2}H$ values ranged from -11.0 ~ -5.3‰ (mean = -6.9‰) and -76 ~ -43‰ (mean = -51‰), respectively. Some variability was also evident in deep groundwater compositions, although only three deep samples were collected during the dry season.

From Figure 3, it can be seen that surface water exhibits a much wider range of $\delta^{18}O$ and $\delta^{2}H$ values relative to groundwater, with shallow groundwater in turn more spatially variable than deep groundwater. Water samples collected in the wet season showed wider ranges of $\delta^{18}O$ and $\delta^{2}H$ values relative to the dry season. Most water samples of all types plot to the right of (below) the LMWL, with some surface water samples showing similar compositions to the local seawater (Fig. 3). The local seawater plots below (more negative) than typically assumed values (e.g. VSMOW = 0‰) for both $\delta^{2}H$ and $\delta^{18}O$, and this water appears to represent an end-member involved in mixing with meteoric-derived waters in both ground and surface water (Fig. 3).

4.2 Water salinity and dissolved ions

TDS (total dissolved solids) concentrations of surface water samples from Dai River range from 0.3g/L~31.4g/L with Na^{+} and Ca^{2+} comprising 22-78% and 4-56% of total cations and Cl^{-} comprising 36-91% of total anions. The composition changes from Ca•Na•Mg-Cl•HCO_3 to Na-Cl water type from upstream to downstream locations along with increasing salinity; Cl^- concentrations vary from approximately 70 mg/L upstream to 16700 mg/L near the coastline, due to marine influence. Similar variation occurs along the Yang River, where samples had TDS concentrations between 0.3-26.1 g/L with increasing concentrations and proportions of Cl^- (63.2-14953.5 mg/L) from upstream to downstream locations. Nitrate concentrations also range from 2.8 to 65.2 mg/L in the surface water samples, increasing downstream.

In the early 1960s, groundwater pumped from the Zaoyuan well field exhibited Ca-HCO_3 water type and chloride concentrations of 90-130 mg/L; this was followed by rapid salinization since the 1980s (see section 2.3). In this study, shallow groundwater is characterized by TDS concentrations of 0.4-4.8 g/L with Cl^- (34-77%), Na^+ (12-85%) and Ca^{2+} (5-69%) being the predominant major anion and cations, respectively. Groundwater hydrochemical types vary from Ca-HCO_3•Cl, Ca•Na-Cl, Na•Ca-Cl to Na-Cl (Figure 4). Deep groundwater has TDS concentrations between 0.3-2.8g/L, dominated by Ca (up to 77% of major cations) in the upstream area and Na (up to 85% or major cations) near the coast, with water type evolving from Ca-Cl•HCO_3 to Ca•Na-Cl and Na•Mg-Cl (Figure 4). At present, the TDS of groundwater from the well field reaches 3.31 g/L with Na-Cl water type (see well G15). The highest observed mixing proportions of seawater occur in shallow well G10 and deep well G2, respectively, with calculated *fsw* values (according to equation 1) of 12.95% and 5.35%, respectively.

Hydrochemical features of thermal water from the Danihe-Luwangzhuang area (Fig. 1A) are distinct from the normal/low temperature groundwater. Previous work by Zeng (1991) and Hui (2009) identified geothermal water with high TDS in the fractures of deep metamorphic rock. The geothermal water was characterized by TDS values between 6.2-10.6 g/L and Ca•Na-Cl water type, while Cl^- concentrations ranged from 5.4 to 6.5 g/L and Sr concentrations from 6.73 to 89.8 mg/L. Some normal/low temperature groundwater samples collected in this study from wells G8, G19, and G9 featured by Ca•Na-Cl water type with relative high TDS ranges (0.8-1.4 g/L, 1.3-1.6 g/L, and1.5-2.8 g/L, respectively) and strontium concentrations (1.1-1.9 mg/L, 4.9-7.1 mg/L, and 7.3-11.6 mg/L, respectively), showing similarity with the geothermal system. Low temperature groundwater sampled in this study had Sr/Cl mass ratios ranging from 2.4×10^{-4} to 1.6×10^{-2}, with higher ratios in deep groundwater (range: 9.4×10^{-4} to 1.3×10^{-2}, median: 3.7×10^{-3}) compared to shallow groundwater (median: 3.1×10^{-3}), and groundwater generally higher than seawater/saline surface water (range: 3.7×10^{-4} to 5.8×10^{-4}, median: 3.9×10^{-4}; Table S1).

Nitrate concentrations in groundwater range from 2.0-178.5 mg/L (mean 90.1 mg/L) for shallow groundwater, and 2.0-952.1 mg/L (mean 232.1 mg/L) for the deep groundwater, respectively, with most samples exceeding the WHO drinking water standard (50 mg/L).

5. Discussion

5.1 Groundwater isotopes and hydrochemistry as indicators of mixing processes

The Quaternary groundwater system in the Yang-Dai River coastal plain may be recharged by precipitation, irrigation return flow, river infiltration and lateral subsurface runoff (e.g. from mountain-front regions). Groundwater geochemical characteristics are then controlled by hydrogeological conditions and mixing processes, including mixing induced by extensive groundwater pumping, as well as natural mixing and water-rock interaction. It is evident from the geochemistry that mixing has occurred between groundwater and seawater in the coastal areas, as well as between normal/low temperature groundwater and geothermal water in the inland areas (e.g. near the Danihe geothermal field). Different sources of water are generally characterized by somewhat distinctive stable isotopic and hydrochemical compositions, allowing mixing calculations to aid understanding of the groundwater salinization and mixing processes, as discussed below.

Stable isotopes of O and H in groundwater and surface water fall on a best-fit regression line (dashed line in Fig. 3) with slope of $\delta^2H=4.4\times\delta^{18}O-21.7$, significantly lower than either the local or global meteoric water lines. Three processes are likely responsible for the observed range of isotopic compositions: 1. Mixing between saline surface water (e.g. seawater or saline river water affected by tidal ingress) and fresher, meteoric-derived groundwater or surface water; 2. Mixing between fresh meteoric-derived groundwater and saline thermal water; 3. Evaporative enrichment of surface water and/or irrigation return-flow, which may infiltrate groundwater in some areas. A sub-group of surface water samples (e.g., S1 to S3, S7 and S12; termed ‘brackish surface water’) show marine-like stable isotopic compositions and major ion compositions (Fig. 3 and Fig. 5). The ‘fresh’ surface water samples (e.g. EC values <1500 μS/cm) exhibit meteoric-like stable isotope compositions, with some samples (such as S9 and S10) showing clear evidence of evaporative enrichment in the form of higher δ^2H and particularly, $\delta^{18}O$ values (Fig. 3).

Fresh groundwater has depleted $\delta^{18}O$ and δ^2H values relative to seawater and show a clear meteoric origin, albeit with modification due to mixing. Theoretically, the mixing of meteoric-derived fresh groundwater and marine water should result in a straight mixing line connecting the two end members; however this is also complicated in the study area by the possible mixing with geothermal water. The thermal groundwater has distinctive stable isotopic and major ion composition (Han, 1988; Zeng, 1991), allowing these mixing processes to be partly delineated. Stable isotopes of thermal groundwater are more depleted than low-temperature groundwater (e.g. $\delta^{18}O$ values of approximately -8‰, Fig. 8), indicating this likely originates in the mountainous areas to the north; Zeng (1991) estimated the elevation of the recharge area for the geothermal field to be from 1200 to 1500 m.a.s.l. Based on a bivariate plot of $\delta^{18}O$ vs. Cl^- with mixing lines and defined fresh and saline end-members, Fig. 5 shows the estimated degree of mixing between fresh groundwater including shallow (G4) and deep (G25) groundwater end-members, and saline water, including seawater and geothermal end-members.

The two fresh end-members were selected to represent a range of different groundwater compositions/recharge sources, from shallow water that is impacted by infiltration of partially evaporated recharge (fresh but with enriched $\delta^{18}O$) to deeper groundwater unaffected by such enrichment (fresh and with relatively depleted $\delta^{18}O$). The narrower range and relatively enriched stable isotopes in shallow groundwater samples collected during the dry season compared with the wet season indicate some influence of seasonal recharge by either rainfall (fresh, with relatively depleted stable isotopes) or irrigation water subject to evaporative enrichment (more saline, with enriched stable isotopes and high nitrate concentrations; Currell et al., 2010) and/or surface water leakage. While there is overlap in the isotopic and hydrochemical compositions of shallow and deep groundwater (Fig. 3 & Fig. 4), this effect appears to only affect the shallow aquifer.

Based on Fig. 5, the shallow groundwater samples (e.g. G15, G10, G11, G14) collected from or around the Zaoyuan well field appear to be characterized by mixing between fresh meteoric water and seawater (plotting in the upper part of Fig. 5); while some deeper groundwater samples (e.g. G13, G2, G16, G14) collected from the coastal zone also appearing to indicate mixing with seawater. Groundwater sampled relatively close to the geothermal field (e.g. G9, G19) shows compositions consistent with mixing between low-temperature fresh water and saline thermal water (lower part of Fig. 5). This is more evident in deep groundwater than shallow groundwater, which is consistent with mixing from below, as expected for the deep-source geothermal water. Other samples impacted by salinization show more ambiguous compositions between the various mixing lines, which may arise due to mixing with either seawater, geothermal water or a combination of both (e.g., G29).

The estimated mixing fraction (f_{sw}) of marine water for the shallow brackish groundwater ranges from 1.2~13.0% and 2.6~6.0% for the deep brackish groundwater. The highest fraction of 13% was recorded in

G10, located in the northerm part of the Zaoyuan well field, which is located near a tidally-impacted tributary of the Yang River (Fig 1). Relatively higher fractions of marine water in relatively shallow samples (including those from the well field) compared to deeper samples may indicate a more 'top down' salinization process, related to leakage of saline surface water through the riverbed, rather than 'classic' lateral sea water intrusion, which typically causes salinization at deeper levels due to migration of a salt water 'wedge' (e.g. Werner et al., 2013); this is consistent with results of resistivity surveys conducted in the region (Fig. 6). The profile of chloride concentrations vs. depth indicates that salinization affects shallow and deep samples alike, with the most saline samples being relatively shallow wells in the Zaoyuan well-field (Fig. 7).

In general, brackish and fresh groundwater samples show distinctive major ion compositions, with the more saline water typically showing higher proportions of Na and Cl (Fig. 4). This contrasts with historic data collected from the Zaoyuan well field, which showed Ca-HCO_3 type water with Cl concentrations ranging from 130 to 170 mg/L. This provides additional evidence that the salinization in this area is largely due to marine water mixing. More Ca-dominated compositions are evident in the region near the geothermal well field further in-land (e.g., G5, G8, G19, G29, and G24); consistent with a component of salinization that is unrelated to marine water intrusion. Plots of ionic ratios of Na/Cl and Mg/Ca vs. Cl also reveal a sub-set of relatively saline deep groundwater samples which appear to evolve towards the geothermal-type signatures with increasing salinity (Fig. 8).

Stronger evidence of mixing of the geothermal water in the Quaternary aquifers (particularly deep groundwater) is provided by examining strontium concentrations in conjunction with chloride (Fig. 9). The geothermal water from Danihe geothermal field has much higher Sr concentrations (up to 89.8 mg/L) than seawater (5.4-6.5 mg/L in this study), due to Sr-bearing minerals (i.e., celestite, strontianite) with Sr contents of 300-2000 mg/kg present in the bedrock (Hebei Geology Survey, 1987). Groundwater sampled from near the geothermal field in this study has the highest Sr concentrations e.g., G9 with Sr concentrations ranging from 7.4 to 11.6 mg/L, and G19 from 4.9 to 7.1 mg/L.

The plot of chloride versus strontium concentrations (Fig. 9) shows that these samples and others (e.g., G16, G20, G27, G29) plot close to a mixing line between fresh low-temperature and saline thermal-groundwater. Mass ratios of Sr/Cl in these samples are also elevated relative to seawater by an order of magnitude or more (e.g. Sr/Cl >5.0×10^{-3}, compared to 3.9×10^{-4} in seawater, Table S1). Other samples from closer to the coast (e.g. G4) also approach the thermal-low temperature mixing line, indicating probable input of thermal water. Samples collected from the Zaoyuan well field generally plot closer to the Sr/Cl seawater mixing line (consistent with salinization largely due to marine water – Fig. 9); however, samples mostly plot slightly above the mixing line with additional Sr, which may indicate more widespread (but volumetrically minor) mixing with the thermal water in addition to seawater.

5.2 Anthropogenic pollution of groundwater

The occurrence of high nitrate (and possibly also sulfate) concentrations in groundwater in both coastal and in-land areas also indicates that anthropogenic pollution is an important process impacting groundwater quality and salinity (Fig. 10; Table 1). Seawater from Bohai Sea is heavily affected by nutrient contamination, showing NO_3^- concentrations of 810 mg/L in this study, and up to 1092 mg/L in seawater further north of the bay near Dalian (Han et al., 2015), primarily due to wastewater discharge into the sea. The historic sampled NO_3^- concentration of groundwater in the well field increased from 5.4 mg/L in May 1985 to 146.8~339.4 mg/L in Aug 2010, while the concentration in seawater changed from 57.4 mg/L in May1985 to 810.1 mg/L in Aug 2010. A bivariate plot of Cl^- vs. NO_3^- concentrations in groundwater (Fig. 10) can thus be used to identify nitrate sources and mixing trends, including infiltration with contaminated seawater, and other on-land anthropogenic NO_3-sources (e.g. domestic/industrial wastewater discharge and/or NO_3^--bearing fertilizer input through irrigation return-flow).

From this plot (Fig. 10) it appears that the major source of NO_3^- in groundwater is on-land anthropogenic inputs rather than mixing with seawater, which would result in relatively large increases in Cl along with NO_3. Samples G10 and G15 (from the well field) are exceptions to this trend, showing clear mixing with nitrate-contaminated seawater. Deep groundwater (e.g. G9, G14) is also extensively contaminated with high NO_3^- concentrations; this is likely associated with leakage from the surface via poorly constructed or abandoned wells - a problem of growing significance in China (see Han et al., 2016b; Currell and Han, 2017). According to one investigation by Zang et al.(2010), 14 of 21 pumping wells in the Zaoyuan well field have been abandoned due to poor water quality, and 307 pumping irrigation wells (occupied 2/3 of total pumping wells for irrigation) in the region have also been abandoned. Local authorities have however not implemented measures to deal with abandoned wells, meaning they are a future legacy contamination risk – e.g. by allowing surface runoff impacted by nitrate contamination to infiltrate down well annuli.

5.3 Hydrochemical evolution during salinization

A hydrogeochemical facies evolution diagram (HFE-D) proposed by Giménez-Forcada (2010), was used to analyze the geochemical evolution of groundwater during seawater intrusion and/or freshening phases (Fig. 11). In the coastal zone, the river water shows an obvious mixing trend between fresh and saline end members. Some shallow groundwaters (e.g., G2, G4, G10, G13, G15) are also close to the mixing line between the surface-water end-members on this figure, indicating mixing with seawater without significant additional modification by typical water-rock interaction processes (e.g. ion exchange). Most brackish groundwaters (e.g., G11, G16, G17, G20, G25, G28, G29) have evolved in the series Ca-HCO_3 → Ca-Cl→ Na-Cl, according to classic seawater intrusion. A relative depletion in Na (shown in lower than marine Na/Cl ratios) and enrichment in Ca (shown as enriched Ca/SO_4 ratios) is evident in groundwater with intermediate salinities (e.g. Fig. 8; Fig. 11), indicating classic base-exchange between Na and Ca during salinization (Appelo and Postma, 2005). Locally, certain brackish water samples (e.g., G1, G12, G26) appear to plot in the 'freshening' part of the HFE diagram (potentially indicating slowing or reversal of salinisation due to reduce in groundwater use), although these do not follow a conclusive trajectory. Water samples from the geothermal field (G5, G8, G9, and G19) plot in a particular corner of the HFE diagram away from other samples (being particularly Ca-rich); a result of their distinctive geochemical evolution during deep transport through the basement rocks at high temperatures.

5.4 Conceptual model of salinization and management implications

Coastal zones encompass the complex interaction among different water bodies (i.e., river water, seawater and groundwater). The interactions between surface- and ground-water in the Yang-Dai River coastal plain have generally been ignored in previous studies. However, the surface water chemistry data show that the distribution of salt water has historically reached more than 10 km inland along the estuary of the Yang River, and approximately 4 km inland in the Dai River (Han, 1988). The relatively higher proportion of seawater-intrusion derived salinity in shallow samples in this study, along with the evidence from resistivity surveys (Fig. 6; Zuo, 2006) indicate that intrusion by vertical leakage from these estuaries is therefore an important process. The hazard associated with this pathway in recent times has been reduced by the construction of a tidal dam, which now restricts seawater ingress along the Yang estuary to within 4 km of the coastline. This may alleviate salinization to an extent in future in the shallow aquifer by removing one of the salinization pathways, however, as described, there are multiple other salinization processes impacting the groundwater in the Quaternary aquifers of the region.

A conceptual model of the groundwater flow system in the Yang-Dai River coastal plain is summarized in Fig. 12. This model presents an advance on the previous understanding of the study area, by delineating four major processes responsible for groundwater salinization in this area. These are: 1. Seawater intrusion by lateral sub-surface flow; 2. Interaction between saline surface water and groundwater (e.g. vertical leakage of saline water from the river estuaries); 3. Mixing between low-temperature groundwater and deep geothermal water; and, 4. Irrigation return-flow and associated anthropogenic contamination. Both the lateral and vertical intrusion of saline water are driven by the long-term over-pumping of groundwater from fresh aquifers in the region. The irrigation return-flow from local agriculture results from over-irrigation of crops, and is responsible for extensive nitrate pollution (up to 340 mg/L NO_3^- in groundwater of this area) probably due to dissolution of fertilizers during infiltration. The somewhat enriched stable isotopes in shallow groundwater (more pronounced in the dry season) also indicate that such return-flow may recharge water impacted by evaporative salinization into the aquifer. The geothermal water, with distinctive chemical composition (e.g. depleted stable isotopes, high TDS, Ca and Sr concentrations), is also demonstrated in this study to be a significant contributor to groundwater salinization, via upward mixing. The study area is therefore in a situation of unusual vulnerability, in the sense that it faces salinization threats simultaneously from lateral, downward and upward migration of saline water bodies.

According to drinking water standards and guidelines from China Environmental Protection Authority (GB 5749-2006) and/or US EPA and WHO, chloride concentration in drinking water should not exceed 250 mg/L. At the salinity levels observed in this study - many samples impacted by salinization contain >500mg/L of chloride (Table 1) - a large amount of groundwater is now or will soon be unsuitable for domestic usage, as well as irrigation or industrial utilization. So far, this has enhanced the scarcity of fresh water resources in this region, leading to a cycle of groundwater level decline → seawater intrusion → loss of available freshwater → increased pumping of remaining fresh water. If this cycle continues, it is likely to further degrade groundwater quality and restrict its usage in the future. Such a situation is typical of the coastal water resources 'squeeze' highlighted by Michael et al., (2017). Alternative management strategies, such as restricting water usage in particular high-use sectors, such as agriculture, industry or tourism, that are based on a comprehensive assessment of the social, economic and environmental benefits and costs of these activities, warrants urgent and careful consideration.

6. Conclusions

Groundwater in the Quaternary aquifers of the Yang-Dai River coastal plain is an important water resource for agricultural irrigation, domestic use (including for tourism) and industrial activity. Extensive groundwater utilization has made the problem of groundwater salinization in this area increasingly prominent, resulting in the closure of wells in the area. Based on the analysis of hydrochemical and stable isotopic compositions of different water bodies, we delineated the key groundwater salinization processes. Seawater intrusion is the main process responsible for salinization in the coastal zone; however this likely includes vertical saltwater infiltration along the riverbed into aquifers as well as lateral seawater intrusion caused by pumping for fresh groundwater at the Zaoyuan wellfield. The upward mixing of highly mineralized thermal water into the Quaternary aquifers is also evident, particularly through the use of stable isotope, chloride and strontium end-member mixing analysis. Additionally, significant nitrate pollution from the anthropogenic activities (e.g., agricultural irrigation return-flow with dissolution of fertilizers) and locally, intrusion of heavily polluted seawater, are also evident.

Groundwater salinization has become a prominent water environment problem in the coastal areas of northern China (Han et al., 2014; Han et al., 2015; Han et al., 2016a), and threatens to create further paucity of fresh water resources, which may prove a significant impediment to further social and economic development in these regions. Since the 1990s, the local government has begun to pay attention to the problem of seawater intrusion, and irrational exploitation of groundwater has been restricted in some cases. The Zaoyuan well field ceased to pump groundwater since 2007, while an anti-tide dam (designed to protect against tidal surge events) established in the Yang River estuary may also reduce saline intrusion in future. However, due to the significant lag-time associated with groundwater systems, a response in terms of water quality may take time to emerge, and in the meantime the other salinization and pollution impacts documented here may continue to threaten water quality. In this regard, we recommend continued monitoring of groundwater quality and levels, and active programs to reduce input of anthropogenic contaminants such as nitrate from fertilizers, and appropriate well-construction and decommissioning protocols to prevent contamination through preferential pathways.

Acknowledgement

This research was supported by Zhu Kezhen Outstanding Young Scholars Program in the Institute of Geographic Sciences and Natural Resources Research, Chinese Academy of Sciences (CAS) (grant number 2015RC102), and Outstanding member program of the Youth Innovation Promotion Association, CAS (grant number 2012040). The authors appreciate the helpful field work and data collection made by Mr

Yang Jilong from Tianjin Institute of Geology and Mineral Resources, Dr. Wang Peng and Dr Liu Xin from Chinese Academy of Sciences.

References

An T.D., Tsujimura M., Phu V.L., Kawachi A., Ha D.T., 2014. Chemical Characteristics of Surface Water and Groundwater in Coastal Watershed, Mekong Delta, Vietnam. The 4th International Conference on Sustainable Future for Human Security, SustaiN 2013. Procedia Environmental Sciences. 20:712-721.

Andersen, M.S., Jakobsen, V.N.R., Postma, D. 2005. Geochemical processes and solute transport at the seawater/freshwater interface of a sandy aquifer. Geochimica et Cosmochimica Acta. 69(16): 3979-3994.

Appelo C.A.J., 1994. Cation and proton exchange, pH variations, and carbonate reactions in a freshening aquifer. Water Resour. Res., 30, 2793-2805.

Appelo C.A.J., Postma D., 2005. Geochemistry, Groundwater and Pollution, second edition. Taylor & Francis Group.

Bao J., 2005. Two-dimensional numerical modeling of seawater intrusion in Qinhuangdao Region. Master's Thesis. Tongji University, Shanghai, China. (Chinese with English abstract)

Barbecot F., Marlin C., Gibert E., Dever L., 2000. Hydrochemical and isotopic characterisation of the Bathonian and Bajocian coastal aquifer of the Caen area (northern France). Applied Geochemistry. 15:791-805.

Bobba A.G., 2002. Numerical modelling of salt-water intrusion due to human activities and sea-level change in the Godavari Delta, India. Hydrological Sciences. 47(S), S67-S80.

Bouchaou L., Michelot J.L., Vengosh A., Hsissou Y., Qurtobi M., Gaye C.B., Bullen T.D., Zuppi G.M., 2008. Application of multiple isotopic and geochemical tracers for investigation of recharge, salinization, and residence time of water in the Souss–Massa aquifer, southwest of Morocco. Journal of Hydrology. 352: 267-287.

Cary L., Petelet-Giraud E., Bertrand G., Kloppmann W., Aquilina L., Martins V., Hirata R., Montenegro S., Pauwels H., Chatton E., Franzen M., Aurouet A., the Team. 2015. Origins and processes of groundwater salinization in the urban coastal aquifers of Recife (Pernambuco, Brazil): A multi-isotope approach. Science of the Total Environment. 530-531:411-429.

Chen M., Ma F., 2002. Groundwater resources and the environment in China. Seismological Press. Beijing. pp255-281. (in Chinese)

Craig, H., 1961. Standard for reporting concentration of deuterium and oxygen-18 in natural water. Science 133, 1833-1834.

Creel L., 2003. Ripple effects: Population and coastal regions. Population Reference Bureau. pp1-7.< http://www.prb.org/Publications/Reports/2003/RippleEffectsPopulationandCoastalRegions.aspx>

Currell M.J., Cartwright, I., Bradley, D.C., Han, D.M., 2010. Recharge history and controls on groundwater quality in the Yuncheng Basin, north China. Journal of Hydrology. 385: 216-229.

Currell M.J., Dahlhaus P.D., Ii H. 2015. Stable isotopes as indicators of water and salinity sources in a southeast Australian coastal wetland: identifying relict marine water, and implications for future change. Hydrogeology Journal. 23: 235-248.

Currell M.J., Han D. 2017. The Global Drain: Why China's water pollution problems should matter to the rest of the world. Environment: Science and Policy for Sustainable Development. 59(1): 16-29.

de Montety V., Radakovitch O., Vallet-Coulomb C., Blavoux B., Hermitte D., Valles V., 2008. Origin of groundwater salinity and hydrogeochemical processes in a confined coastal aquifer: Case of the Rhône delta (Southern France). Applied Geochemistry. 23: 2337-2349.

Edmunds W. M., 1996. Bromine geochemistry of British groundwaters. Mineral. Mag., 60, 275–284.

El Yaouti F., El Mandour A., Khattach D., Benavente J., Kaufmann O., 2009. Salinization processes in the unconfined aquifer of Bou-Areg (NE Morocco): A geostatistical, geochemical, and tomographic study. Applied Geochemistry. 24:16-31.

Ferguson G., Gleeson T., 2012. Vulnerability of coastal aquifers to groundwater use and climate change. Nature Climate Change. 2, 342-345.

Fidelibus M.D., Giménez E., Morell I., Tulipano L., 1993. Salinization processes in the Castellon Plain aquifer (Spain). In: Custodio, E., Galofré, A. (Eds.), Study and Modelling of Saltwater Intrusion into Aquifers. Centro Internacional de Métodos Numéricos en Ingeniería, Barcelona, pp267-283.

Garing C., Luquot L., Pezard P.A., Gouze P., 2013. Geochemical investigations of saltwater intrusion into the coastal carbonate aquifer of Mallorca, Spain. Applied Geochemistry. 39:1-10.

Ghassemi F., Chen T.H., Jakeman A.J., Jacobson G., 1993. Two and three-dimensional simulation of seawater intrusion: performances of the "SUTRA" and "HST3D" models. AGSO J. Aust.Geol.Geophys. 14(2-3):219-226.

Ghiglieri G., Carletti A., Pittalis D., 2012. Analysis of salinization processes in the coastal carbonate aquifer of Porto Torres (NW Sardinia, Italy). Journal of Hydrology. 432-433:43-51.

Giambastiani B.M.S., Antonellini M., Oude Essink G.H.P., Stuurman R.J., 2007. Saltwater intrusion in the unconfined coastal aquifer of Ravenna (Italy): A numerical model. Journal of Hydrology. 340:91-104.

Giménez-Forcada E., 2010. Dynamic of sea water interface using hydrochemical facies evolution diagram, Ground Water. 48, 212-216.

Gingerich S., Voss C., 2002. Three-dimensional variable-density flow simulation of a coastal aquifer in southern Oahu, Hawaii, USA, in Proceedings SWIM17 Delft 2002, edited by R. Boekelman, pp.93-103, Delft Univ. of Technol., Delft, Netherlands.

Han D.M., Kohfahl C., Song X.F., Xiao G.Q., Yang J.L., 2011. Geochemical and isotopic evidence for palaeo-seawater intrusion into the south coast aquifer of Laizhou Bay, China. Applied Geochemistry, 26(5):863-883.

Han D.M., Song, X.F., Currell, M.J., Yang, J.L., Xiao G.Q. 2014. Chemical and isotopic constraints on the evolution of groundwater salinization in the coastal plain aquifer of Laizhou Bay, China. Journal of Hydrology 508: 12-27.

Han D., Post V.E.A., Song X., 2015. Groundwater salinization processes and reversibility of seawater intrusion in coastal carbonate aquifers. Journal of Hydrology. 531:1067-1080.

Han, D., Song, X., Currell, M. 2016a. Identification of anthropogenic and natural inputs of sulfate into a karstic coastal groundwater system in northeast China: evidence from major ions, $\delta^{13}C_{DIC}$ and $\delta^{34}S_{SO4}$. Hydrology and Earth System Sciences 20(5): 1983-1999.

Han, D., Currell, M.J., Cao, G. 2016b. Deep challenges for China's war on water pollution. Environmental Pollution. 218: 1222-1233.

Han Z., 1988. Seawater intrusion into coastal porous aquifer- a case study of the alluvial plain of Yang River and Dai River in Qinhuangdao City. China University of Geosciences, Beijing, China. (Chinese with English abstract)

Han Z., 1990. Controlling and harnessing of the seawater intrusion the alluvial plain of Yang River and Dai River in Qinhuangdao.Geoscience (Journal of Graduate School, China University of Geosciences). 4(2):140-151. (Chinese with English abstract)

Hebei Geology Survey, 1987. Report of regional geological and tetonic background in Hebei Province.

Internal materials.

Hui G., 2009. Characteristics and formation mechanism of hydrochemistry of geothermal water in Danihe, Funing District of Qinhuangdao region. Science & Technology Informaion. 9:762-763. (in Chinese)

IAEA/WMO, 2006. Global Network of Isotopes in Precipitation. The GNIP Database, Vienna. <http://www-naweb.iaea.org/napc/ih/IHS_resources_gnip.html>.

IPCC, Climate Change 2007: The Physical Science Basis, Contribution of Working Group I to the Fourth Assessment Report of the Intergovernmental Panel on Climate Change, S. Solomon et al., Eds. (Cambridge Univ. Press, Cambridge, 2007).

Jones B.F., Vengosh A., Rosenthal E. Yechieli Y., 1999. Geochemical investigations. In: Bear et al. (eds) Seawater Intrusion in Coastal Aquifers - Concepts, Methods and Practices, pp51-72.

Langevin C.D., Zygnerski M.R., White J.T., Hughes J.D., 2010. Effect of sea-level rise on future coastal groundwater resources in southern Florida, USA. SWIM21-21st Salt Water Intrusion Meeting. Azores, Portugal., June 21-26, 2010. Pp125-128.

Larsen, F., Tran, L.V., Hoang, H.V., Tran, L.T., Chistiansen, A.V., Pham, N.Q., 2017. Groundwater salinity influenced by Holocene seawater trapped in the incised valleys in the Red River delta plain. Nature Geoscience 10: 376-382.

Lee, S., Currell, M., Cendon, D.I., 2016. Marine water from mid-Holocene sea level highstand trapped in a coastal aquifer: Evidence from groundwater isotopes, and environmental significance. Science of the Total Environment. 544: 995-1007

Masterson J.P., 2004. Simulated interaction between freshwater and saltwater and effects of ground-water pumping and sea-level change, Lower Cape Cod aquifer system, Massachusetts: U.S. Geological Survey Scientific Investigations Report 2004-5014, 72 p.

Mazi, K., Koussis, A.D., Destouni, G., 2014. Intensively exploited Mediterranean aquifers: proximity to tipping points and control criteria for sea intrusion. Hydrol. Earth Syst. Sci. 18, 1663-1677.

Meng F., 2004. Rational development of groundwater resources on the coastal zone of Qinhuangdao area. Marine Geology Letters. 20(12):22-25. (Chinese with English abstract)

Michael H.A., Post V.E.A., Wilson A.M., Werner A.D. 2017. Science, society and the coastal groundwater squeeze. Water Resources Research. 53. 2610-2617.

Mondal N.C., Singh V.P., Singh V.S., Saxena V.K., 2010. Determining the interaction between groundwater and saline water through groundwater major ions chemistry. Journal of Hydrology. 388:100-111.

Montenegro S.M.G., de A. Montenegro A.A., Cabral J.J.S.P., Cavalcanti G., 2006. Intensive exploitation and groundwater salinity in Recife coastal plain (Brazil): monitoring and management perspectives. Proceedings 1st SWIM-SWICA Joint Saltwater Intrusion Conference, Cagliari-Chia Laguna, Italy - September 24-29, 2006. pp79-85.

Moore W.S., 1996. Large groundwater inputs to coastal waters revealed by 226Ra enrichments. Nature 380,612-214.

Narayan K.A., Schleeberger C., Bristow K.L., 2007. Modelling seawater intrusion in the Burdekin Delta Irrigation Area, North Queensland, Australia. Agricultural Water Management. 89:217-228.

Pan G., Yang Y., Zhang L., 1990. Survey report of geothermal water in Qinhuangdao city of Hebei Province. Team of mineral hydrological and engineering geology from the Bureau of Geology and mineral Resources of Hebei Province, China. (in Chinese)

Post V.E.A., 2005. Fresh and saline groundwater interaction in coastal aquifers: Is our technology ready for the problems ahead? Hydrogeology Journal. 13:120-123.

Price R.M., Herman J.S., 1991. Geochemical investigation of salt-water intrusion into a coastal carbonate

aquifer: Mallorca, Spain. Geological Society of America Bulletin. 103:1270-1279.
Pulido-Leboeuf P., 2004. Seawater intrusion and associated processes in a small coastal complex aquifer (Castell de Ferro, Spain). Applied Geochemistry. 19:1517-1527.
Radhakrishna I., 2001. Saline fresh water interface structure in Mahanadi delta region, Orissa, India. Environmental Geology. 40(3):369-380.
Rahmawati N., Vuillaume J., Purnama I.L.S., 2013. Salt intrusion in Coastal and Lowland areas of Semarang City. Journal of Hydrology. 494:146-159.
Robinson M.A., Gallagher D.L., Reay W.G., 1998. Field observations of tidal and seasonal variations in ground water discharge to estuarine surface waters. Ground Water Monitoring and Remediation. 18 (1): 83-92.
Shen Z., Zhu Y., Zhong Z., 1993. Theoretical basis of hydrogeochemistry. Geological Publishing House. Beijing, China. (in Chinese)
Sherif M.M., Singh V.P., 1999. Effect of climate change on sea water intrusion in coastal aquifers. Hydrological Processes 13, 8:1277-1287.
Shi M.Q., 2012. Spatial distribution of population in the low elevation coastal zone and assessment on vulnerability of natural disaster in the coastal area of China. Master thesis of Shanghai Normal University, 24–32.(Chinese with English abstract)
Simpson, M.J., Clement, T.P., 2004. Improving the worthiness of the Henry problem as a benchmark for density-dependent groundwater flow models. Water Resources Research 40 (1), W01504 doi:10.1029/2003WR002199.
Sivan O., Yechieli Y., Herut B., Lazar B., 2005. Geochemical evolution and timescale of seawater intrusion into the coastal aquifer of Israel. Geochimica et Cosmochimica Acta. 69(3):579-592.
Smith A.J., Turner J.V., 2001. Density-dependent surface water-groundwater interaction and nutrient discharge in the Swan-Canning Estuary. Hydrolological Processes. 15:2595-2616.
SOA (State Oceanic Administration of the People's Republic of China), 2015. China's Marine Environment Bulletin: 2014. Released 11th March, (in Chinese).
Sun J., Yang Y., 2007. Seawater intrusion characteristics in Qinhuangdao. Journal of Environmental Management College of China. 17(2):51-54. (Chinese with English abstract)
UN Atlas, 2010. UN Atlas: 44 Percent of us Live in Coastal Areas. <http://coastalchallenges.com/2010/01/31/un-atlas-60-of-us-live-in-the-coastal-areas/>.
Vengosh A., Spivack A.J., Artzi Y., Ayalon A. 1999. Geochemical and boron, strontium, and oxygen isotopic constraints on the origin of the salinity in groundwater from the Mediterranean coast of Isreal. Water Resources Research. 35(6): 1877-1894.
Walraevens, K., Cardenal-Escarcena, J., Van Camp, M., 2007. Reaction transport modelling of a freshening aquifer (Tertiary Ledo-Paniselian Aquifer, Flanders-Belgium). Applied Geochemistry. 22: 289-305.
Wang, J., Yao, P., Bianchi, T.S., Li, D., Zhao, B., Cui, X., Pan, H., Zhang, T., Yu, Z., 2015. The effect of particle density on the sources, distribution, and degradation of sedimentary organic carbon in the Changjiang Estuary and adjacent shelf. Chemical Geology. 402:52-67.
Weber, K., Stewart, M., 2004. A critical analysis of the cumulative rainfall departure concept. Ground Water 42 (6), 935–938.
Werner, A.D., 2010. A review of seawater intrusion and its management in Australia. Hydrogeology Journal. 18(1):281-285.
Werner A.D., Bakker M., Post V.E.A., Vandenbohede A., Lu C., Ataie-Ashtiani B., Simmons C.T., Barry D.A., 2013. Seawater intrusion processes, investigation and management: Recent advances and future

challenges. Advances in Water Resources.51:3-26.
Werner A.D., Simmons C.T., 2009. Impact of sea-level rise on seawater intrusion in coastal aquifers. Ground Water. 47:197-204.
Westbrook S.J., Rayner J.L., Davis G.B., Clement T.P., Bjerg P.L., Fisher S.J., 2005. Interaction between shallow groundwater, saline surface water and contaminant discharge at a seasonally and tidally forced estuarine boundary. Journal of Hydrology, 302:255-269.
Wilhite D.A., 1993.Drought Assessment, Management, and Planning: Theory and Case Studies. Springer U S. p628.
Xu G., 1986. Analysis of seawater intruding into aquifer system in Beidaihe Region.Hydrogeology & Engineering Geology. 2:7-10. (in Chinese)
Xue Y.Q., Wu J.C., Ye S.J., Zhang Y.X., 2000. Hydrogeological and hydrogeochemical studies for salt water intrusion on the South Coast of Laizhou Bay, China. Ground Water. 38, 38-45.
Yang L., 2011. Formation mechanism of bedrock fracture type-geothermal water in Qinhuangdao area. West-china Exploration Engineering. Urumchi, China. 10:151-152. (in Chinese)
Yang Y., Gao S., Xie Y., 2008. Assessment and control countermeasures of seawater intrusion hazard on Qinhuangdao Region. The Chinese Journal of Geological Hazard and Control. 19(3):139-143. (Chinese with English abstract)
Yang Y., He Q., Xie Y., Cao C., 1994. Grey model prediction of seawater intrusion of Qinhuangdao. The Chinese Journal of Geological Hazard and Control. 5(sup.):181-183. (Chinese with English abstract)
Yechieli Y., Kafri U., Sivan O., 2009. The inter-relationship between coastal sub-aquifers and the Mediterranean Sea, deduced from radioactive isotopes analysis. Hydrogeology Journal. 17:265-274.
Zang W., Liu W., Guo J., Zhang X., 2010. Geological hazards of seawater intrusion and its control measures in Qinhuangdao City, Hebei Province. The Chinese Journal of Geological Hazard and Control. 21(4):120-125. (Chinese with English abstract)
Zeng J., 1991. Geochemistry of geothermal water in Qinhuangdao area, Hebei Province. Bull. Institute of Hydrogeology and Engineering Geology, Chinese Academy of Geological Sciences. 7:111-127.
Zhang B., 2012. Mechanism of Seawater Intrusion Using Hydrochemistry and Environmental Isotopes in Qinhuangdao Yang Dai River Plain. Master's Thesis. Xiamen University, Fujian, China. (Chinese with English abstract)
Zhang Q., Volker R.E., Lockington D.A., 2004. Numerical investigation of seawater intrusion at Gooburrum, Bundaberg, Queensland, Australia. Hydrogeol. J. 12 (6), 674-687.
Zuo W., 2006. Survey and Research on Seawater Intrusion in the Yandaihe Plain of Qinhuangdao City. Doctoral Thesis. China University of Geosciences, Beijing, China. (Chinese with English abstract)
Zuo W., Yang Y., Dong Y., Liang M., 2009. The numerical study for seawater intrusion in Yanghe and Daihe coastal plain of Qinhuangdao City. Journal of Natural Resources. 24(12):2087-2095. (Chinese with English abstract)

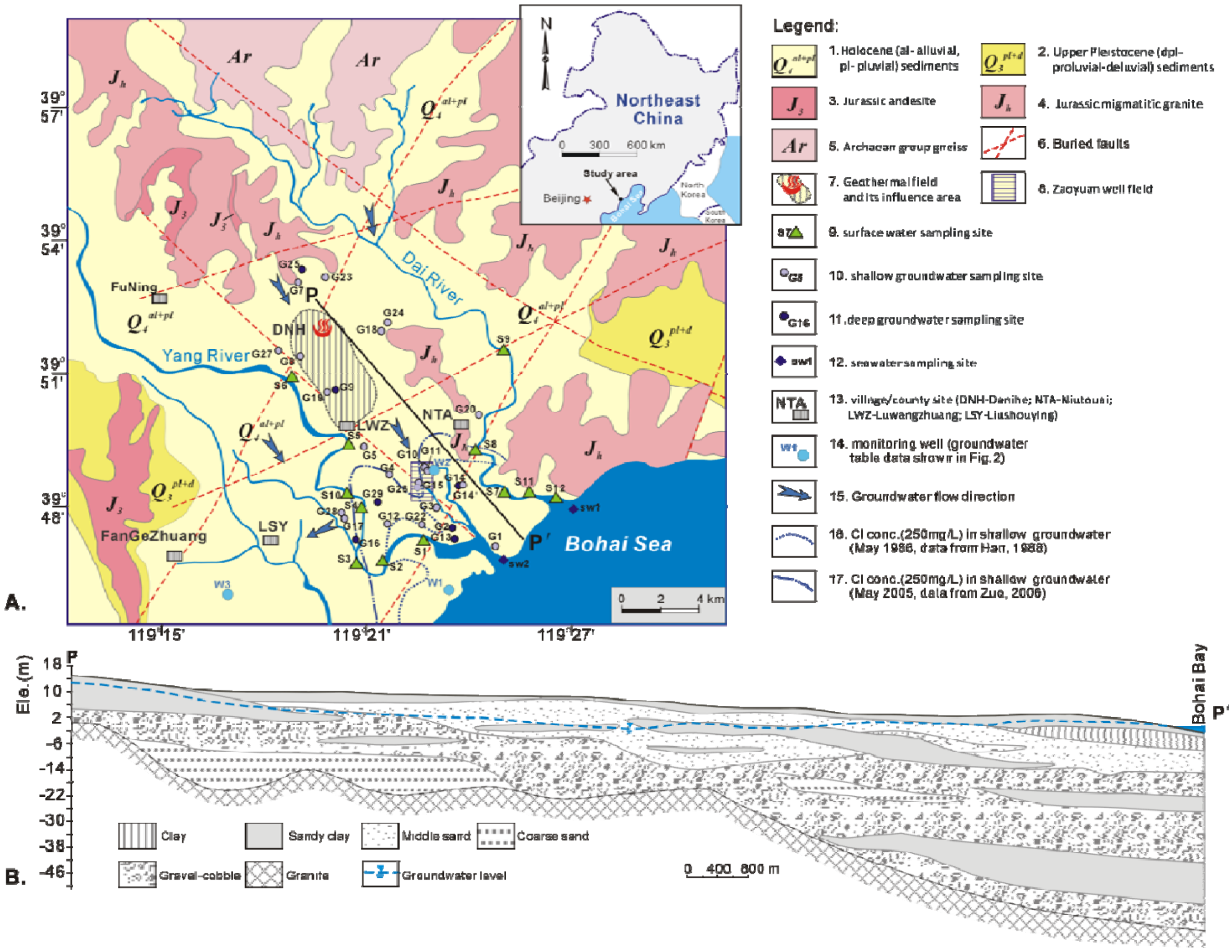

Figure 1. Location map (A.) for showing geological background and water sampling sites in the study area, and (B.) hydrogeological cross-section of Yang-Dai River Plain (P-P′ in A.) (modified from Han, 1988). The surface area covered from >250 mg Cl/L contour line to coastline refers the seawater zones.

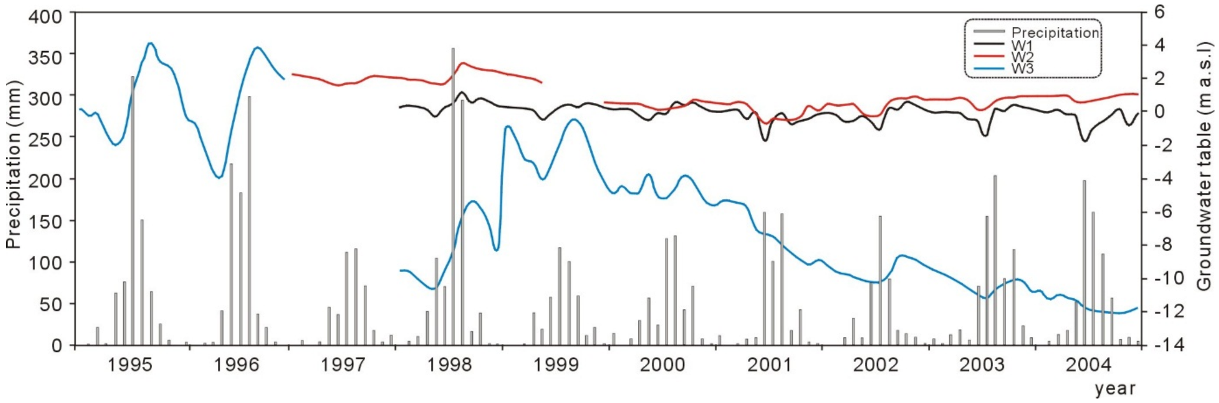

Figure 2. Distribution of precipitation and dynamics of groundwater table in the study area. Locations of the monitoring wells (W1, W2 and W3) can be seen from Fig. 1.

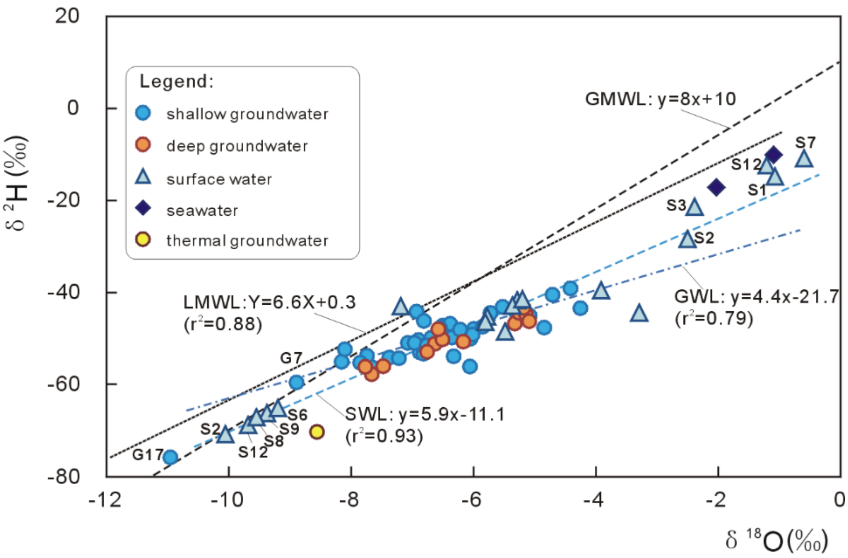

Figure 3. Stable isotope compositions of different water samples collected from the study area LMWL - local meteoric water line; GMWL – global meteoric water line (Craig, 1961); GWL – groundwater line; SWL – surface (river) water line.

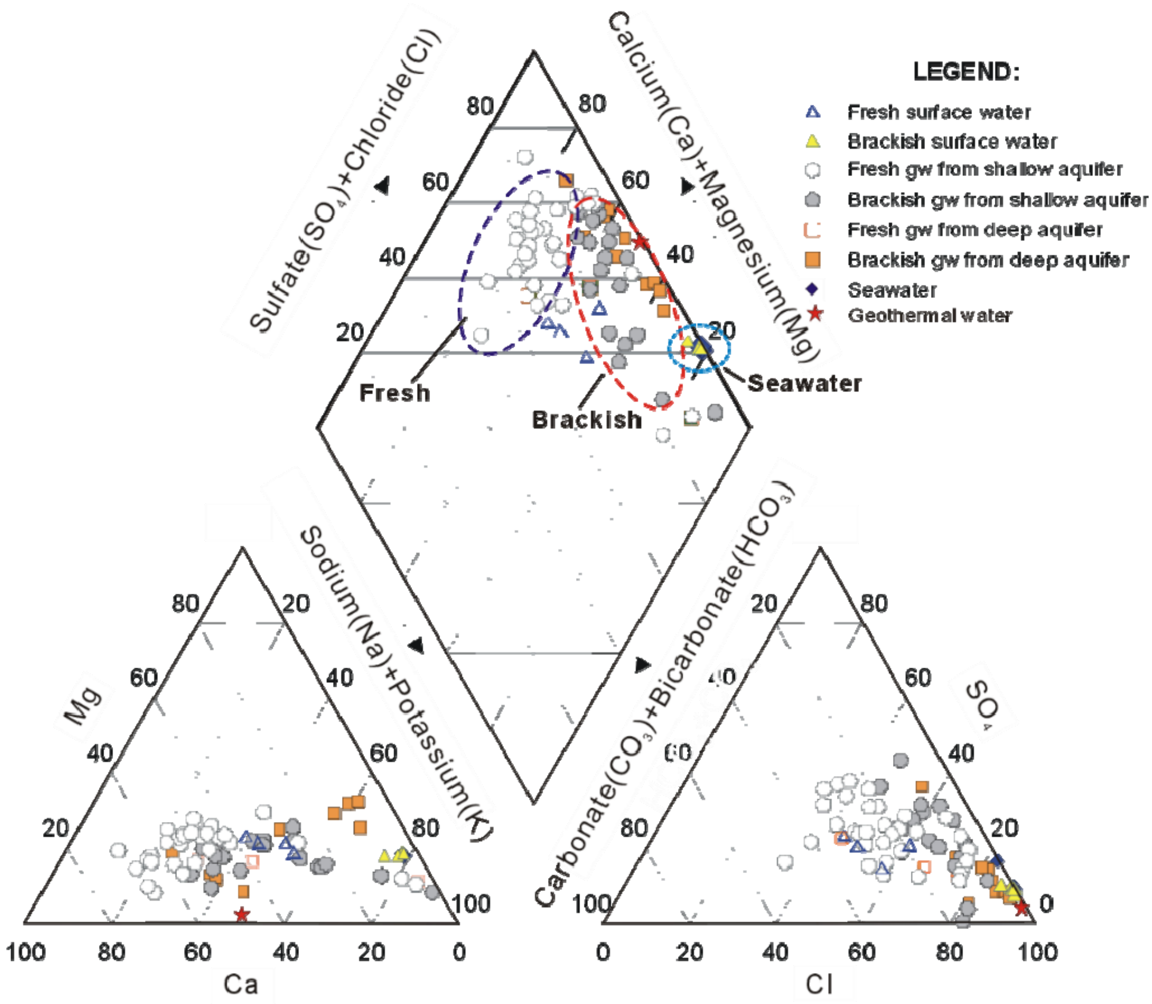

Figure 4. Piper plot of different water samples

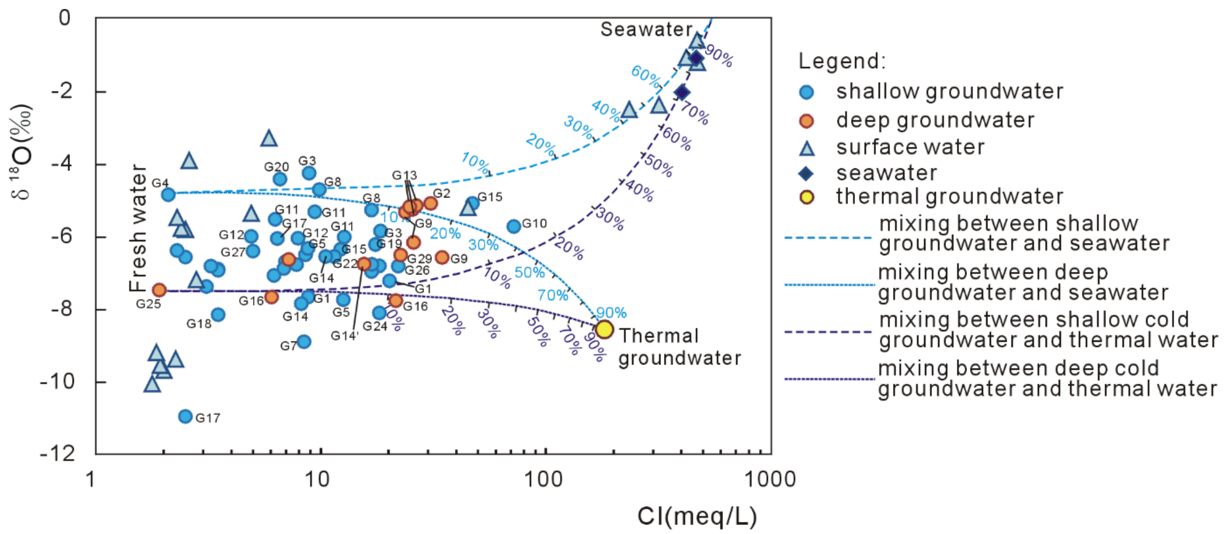

Figure 5. Relationship between chloride content and isotopic signature of different water samples as a means to differentiate mixing processes in the area. The data of thermal water are from Zeng (1991).

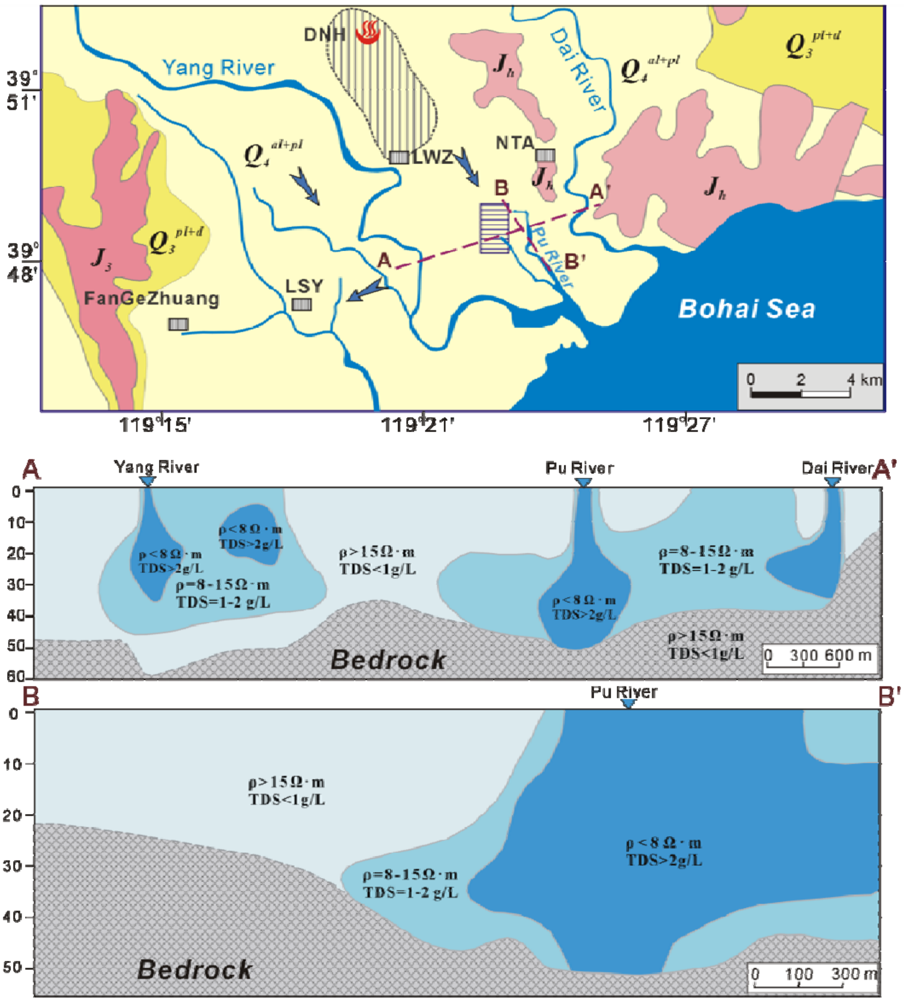

Figure 6. Cross-sections showing results obtained from application of geophysical resistivity method (employed in May, 2004, data and methods described in Zuo, 2006)

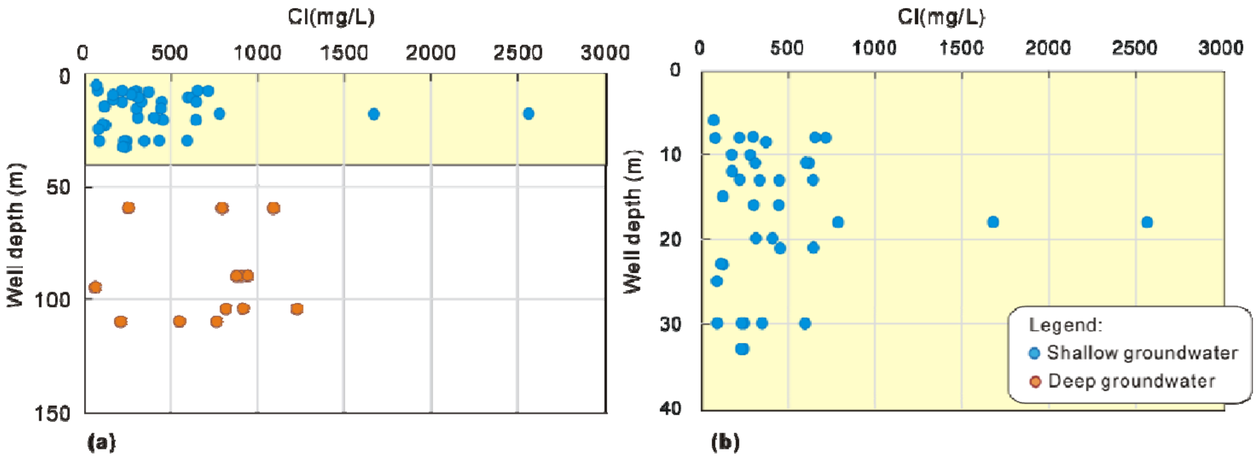

Figure 7. Chloride concentration vs. well depth for groundwater samples.

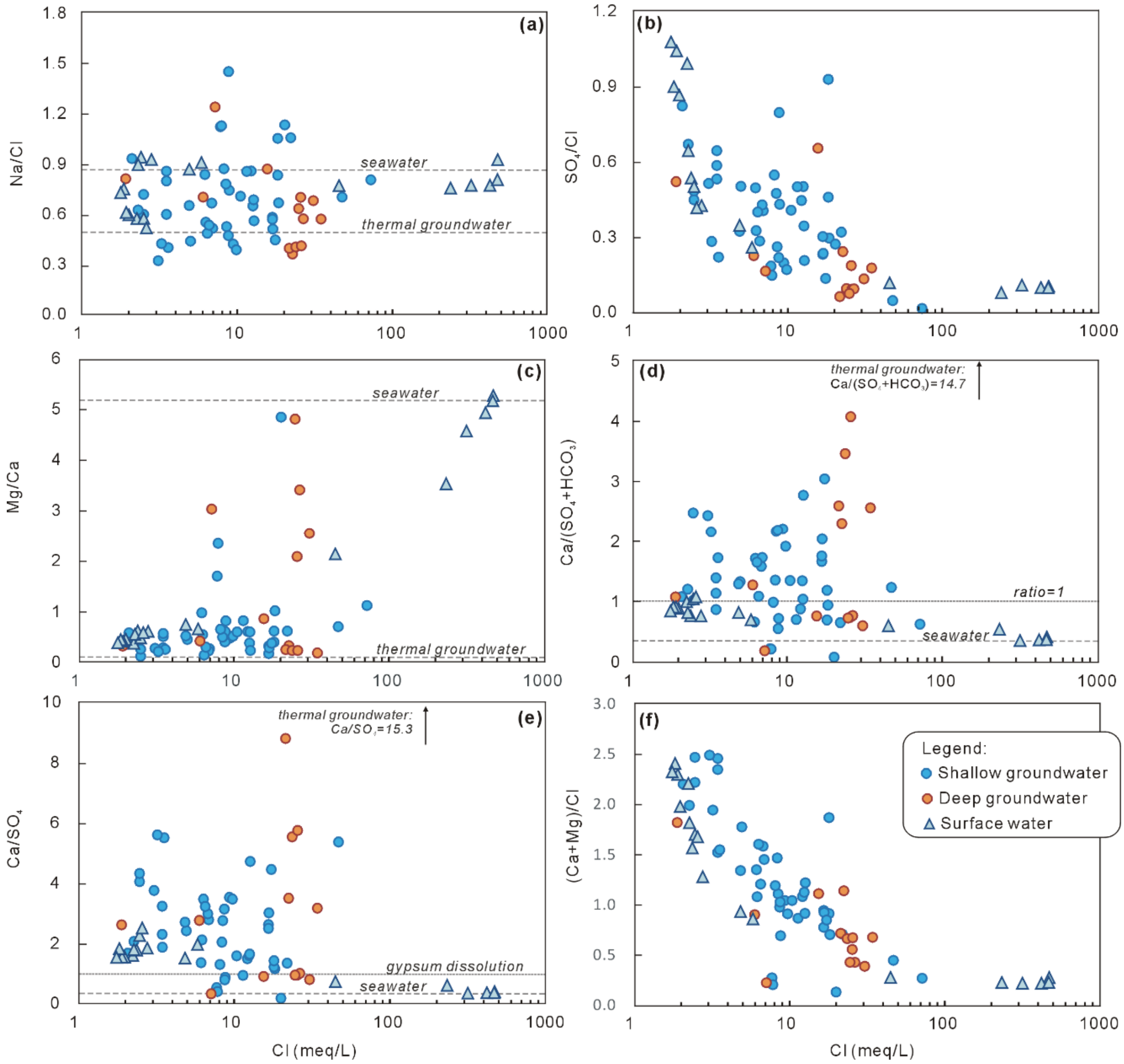

Figure 8. Molar ratios of major ions versus chloride concentrations for different water samples from the study area

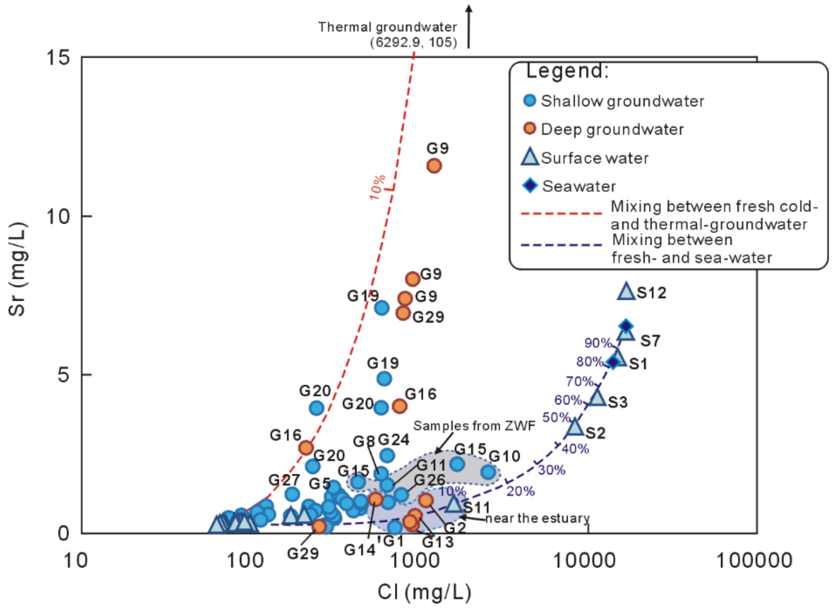

Figure 9. Chloride versus strontium concentrations of different water samples ZWF- Zaoyuan well field

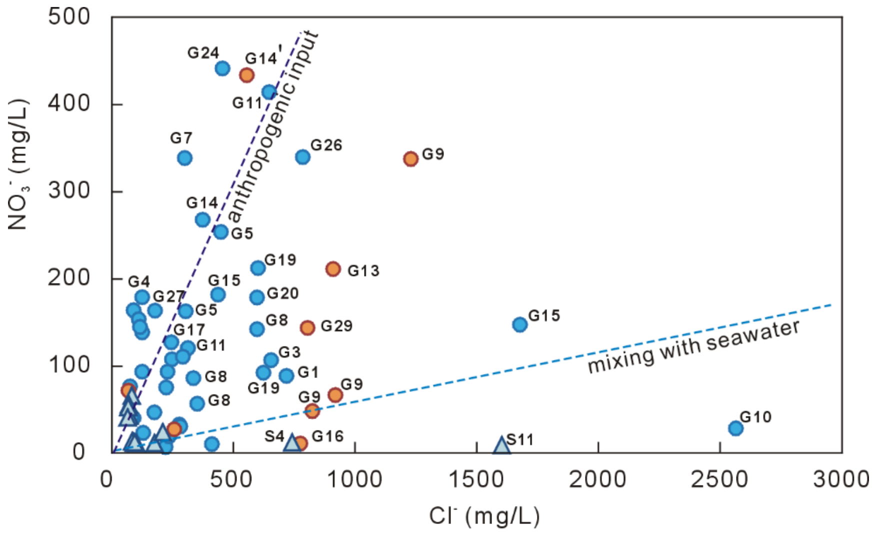

Figure 10. Plot of chloride versus nitrate concentrations in groundwater, with seawater and anthropogenic pollution mixing trajectories

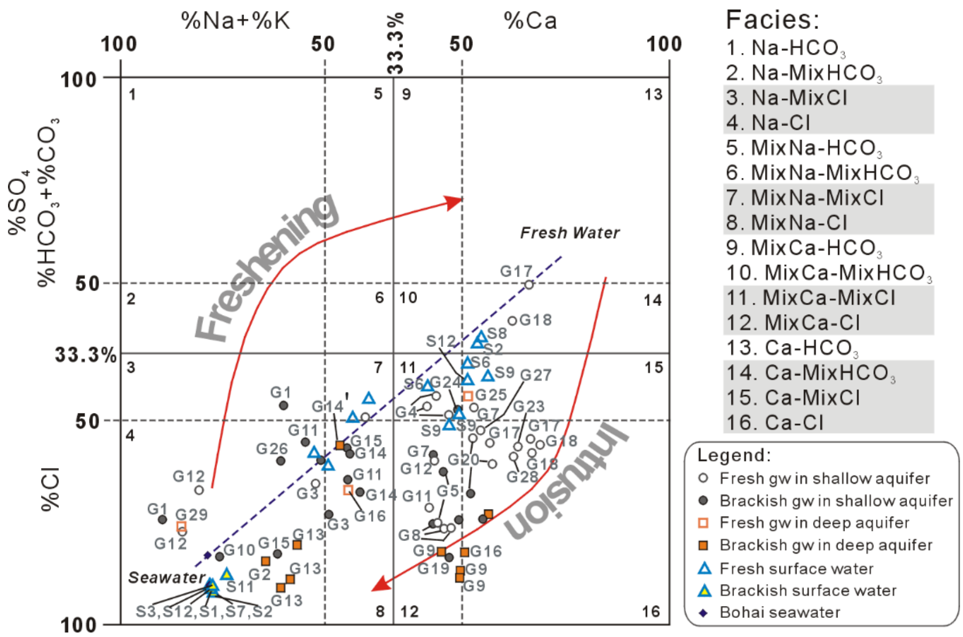

Figure 11. Hydrogeochemical facies evolution diagram (HFE-D) for the collected water samples

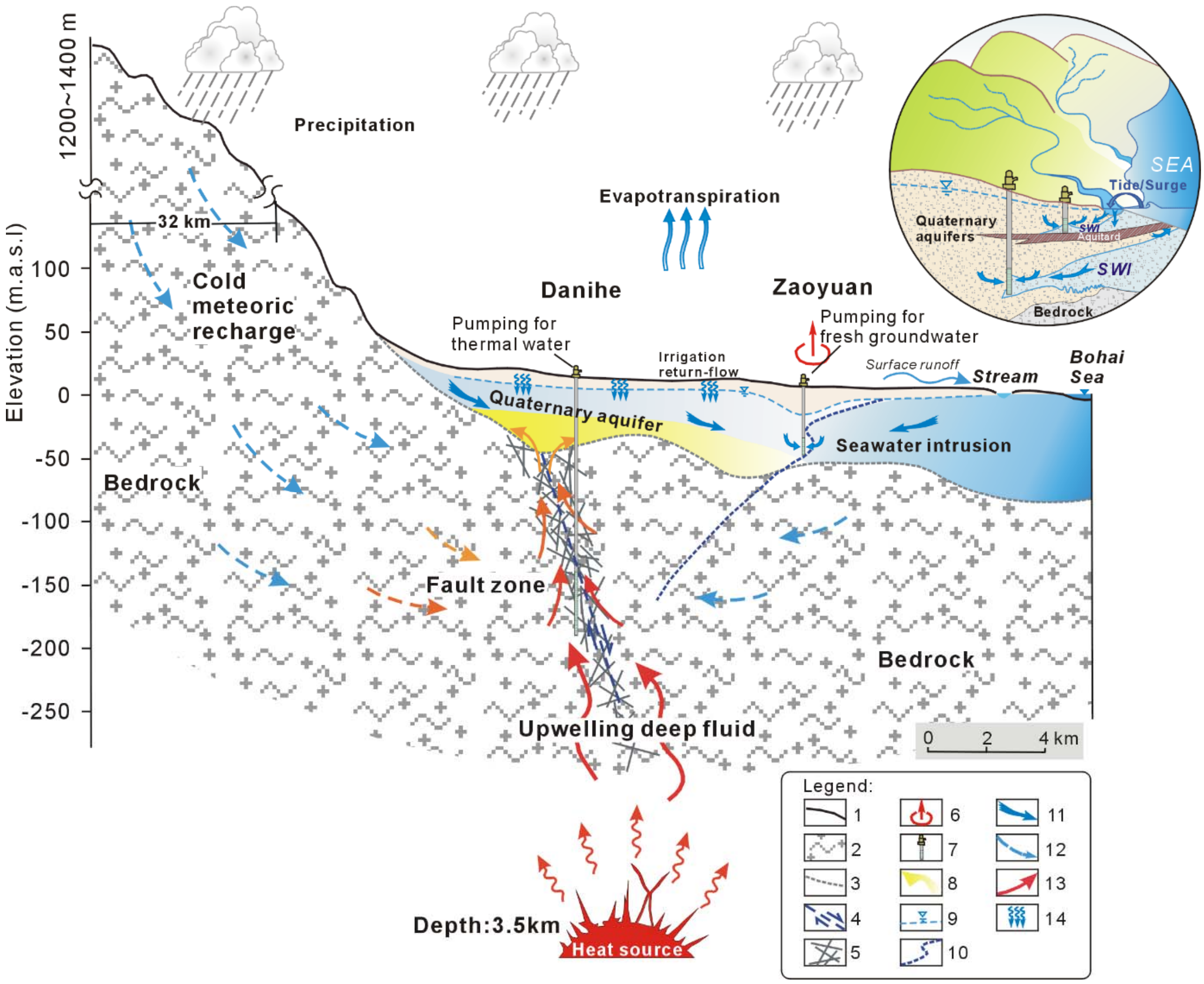

Figure 12. Conceptual model of groundwater flow system in the Yang-Dai River coastal plain

Explanation: 1- Land surface; 2- Bedrock; 3- Boundary between Quaternary sediments and bedrock; 4-Fault; 5- Permeable fracture zone; 6- Concentrated groundwater pumping zone; 7- Pumping wells; 8- Zone affected by upflow of geothermal fluids; 9- Groundwater table; 10- Potential interface between fresh- and salt-water; 11-Groundwater flow direction in Quaternary aquifers; 12- Groundwater flow in bedrocks; 13- Geothermal groundwater flow direction; 14- Irrigation return-flow.

Table 1. Physical, hydrochemical and isotopic data of the water samples collected from the Yang-Dai River coastal plain

WaterType	ID	Sampling Time	Ele. m	WellDepth m	WaterTable Depth(m)	EC μs/cm	pH	T ^{o}C	ORP mV	DO mg/L	Cl^- mg/L	NO_3^- mg/L	SO_4^{2-} mg/L	HCO_3^- mg/L	Ca^{2+} mg/L	Na^+ mg/L	K^+ mg/L	Mg^{2+} mg/L	Sr mg/L	δ^2H ‰	$\delta^{18}O$ ‰
Shallow groundwater samples:																					
Fresh Groundwater	G4	Aug.2010	5	15	4.2	741	6.5	20.5	6	3.9	124.3	92.6	89.7	136.9	70.3	69.2	2.3	21.8	0.67	-50	-6.9
	G27	Aug.2010	3	12		1014	6.4	14.8	16	3.8	177.5	163.0	121.0	128.0	122.0	50.6	2.6	33.4	1.22	-50	-6.4
	G12	Aug.2010	8	10		1152	7.2	25.0	9	5.9	276.9	31.9	69.8	148.8	15.8	201.9	11.1	16.2	0.25	-51	-6.8
	G17	Aug.2010	5	25	5.7	624	7.1	19.1	13	3.3	88.8	39.5	58.3	223.3	98.4	41.4	4.3	7.5	0.33	-76	-11.0
	G18	Aug.2010	5	23	1.7	934	7.4	14.9	12	7.1	124.3	137.8	98.7	235.2	133.3	48.3	2.2	23.2	0.71	-55	-8.2
	G1	Sep.2009	6	8	2.4	1673	8.3	19.4			220.1	2.0	148.3	207.9	84.3	119.6	17.1	49.9	0.66	-51	-7.1
	G4	Sep.2009	6	15	4.6	1295	7.9	13.9			124.3	178.5	108.7	92.4	104.4	64.4	2.7	35.9	0.85	-44	-6.9
	G5	Sep.2009	11	16	6.5	1544	7.8	13.3			303.4	162.3	108.2	38.5	124.5	103.7	1.1	39.1	1.14	-47	-6.5
	G23	Sep.2009	15	30	3.0	556	7.9	14.9			88.8	163.4	54.0	51.9	97.4	34.5	0.5	15.6	0.55	-48	-6.6
	G7	Sep.2009	17	8	1.7	901	8.4	14.9			81.7	41.2	74.2	69.3	64.0	33.2	1.0	16.5	0.41	-47	-6.4
	G8	Sep.2009	4	13	4.3	1621	7.8	14.0			334.6	85.4	90.1	69.3	132.5	91.9	1.4	38.5	1.19	-44	-5.3
	G11	Sep.2009	4	13		1237	8.6	18.4			222.9	74.5	98.7	30.8	87.4	80.1	1.8	29.0	0.84	-43	-5.5
	G12	Sep.2009	8	10		1114	7.9	15.0			174.0	46.0	76.4	107.8	86.2	73.6	4.3	27.2	0.53	-48	-6.0
	G28	Sep.2009	6	23	6.8	1748	8.2	14.6			127.8	22.5	38.4	107.8	88.2	33.3	1.3	14.0	0.58		
	G18	Sep.2009	9	23	5.5	2850	7.8	13.7			110.1	152.9	76.7	53.9	120.3	23.1	1.1	20.5	0.65	-54	-7.4
	G20	Sep.2009	12	30		1602	7.7	19.5			246.9	107.1	135.9	107.8	158.2	82.8	1.7	26.3	3.94	-50	-6.7
	G17	Sep.2009	6	33	7.9	819	8.1	14.3			243.5	126.4	141.7	161.7	176.3	105.5	1.8	24.6	0.71	-53	-6.9
	G3	Jun.2008	4	20		1573	7.3	14.5			315.0		184.4	54.9	67.3	152.1	3.8	33.2	0.46	-43	-4.2
	G4	Jun.2008	6	6		688	7.5	14.1			74.6	75.8	83.2	60.4	58.2	45.2	1.2	20.6	0.47	-48	-4.8
	G5	Jun.2008	5	11		1455	7.4	14.7			310.9	119.5	92.7	52.2	121.3	95.4	0.9	29.9	1.43	-54	-6.3
	G8	Jun.2008	4	30		1402	7.3	14.7			349.7	55.9	81.5	85.1	118.0	88.1	1.2	36.9	1.08	-40	-4.7
	G12	Jun.2008	8	10		1285	7.6	19.3			281.0	29.8	56.8	74.1	9.7	205.7	11.0	13.7	0.19	-50	-6.0
	G17	Jun.2008	6	33		1462	8.1	15.0			227.9	92.6	123.8	175.7	179.2	72.1	1.1	15.9	0.57	-56	-6.1
	G18	Jun.2008	9	23		1125	7.9	18.8			115.5	144.2	44.4	90.6	103.7	31.8	1.4	13.7	0.41	-53	-6.8
	G20	Jun.2008	12	30		1210	9.1	28.3			234.3	18.2	90.6	230.6	122.0	81.4	2.6	22.4	2.10	-39	-4.4
Brackish Groundwater	G1	Aug.2010	6	11		2750	7.4	17.3	143	1.5	312.4	120.0	337.1	205.4	112.0	294.4	29.9	41.3	0.54	-56	-7.7
	G3	Aug.2010	4	8		2490	5.9	14.7	74	1.4	654.3	106.0	263.7	86.3	128.2	283.6	6.6	78.6	0.97	-47	-5.8
	G15	Aug.2010	4	30		2290	6.6	15.4	3	3.3	435.7	181.3	263.7	244.1	164.3	242.8	6.6	60.8	1.60	-50	-6.3
	G26	Aug.2010	4	18	1.8	4060	6.4	15.2	145	1.3	784.6	339.4	341.4	485.2	192.3	538.2	36.0	72.1	1.20	-46	-6.8
	G11	Aug.2010	6	13	2.3	3490	6.5	15.0	47	1.3	646.1	414.1	402.7	402.6	204.8	441.8	34.9	76.3	1.51	-52	-6.8
	G20	Aug.2010	12	30		1513	6.7	18.8	4	4.3	596.4	177.9	245.0	184.6	268.6	225.4	2.0	29.2	3.95	-51	-7.0
	G5	Aug.2010	5	16	5.4	1500	6.2	15.6	7	5.9	447.3	253.3	304.7	79.3	204.1	188.6	0.8	47.5	0.78	-54	-7.7
	G8	Aug.2010	4	30	2.1	1563	6.3	15.7	120	4.9	596.4	141.4	188.1	104.2	196.3	220.8	3.2	38.7	1.87	-44	-5.3
	G7	Aug.2010	5	8	0.9	1438	6.8	19.3	24	6.1	299.6	338.3	192.7	128.0	164.2	151.8	0.3	50.0	0.66	-60	-8.9
	G19	Aug.2010	8	11	2.8	2380	6.5	16.1	42	3.2	600.0	211.9	192.1	119.1	241.4	199.5	6.6	42.4	7.10	-52	-6.8
	G24	Aug.2010	4	21		4400	6.8	15.5	4	5.9	646.1	952.1	813.3	223.3	484.1	349.6	3.4	117.4	2.44	-52	-8.1
	G22	Sep.2009	2	20	2.0	2170	8.0	17.8			408.3	2.0	277.5	130.9	109.2	226.8	21.3	54.2	0.70	-48	-6.5
	G10	Sep.2009	3	18		9770	7.5	15.1			2563.1	27.7	25.3	870.2	181.4	1340.0	98.1	123.0	1.92	-44	-5.7
	G14	Sep.2009	2	8.5		1886	8.5	16.6			291.1	109.8	216.4	92.4	117.8	164.7	19.3	46.5	0.82	-55	-7.9

	G24	Sep.2009	11	21	5.3	1003	7.8	13.6			454.4	441.5	128.1	115.5	252.3	165.6	0.6	36.2	0.93		
	G19	Sep.2009	12	11	4.7	2560	8.1	14.6			622.0	91.5	115.6	69.3	214.9	180.7	6.0	49.4	4.87	-48	-6.2
	G1	Jun.2008	6	8		3150	8.5	15.0			717.1	87.7	265.6	98.8	9.1	527.4	26.7	26.6	0.17	-54	-7.2
	G11	Jun.2008	6	13		2370	7.2	12.2			451.2		211.3	162.0	145.1	201.2	22.0	52.6	1.00	-49	-6.0
	G14	Jun.2008	3	8.5		2050	7.4	18.6			372.8	267.3	206.1	49.4	136.4	171.3	12.7	49.5	0.93	-48	-6.5
	G15	Jun.2008	4	18		5990	7.5	15.6			1675.6	146.8	110.1	474.9	246.5	764.7	20.2	104.9	2.17	-45	-5.1
Deep Groundwater samples:																					
Fresh Groundwater	G25	Aug.2010	4	95		444	6.6	23.5	41	4.4	68.1	71.0	48.2	89.3	52.5	35.9	1.1	10.4	0.25	-56	-7.5
	G16	Sep.2009	3	110		1214	7.9	19.9			214.4		66.1	100.1	76.3	97.8	2.8	19.5	2.68	-58	-7.7
	G29	Sep.2009	6	60		1291	8.1	20.9			255.6	26.3	57.5	69.3	8.0	205.9	12.3	14.6	0.20	-51	-6.6
Brackish Groundwater	G29	Aug.2010	6	60	6.2	3220	7.2	24.1	12	5.6	803.4	143.0	264.7	178.6	386.8	189.3	4.3	77.6	6.95	-50	-6.5
	G16	Aug.2010	3	110		1733	7.3	21.5	16	4.8	766.8	5.5	67.1	205.4	246.2	197.8	4.5	37.9	4.00	-56	-7.8
	G9	Jun.2008	9	104		3110	7.8	15.0			823.6	47.4	110.5	85.1	255.1	222.2	5.1	36.7	7.40	-47	-5.3
	G9	Sep.2009	9	104		3190	8.5	20.4			917.4	65.8	116.6	61.6	279.8	245.1	5.7	40.6	8.02	-51	-6.2
	G9	Aug.2010	9	104		4600	6.3	24.3	18	4.0	1228.3	337.4	296.3	92.3	392.2	455.4	5.5	45.3	11.59	-48	-6.6
	G14'	Aug.2010	5	110	2.1	2850	6.1	22.9	120	1.8	553.8	433.7	491.4	134.0	186.0	312.8	52.3	96.6	1.06	-53	-6.8
	G13	Aug.2010	3	90		3230	8.9	19.2	36	2.4	908.8	210.6	231.8	92.3	92.0	413.5	29.0	115.7	0.26	-45	-5.2
	G13	Jun.2008	3	90		3180	7.9	13.5			945.4		122.2	52.2	51.4	351.9	25.0	105.4	0.55	-45	-5.1
	G13	Sep.2009	3	90	2.6	3070	8.1	15.3			882.0		91.9	38.5	36.5	362.9	26.0	105.3	0.35	-43	-5.2
	G2	Jun.2008	2	60		3780	7.7	18.5			1093.4		200.3	96.1	67.3	484.1	25.8	103.1	1.03	-46	-5.1
River water samples:																					
Fresh water samples																					
Dai River	S9	Aug.2010				511	7.2	22.2	22	5.5	80.3	65.2	107.9	86.3	72.1	29.9	3.7	16.7	0.34	-66	-9.4
Dai River	S12	Aug.2010				485	7.5	25.8	18	7.3	71.3	41.9	83.7	83.4	54.3	27.6	4.0	15.1	0.30	-69	-9.7
Dai River	S8	Aug.2010				495	7.3	22.1	24	5.8	68.6	54.9	96.8	89.3	62.3	27.2	4.1	15.9	0.32	-67	-9.6
Yang River	S6	Aug.2010				507	7.0	23.3	17	4.5	66.0	51.9	80.5	107.2	61.6	32.2	3.8	16.8	0.30	-65	-9.2
Yang River	S2	Aug.2010				435	7.3	7.3	6	4.9	63.2	40.2	92.2	101.2	59.3	29.9	4.3	14.0	0.26	-71	-10.1
Yang River	S5	Sep.2009				718	8.4	24.4			85.2	12.9	62.0	107.8	46.1	52.0	6.4	17.4	0.36	-45	-5.8
Yang River	S4	Sep.2009				2630	8.1	24.7			733.1	6.6	142.2	115.5						-42	-5.3
Yang River	S6	Sep.2009				718	8.3	25.6			99.4	6.6	57.5	107.8	44.3	59.8	5.0	16.4	0.30	-43	-7.2
Dai River	S9	Sep.2009			2.0	560	8.0	23.6			88.8	6.8	60.5	92.4	57.2	33.2	3.3	16.7	0.36	-46	-5.8
Dai River	S8	Sep.2009				1013	8.2	23.6			174.0	6.4	82.2	92.4	52.1	98.1	6.0	23.6	0.55	-43	-5.4
Yang River	S6	Jun.2008				1166	7.5	12.6			81.7	12.6	71.3	112.5	53.6	47.5	4.9	18.0	0.31	-49	-5.5
Dai River	S10	Jun.2008				1255	9.1	28.0			208.9	23.1	73.7	175.7	60.7	123.2	10.8	24.2	0.57	-44	-3.3
Dai River	S9	Jun.2008				1163	7.8	11.8			92.3	7.5	52.2	90.6	54.7	31.1	3.6	19.5	0.35	-40	-3.9
Brackish and salt water samples																					
Yang River	S3	Sep.2009				34800	7.8	15.5			11289.4		1684.7	115.5	251.0	5658.7	231.3	690.1	4.29	-21	-2.4
Dai River	S12	Sep.2009				47100	7.5	23.7			16766.3		2416.5	77.0	412.1	10074.3	398.2	1306.0	7.64	-12	-1.2
Dai River	S11	Sep.2009				52500	8.5	23.4			1601.5	2.8	258.7	84.7	79.7	801.4	32.9	102.7	0.93	-41	-5.2
Yang River	S1	Jun.2008				39800	8.7	24.2			14953.5		2035.9	134.5	313.0	7496.0	270.5	928.3	5.55	-15	-1.1
Yang River	S2	Jun.2008				20200	8.8	28.5			8328.3		912.1	189.4	233.4	4094.2	147.9	495.9	3.37	-28	-2.5
Dai River	S7	Jun.2008				49500	8.4	11.5			16677.1		2261.3	113.9	349.0	8730.0	326.4	1084.0	6.36	-11	-0.6
	SW1	Aug.2010				45600	7.8	25.5	83	4.90	14768.3	810.1	4047.0	148.8	312.7	8326.4	293.6	1007.0	5.79	3.8	1.1
Seawater:	SW1	Sep.2009				47700	7.8	24.2			16568.0		2394.3	92.4	352.2	8922.0	322.2	1107.0	6.45	-10	-1.1
	SW2	Sep.2009				39500	7.3	23.2			14484.8		1926.6	107.8	313.2	7214.0	267.9	916.9	5.43	-17	-2.0

~~Hydrochemical and isotopic evidences for deciphering conceptual model of groundwater~~ Delineating multiple salinization processes in a coastal plain aquifer, northern China: hydrochemical and isotopic evidence

Han Dongmei[a,b], Matthew Currell[c]

a Key Laboratory of Water Cycle & Related Land Surface Processes, Institute of Geographic Sciences and Natural Resources Research, Chinese Academy of Sciences, Beijing, 100101, China

b College of Resources and Environment, University of Chinese Academy of Sciences, Beijing 100049, China

c School of Engineering, RMIT University, Melbourne VIC 3000, Australia.

Abstract

Groundwater is ~~the~~ an important water resource for agricultural irrigation, urban ~~and tourism development~~ and industrial utilization in the coastal regions of northern China. In the past five decades, coastal groundwater salinization in the Yang-Dai River ~~coastal~~ plain has become ~~more~~ increasingly serious ~~than ever before~~ under the influence of ~~natural climate change and~~ anthropogenic activities and climatic change. It is pivotal for the scientific management of coastal water resources to accurately understand groundwater salinization processes and ~~its inducement~~their causative factors. Hydrochemical (major ion and trace element) and stable isotopic ($\delta^{18}O$ and $\delta^{2}H$) analysis ~~for~~ of ~~the~~ different water bodies (surface water, groundwater, geothermal water, and seawater) were ~~applied~~ conducted to ~~provide a better~~improve understanding of ~~the processes of~~ groundwater salinization processes in the ~~the~~ plain's Quaternary aquifer~~s~~. Saltwater intrusion due to intensive groundwater pumping is ~~the~~ a major ~~aspect~~ process, ~~and can be caused by~~ either by vertical infiltration along ~~the~~ riverbeds which convey saline surface water inland, ~~at the downstream areas of rivers during the tide/surge period,~~ and/or direct subsurface lateral inflow ~~into fresh aquifer derived from intensively pumping groundwater~~. Trends in salinity with depth indicate that the former may be more important than previously assumed. The ~~Seawater~~ proportion of seawater in groundwater is estimated to have ~~can~~ reached up to ~13% in ~~the~~ shallow groundwater of a local well field. End-member mixing calculations also indicate that h~~H~~ighly mineralized geothermal water (TDS of up to 10.6 g/L) with depleted stable isotope compositions and elevated strontium concentrations (>10 mg/L) ~~with the indicator of paleoseawater relics (lower Cl/Br ratios relative to modern seawater)~~ also locally ~~overflows~~ mixes with water in~~to~~ the ~~cold~~ overlying Quaternary aquifers. This is particularly evident in samples with elevated Sr/Cl ratios (>0.005 mass ratio). ~~Groundwater~~ Deterioration of groundwater quality by salinization ~~can~~ is ~~also be~~ also clearly exacerbated by ~~the~~ anthropogenic ~~activities~~pollution. Nitrate contamination via intrusion of heavily polluted marine water is evident locally (e.g. in the Zaoyuan well field); however, more

widespread nitrate contamination due to other local sources such as ~~(e.g., irrigation return-flow with solution of~~ fertilizers and/or ~~,~~ domestic wastewater– is evident on the basis of NO_3/Cl ratios~~discharge)~~. ~~Additionally, the interaction between surface water and groundwater can make the groundwater freshening or salinizing in different sections to locally modify the groundwater hydrochemistry. The cease of the well field and establishment of anti-tide dam in the Yang River estuary area have effective function to contain the development of saltwater intrusion.~~ This study provides an example of how multiple geochemical indicators can delineate different salinization processes and guide ~~the~~ future water management practices~~,~~ ~~and provide research approaches and foundation for further investigation of seawater intrusion~~ in ~~this~~ a densely populated water-stressed coastal region~~and similar region~~.

Key words: Groundwater salinization; Stable isotopes; Coastal aquifers, Water quality

1. Introduction

Coastal regions ~~is~~ are ~~the~~ key areas for the world's social and economic development. Approximately 40% of the world's population lives~~s~~ within 100 kilometers of the coast (UN Atlas, 2010). ~~The w~~Worldwide, ~~coastal~~ these areas have~~s~~ become increasingly urbanized, with 14 of the world's 17 largest cities located along coasts (Creel~~ L.~~, 2003). China has 18,000 km of continental coastline, ~~about~~ and around 164 million people (~~about~~ approximately 12% of the total ~~Chinese~~ population) living~~e~~ in 14 coastal provinces;~~, and~~ nearly 80% of these people inhabit~~em distribute in the~~ three coastal 'economic zones'~~economic regions~~, namely Beijing-Tianjin-Hebei~~ economic region~~, the Yangtze River delta ~~economic region~~ and the Pearl River delta ~~economic region~~ (Shi, 2012). The rapid economic development and ~~the~~ growing population in these ~~coastal~~ regions have greatly increased demand~~s~~ for fresh water.~~,~~ ~~meanwhile~~ Meanwhile, ~~been~~ they are also confronted with ~~the threat from~~ increased ~~waste and~~ sewage and other wastewater discharge into coastal ~~ecosystems~~environments.

~~Coastal g~~Groundwater resources play crucial roles ~~on~~ in the social, economic and ecologic function ~~in~~ of ~~the~~ global coastal systems (IPCC, 2007). ~~Coastal groundwater~~Coastal aquifers~~ system~~ connect with~~s~~ the ocean and with ~~the~~ continental hydro-ecological systems (Moore, 1996; Ferguson and Gleeson, 2012). ~~Groundwater a~~As an important freshwater resource, groundwater ~~could~~ may be over-~~-~~extracted ~~due to that the~~during periods of high~~est~~ demand, which ~~(e.g., agricultural irrigation and tourist seasons)~~ are often ~~the~~ periods of low~~est~~ recharge and/or surface water availability ~~rates~~ (Post, 2005). ~~In addition to occurrence of some environmental issues, such as land subsidence, contaminants transport, the over~~Over-exploitation of groundwater can therefore ~~readily~~ result in seawater intrusion~~ in the coastal area~~, as well as related environmental issues such as land subsidence. Seawater intrusion has become a global issue and ~~the~~ related studies can be found from ~~the~~ coastal aquifers ~~system of different countries~~around the world, ~~such as~~including Israel (Sivan et al., 2005;Yechieli et al., 2009; Mazi et al., 2014), Spain (Price and Herman, 1991; Pulido-Leboeuf, 2004; Garing et al., 2013), France (Barbecot et al., 2000; de Montety et al., 2008), Italy (Giambastiani et al.~~.~~, 2007; Ghiglieri et al., 2012), Morocco (Bouchaou et al., 2008; El Yaouti et al., 2009), USA (Gingerich and Voss, 2002; Masterson, 2004; Langevin et al., 2010), Australia (Zhang et al., 2004; Narayan et al., 2007; Werner, 2010), China (Xue et al.~~.~~, 2000; Han et al., 2011, 2015), Vietnam (An et al., 2014), Indonesia (Rahmawati et al., 2013), India (Radhakrishna, 2001; Bobba, 2002) and~~,~~ Brazil (Montenegro et al., 2006; Cary et al., 2015)~~, etc. ~~. Werner et al. (2013) ~~gave an excellent~~ provides a comprehensive review ~~on~~ of seawater intrusion processes, investigation and management.

~~A variety of approaches have been used to investigate seawater intrusion, including head measurement, geophysical methods, geochemical methods (environmental tracers combined hydrochemical and isotope data), conceptual and mathematical modeling (see reviews by Jones et al., 1999; Werner et al., 2013).~~

Seawater/saltwater intrusion is a complicated hydrogeological process, due to the impact of aquifer properties, anthropogenic activities (e.g., intensive groundwater pumping, irrigation practices), recharge rates, variable density flow, ~~between the estuary and adjacent fresh groundwater system,~~ tidal~~/surge~~ activity and effects relating to global climate change, such as sea level rise (Ghassemi et al., 1993; Robinson et al., 1998; Smith and Turner, 2001; Simpson and Clement, 2004; Narayan et al., 2007; Werner and Simmons, 2009; Wang et al., 2015). Understanding the complex interactions between groundwater, surface water, and seawater is thus essential for effective management of coastal water resources (Mondal et al., 2010). ~~Brockway et al. (2006) reported the negative relationship between saltwater intrusion length and river discharge. Understanding the complex interactions between groundwater and surface water, groundwater and seawater is essential for the effective management of water resources (Sophocleus, 2002; Mondal et al., 2010). There was a v~~Vastly~~ery~~ different salinization patterns may arise as a result of diverse interactions~~result based on numerical simulations~~ in coastal settings ~~for the additional distance of intrusion in the Nile Delta Aquifer of Egypt and in the Bay of Bengal under the same sea level rise~~ (Sherif and Singh, 1999; Bobba, 2002; Westbrook et al., 2005)~~. Bobba (2002) also employed numerical simulations to demonstrate an apparent risk of saltwater intrusion in the Godavari delta, India due to sea level rise. Westbrook et al. (2005) defined the hyporheic transition zone of mixing between river water and~~

~~groundwater influenced by tidal fluctuations and the contaminant distribution.~~ . ~~Modelling~~Modeling ~~seawater intrusion in the Burdekin Delta irrigation area, North Queensland (Australia)~~has shown that generally, seawater intrusion is ~~far~~ more sensitive to groundwater pumping and recharge rates ~~and recharge than to aquifer properties (e.g., hydraulic conductivity), and compared to the effects of groundwater pumping, the effect~~in comparison to ~~of~~ tidal fluctuation and sea level rise~~s on saltwater intrusion can be neglected~~ (Narayan et al., 2007; Ferguson and Gleeson, 2012). However, most models of seawater intrusion require simplification of the coastal interface zone. Relatively ~~rare~~ few studies have focused on delineating ~~the~~complex interactions among the surface-ground-sea-water continuum~~s~~ in estuarine environments, ~~and~~ including the effects of vertical infiltration of seawater into ~~the off-shore~~ aquifers –through river channels, ~~vs.~~as compared to ~~– the~~ sub-surface lateral landward migration of the freshwater-saltwater interface. Recent data indicate that such processes may be more important in causing historical salinization of coastal groundwater than previously appreciated (e.g. Cary et al., 2015; Lee et al., 2016; Larsen et al., 2017).

Additionally, groundwater in coastal aquifers may be affected by other salinization processes, such as input of anthropogenic contaminants or induced mixing with saline water from deeper or adjacent formations, which may include mineralized geothermal water or brines emplaced in the coastal zone over geologic history.

The data ~~of~~ from China's marine environment bulletin released on March 2015 by the State Oceanic Administration ~~People's Republic of China~~ showed that the major bays, including Bohai Bay, Liaodong Bay and ~~,~~Hangzhou Bay, are ~~polluted~~ seriously polluted, with ~~the~~ inorganic nitrogen and active phosphate being ~~as~~ the major pollutants (SOA, 2015). Seawater intrusion in China is ~~the~~ most serious ~~around~~ in the Circum-Bohai-Sea region (Han et al., 2011~~; Han et al.~~, 2016a); and~~.~~ due to the heavy marine pollution, t~~T~~he ~~escalating~~ impacts of anthropogenic activities on groundwater quality ~~seawater intrusion~~ in ~~the~~ future may ~~be~~ not simply be a case of ~~a simple problem related to groundwater salinization~~ simple salt-water intrusion. This region is also characterized by deep brines and geothermal waters (e.g. Han et al., 2014), which may migrate and mix with fresher groundwater under due to intensive water extraction. Depending on the specific processes involved, additional contaminants may mix with fresh groundwater resources in parallel with seawater intrusion, and ~~in this region.~~ i~~I~~t is thus likely to be more difficult to mitigate and remediate groundwater pollution ~~caused by the contaminated seawater~~.

A variety of approaches can be used to investigate and differentiate seawater intrusion and other salinization processes, including time-series water level and salinity measurements, geophysical methods, conceptual and mathematical modeling as well as geochemical methods (see reviews by Jones et al., 1999; Werner et al., 2013). Geochemical techniques are particularly valuable in areas where the dynamics of saline intrusion are complicated and may involve long-term processes pre-dating accurate water level records, or where multiple salinization processes may be occurring simultaneously. These techniques typically employ the use of major ion ratios such as Cl/Br and Cl/Na, which are indicative of solute origins (Edmunds, 1996; Jones et al., 1999). Other ionic ratios, involving Mg, Ca, Na, HCO_3 and SO_4, and characterization of water 'types' can also be useful in determining the geochemical evolution of coastal groundwater, for example, indicating freshening or salinization, due to commonly associated ion exchange and redox reactions (Anderson et al., 2005; Walraevens, 2007). Trace elements such as strontium, lithium and boron can provide additional valuable information about sources of salinity and mixing between various end-members, as particular waters can have distinctive concentrations (and/or isotopic compositions) of these elements (e.g., Vengosh et al., 1999). Stable isotopes of water ($\delta^{18}O$ and $\delta^{2}H$) are also commonly used in such studies, as they are sensitive indicators of water and salinity sources, allowing seawater to be distinguished from other salt sources (e.g., Currell et al., 2015).

This study ~~will take~~examines the Yang-Dai River coastal plain in Qinhuangdao City, Hebei province ~~of~~, north China, specifically focusing on salinization of fresh groundwater caused by groundwater exploitation in the Zaoyuan well field and surrounding areas.~~,~~ The study ~~as an example to~~ investigates groundwater salinization processes and interactions among surface water, ~~groundwater and~~ seawater and geothermal groundwater~~, and~~ in a dynamic environment, with significant pressure on water resources~~the seawater intrusion caused by groundwater exploitation in Zaoyuan well field~~. Qinhuangdao is an important port and tourist city of northern China. In the past 30 years, many ~~sprevious s~~studies ~~had done to~~have investigated ~~distribution of~~ seawater intrusion and its influencing~~e~~ factors in the region using hydrochemical analysis ~~of groundwater~~ (Xu, 1986; Yang et al., 1994, 2008; Chen and Ma, 2002; Sun and Yang, 2007; Zhang, 2012) and numerical simulations (Han, 1990; Bao, 2005; Zuo, 2009). However, these studies have yet to provide clear resolution of the different mechanisms contributing to salinization, and have typically ignored the role of anthropogenic pollution and groundwater-surface water interaction. This study is thus a continuation of previous investigations of the ~~coastal plain aquifers in Qinhuangdao~~region, using a range of ~~.~~h~~ H~~ydrochemical and stable isotopic ~~compositions of collected water samples were analyzed for~~data to ~~making up the knowledge gap of surface-, ground and sea-water interactions in this region. This study aims to describe the conceptual model of the complex processes for the groundwater~~

~~salinization of the coastal aquifers, to reveal~~delineate the major ~~aspects~~ processes responsible for ~~the~~ increasing groundwater salinity ~~in the coastal aquifers~~, including lateral sub-surface sea-water intrusion, vertical leakage of marine-influenced surface water, induced mixing of saline geothermal water, and anthropogenic pollution. The goal is to ~~and~~ ~~to~~ obtain a more robust conceptual model ~~model for deciphering~~of the interconnections between ~~groundwater~~the various water sources under the impact of groundwater exploitation. ~~flow system of the study area.~~ The results ~~will be helpful for the further numerical simulations of coastal groundwater system. It is~~provide ~~very~~ significant new information ~~for~~ to assist water resources management in the coastal plain of Bohai bay, and other similar coastal areas globally.

2. Study area

The Yang-Dai River coastal plain (Fig. 1) covers approximately 200km^2 ~~in~~ of the west side of Beidaihe District of Qinhuangdao City, ~~the~~ northeastern Hebei Province. It ~~connects the eastern section of~~is surrounded by the Yanshan ~~Mountain~~ Mountains to the north and west, and ~~and surrounded by mountains.~~ t~~T~~he southern boundary of the study area is the Bohai Sea. The plain ~~become low from~~declines in topographic elevation (with an average slope of 0.008) from approximately 390m above sea-level in the northwest to 1-25m in the southeast, forming ~~and~~ a fan-shaped distribution of ~~the~~ incised piedmont- ~~coastal inclined~~ alluvial plain sediments. ~~Elevation ranges from 390 in the west and to 40-100 m in the north, and 25-40 in the east, and 25-1m in the south coastal region, with the average slope of 0.008.~~ Zaoyuan well field, located in the southern edge of the alluvial fan, approximately 4.3km from the Yang River estuary, was built in 1959 (Xu, 1986) as a major water supply for ~~this~~ the region ~~. It is 4.3 km from the southeastern well field to Yang River estuary~~(Fig. 1).

2.1 Climate and hydrology

The study area is in a warm and semi-humid monsoon climate. On the basis of a 56-~~a~~ year record in Qinhuangdao ~~area~~, the mean annual rainfall is ~~estimated to be~~approximately 640 mm, the average annual temperature ~~is about~~approximately 11^{o}C, and mean potential evaporation ~~of~~ 1469 mm. 75% of the total annual rainfall falls in July-September (Zuo, 2006), during the East Asian Summer Monsoon. The average annual tide level is 0.86m (meters above Yellow Sea base level), while the high~~est~~ and low tides ~~is~~ are approximately 2.48m~~,~~ and ~~the lowest is~~ -1.43m.

The Yanghe River and Daihe River, originat~~ed~~ing from the Yanshan Mountains, are the major surface water bodies~~y~~ in the~~is~~ area, flowing southward into the Bohai ~~s~~Sea (Fig. 1). The Yang River is approximately 100 km long with a catchment area of 1029 km^2 and average annual runoff of 1.11×10^8 m^3/a (Han, 1988). Dai River has a length of 35 km and catchment area of 290 km^2, with annual runoff of 0.27×10^8 m^3/a. The rivers become ~~soared~~ full during ~~when heavy~~intense rain events~~s happened with short peak duration~~, ~~whereas it~~ and revert to~~became~~ minimal flow ~~or drying~~ during the dry season – in part this is related to impoundment of flow in upstream reservoirs.~~ The Yang River is about 100 km long with the catchment area of 1029 km^2, and the average annual runoff of 1.11×10^8 m^3/a (Han, 1988). Dai River has the length 35 km and catchment area of 290 km^2, with annual runoff of 0.27×10^8 m^3/a and average gradient of 11.4‰. The two rivers flow into the southern Bohai Sea.~~

2.2 Geological and hydrogeological setting

Groundwater in ~~this~~ the area ~~mainly~~ includes water in Quaternary porous sediment ~~fissure~~ as well as fractured bedrock ~~water in the bedrock and water in the Quaternary porous media. The bedrock fissure water is distributed~~ in the northern platform area. ~~Its water abundance is~~Fractured rock groundwater volume mainly depends~~ed~~ on the degree of weathering and the nature and regularity of fault zones (Fig. 1). The strata outcropping in the west, north and eastern edge of the plain include~~s the~~ Archean ~~gneiss~~, Proterozoic ~~mixed granite and~~ and Jurassic aged metamorphic and igneous rocks, which also underlie the ~~The ex-Quaternary, which is exposed in the offshore area of the region, is mainly the Archean metamorphic granite, which is widely distributed. The mineral composition includes mainly quartz, feldspar, and biotite. The~~ Quaternary sediments of the plain (from which most samples in this study were collected)~~are mostly underlain by the Archean gneisses and Proterozoic mixed granites~~. The basement faults under ~~the~~ Quaternary cover are mainly ~~include the~~ NE-trending ~~fault~~ and ~~the~~ NW-trending (Fig. 1) ~~fault~~;~~. The Quaternary aquifer system of the Yang-Dai River coastal plain is a complete groundwater system from the piedmont to the coast (see P-P' cross-section of Figure 2).~~ these ~~Geological technics~~ structures control the development and ~~deformation~~ thickness of the overlying sediments~~,–~~, as well as the distribution of hot springs and geothermal anomalies. Fault zones are ~~also~~ thought to be the main channel for ~~deep-water cycle and~~transport of thermal ~~convection~~water from deeper to shallower depths.

The Quaternary sediments are widely distributed in the area, with the thickness ranging from approximately 5-80 m (mostly 20-40 m), up to more than 100 m immediately adjacent to the coastline. The bottom of the Holocene (Q_4) unit in most areas ~~has clay or~~consists of clay ~~layers~~, ~~which make~~ making the groundwater in the coastal zone ~~under~~ confined or semi-confined~~ status~~, although ~~. T~~there are no regional, continuous aquitards between several layers of aquifer-forming sediments (Fig. ~~2~~1b~~B~~)~~aquifers. The thickness of the Quaternary strata has a range of 5-80 m, mostly 20-40 m, and up to more than 100 m near the coastline~~. The aquifer is mainly composed of medium sand, coarse sand and gravel layers with ~~thickness of 10-20 m and~~a water table depth of 1-4 m in the phreatic aquifer, and deeper semi-confined groundwater (where present and hydraulically separated from the phreatic aquifer) ~~thickness of 10-30 m and~~ hosted in similar deposits with a ~~water table depth~~ potentiometric surface ~~of~~ 1-5 m below topographic elevation ~~in the confined aquifer~~ (Zuo, 2006).

~~In the yearly peak season of agricultural water, the groundwater level decline sharply and reaches the lowest water table in April-May period, and become highest in January-February. The main sources of aquifer recharge are from rainfall infiltration, river water and irrigation return-flow, lateral subsurface runoff from the piedmont area. Apart from the phreatic water evaporation, groundwater pumping it the main pathway of groundwater discharge for agricultural, industrial, tourism and sanatorium's utilization.~~ The general flow direction of groundwater is from northwest to south, according to the topography. The main sources of recharge are from infiltration of rainfall, river water and irrigation return-flow, as well as lateral subsurface inflow from the piedmont area. Naturally, groundwater discharges into the rivers and the Bohai Sea. Apart from phreatic water evaporation, groundwater pumping for agricultural, industrial and domestic usage (including seasonal tourism) are currently the main pathways of groundwater discharge.

~~The g~~Geothermal water discharges into shallow Quaternary sediments near the fault zones~~, discharges into shallow Quaternary sediments, which is the overlying strata in~~ evident as geothermal ~~anomalous area~~anomalies (Hui, 2009). The temperature of thermal water ~~water~~ ranges ~~is~~ from 27-57~~–~~$^{\circ}$C in this low-to-medium temperature geothermal field (Zeng, 1991). ~~The thickness of the overlying strata is varied from 24.6 to 58.8 m and consists of alluvial sand, gravel, clayey loam, clay and silt. The t~~Deeper thermal water is stored in the Archaeozoic granite and metamorphic rocks~~, which are composed of migmatite, gneiss, and amphibole plagio-gneiss (Pan, 1990).~~; m~~M~~ajor ~~deep~~ fracture zones ~~are the good~~provide pathways ~~passage for the geothermal water movement (Yang, 2011). The heated groundwater in the deep zones could upward transport along the fault and mix with~~into the overlying ~~cold groundwater in the~~ Quaternary ~~aquifers~~ sediments (Pan, 1990; Shen et al., 1993; Yang, 2011).

2.3 ~~Environmental issues~~Groundwater usage and seawater intrusion history

~~The s~~Shallow groundwater pumped from the Quaternary aquifer occupies 94% of ~~the~~ total groundwater exploitation, and is ~~which is~~ used for agricultural irrigation (~~accounts for~~ 52% of ~~the~~ total groundwater use), industrial ~~–~~(32%) and domestic water (16%) (Meng, 2004). Many large and medium-sized reservoirs were built in the 1960s and 1970s ~~and resulted in~~meaning that the surface water was intercepted and ~~the~~ downstream runoff dropped sharply, even ~~became~~ causing rivers to dry up in drought years. With the intensification of human socio-economic activities and growing urbanization, coupled with extended drought years (severe drought during 1976-1989 in north China) (Wilhite,1993; Han et al., 2015), increased groundwater exploitation to meet the ever-growing fresh water demand~~s~~ has resulted in groundwater level ~~declining~~ declines and seawater intrusion (SWI) in the ~~coastal~~ aquifers.

The pumping rate in the Zaoyuan well field ~~was~~ gradually increased from 1.25 million m^3/a in the early 1960s to 3.5 million m^3/a in the late 1970s, and beyond 10 million m^3/a in the 1980s. During 1966-1989, ~~the major agricultural~~ planting ~~in this region is~~of paddy fields became common, ~~with big~~resulting in significant agricultural water consumption. This caused formation of a cone of depression in the Quaternary aquifer system. ~~The g~~Groundwater pumping ~~time is~~ in this region mainly occurs ~~from May to October~~in spring and early summer, ~~–~~with typical pumping rates of ~~of~~ 7~80,000 m^3/d. Pumping from the Zaoyuan well-field occurs in wells approximately 15 to 20m deep. ~~, which was over-exploited and resulted in formation of groundwater level declining depression.~~ Groundwater levels decline sharply and reach their lowest level during May, before the summer rains begin, and recover to their yearly high in January-February (Fig. 2). In May 1986, the groundwater level in the depression center, which is located in Zaoyuan-Jiangying (~~Supplementary~~ Figure S1), ~~was~~ decreased to ~~below~~ -2 ~~–~~m.a.s.l.~~–~~(meters above sea level)~~, with~~and the ~~depression~~ area~~, which has~~ with groundwater levels below ~~the~~ sea level ~~,~~covered 28.2 km^2. The local government commenced reduction in groundwater exploitation in this area after 1992, and groundwater levels began to decrease more slowly after 1995, even showing recovery in some wells. However, during an extreme drought year (1999), increased water demand resulted in renewed groundwater level declines in the region (Fig. ~~3~~2). Since 2000, the groundwater levels have responded seasonally to water demand peaks and recharge (Fig. 2; Fig. S1).

~~Since~~ From 1990, the rapid development of township enterprises ~~in the 1980s~~ (mainly ~~refer to~~ paper mills), also began to cause groundwater over-exploitation in the western area of the plain. ~~(~~The groundwater~~i.e. the groundwater~~ pumping rate for paper mills ~~development~~ reached 55,000 m^3/d in 2002.~~)~~

resulting~~ed~~ in ~~the~~ groundwater level depressions around Liushouying and Fangezhuang (Fig. 1). The ~~lowest~~ groundwater level in the western depression ~~center~~associated with this pumping ~~in 1991 was up to~~reached -11.6 m.a.s.l. in 1991~~,~~ and -17.4 ~~m.a.s.l.~~ in 2002. After the implementation of “Transfering Qing River water to Qinhuangdao” project ~~since~~ in 1992, the intensity of groundwater pumping generally ~~became slowed down~~reduced, and the~~. The depression center moved to Liushouying area. The~~ groundwater level ~~of the~~in the depression center ~~was~~ recovered to -4.3 m.a.s.l. in July 2006.

Overall, the depression area (groundwater levels below mean sea level) was recorded as 132.3km^2 in May 2004 and t~~T~~he shape of the depression ~~was~~ has generally been elliptical with the major axis ~~of the~~aligned E-W~~ direction~~. ~~The depression area developed to 132.3km^2 in May 2004.~~In addition to groundwater over-exploitation, climate change-induced recharge reduction has also likely contributed to groundwater level declines and hence seawater intrusion ~~–~~(Fig. S2). The annual average rainfall declined from 639.7 mm between 1954 - 1979 to 594.2 mm between 1980-2010; a significant decrease over the last 30 years (Zhang, 2012). As indicated in Figure S2, the severity of seawater intrusion (indicated by changes in Cl concentration, and the total area impacted by SWI, as defined by the 250mg/L Cl contour) correlates with periods of below average rainfall – indicated by monthly cumulative rainfall departure (CRD, Weber and Stewart, 2004).

~~The g~~Groundwater quality of the~~is~~ area ~~has become~~ gradually became more salini~~e~~~~zed~~ ~~since~~ from the early 1980s, with~~.~~ c~~C~~hloride concentrations increasing~~ed~~ year by year. As early as 1979, seawater intrusion ~~occurred~~ was recorded in the Zaoyuan well field. The intrusion area with groundwater chlori~~d~~ne concentration greater than 250 mg/L ~~has been developed~~was ~~to~~ 21.8 km^2 in 1984, ~~and~~ 32.4 km^2 in 1991, 52.6 km^2 in 2004 and~~,~~ 57.3 km^2 in 2007 (Zuo, 2006; Zang et al., 2010). The chloride concentration of groundwater pumped from the a monitored well-field well (depth of 18 m, ~~this well field~~G10 in Fig. 1) changed from 90 mg/L in 1963 to~~,~~ 218 mg/L in 1978, 567 mg/L in 1986, 459 mg/L in 1995, and 1367 mg/L in 2002 (Zuo, 2006), reducing to 812 mg/L in July 2007~~ (this study)~~. The distance of estimated seawater intrusion into the inland area from the coastline had reached 6.5 km ~~inland~~ in 1991, and ~~developed to~~ 8.75 km in 2008 (Zang et al., 2010). ~~At~~ In the early 1990s, 16 of 21 pumping wells in the well field ~~have been~~were ~~abundant~~ abandoned due to the salin~~e~~~~ized~~ water quality (Liang et al., 2010). Additionally, 370 of 520 pumping wells were abandoned ~~has been abundant~~ in the wider Yang-Dai River coastal plain during 1982-1991 (Zuo, 2006).

3. Methods

~~Totally~~ In total, 80 water samples were collected from the Yang-Dai River coastal plain, including 58 groundwater samples, 19 river water samples (from 12 sites)~~,~~ and 3 seawater samples, during three sampling campaigns ~~, namely,~~ (June 2008, September 2009 and August 2010). Groundwater samples were pumped from 28 ~~productive~~ production wells with ~~well~~ depths ~~of~~ between 6 and -110m, including 7 deep wells with~~, which has well~~ depths greater ~~more~~ than 60m (Fig. 1). While ideally, sampling for geochemical parameters would be conducted on monitoring wells, due to an absence of these, production wells were utilised. In most cases, the screened interval of these wells encompasses aquifer thicknesses of approximately 5 to 15m above the depths indicated in Table 1.

~~The water sampling sites can be shown in Figure.1.~~ In this study, ~~we~~ sampling ~~investigated~~ focused predominantly on low temperature~~cold~~ groundwater; ~~—from the productive wells. H~~however, ~~the~~ geothermal water ~~existing~~ from around Danihe ~~cannot be ignored~~was also considered a potentially important ongoing source of groundwater salinity. As such, while geothermal water samples were not accessible during our sampling campaigns (as the area is now protected), ~~. The related data can be available and referenced~~data reported by ~~from~~ Zeng (1991) ~~due to that we cannot obtain the hot water samples from the current geothermal field~~were compiled and analyzed in conjunction with the sampled wells.

Measurements of ~~some physical~~physico-chemical parameters (~~i.e.~~ pH, temperature, and electrical conductivity (EC)) were conducted in situ using a portable meter (WTW Multi 3500i). All water samples were filtered ~~to~~ with 0.45-μm membrane filters before ~~collection for~~ analysis of hydrochemical composition. Two aliquots in polyethylene 100mL bottles at each site were collected~~:~~ for major cation and anion analysis, respectively. Samples for cation analysis (Na^+, K^+, Mg^{2+} and Ca^{2+}) were ~~added~~ treated with 6-N HNO_3 to prevent precipitation. Water samples were sealed and stored at 4 °C until ~~determination~~analysis. Bi~~o~~carbonate~~s~~ wa~~ere~~s determined by titration within 12 hours ~~hours after~~of sampling. ~~The c~~Concentrations of cations and some trace elements (~~i.e.~~ B, ~~and~~ Sr, Li) were analyzed by inductively coupled plasma-optical emission spectrometry (ICP-OES) ~~on filtered samples~~ in the chemical laboratory of the Institute of Geographic Sciences and Natural Resources Research (IGSNRR), Chinese Academy Sciences (CAS). Only the Sr data are reported here, as the other trace elements were not relevant to the interpretations discussed (Table 1). The detection limits for analysis of Na^+, K^+, Mg^{2+} and Ca^{2+} are 0.03, 0.05, 0.009, and 0.02 mg/L.

Concentrations of major anions (i.e. Cl^-, SO_4^{2-}, NO_3^- and F^-) were analyzed ~~by a~~using a High Performance Ion Chromatograph (SHIMADZU, LC-10ADvp) at the IGSNRR, CAS. The detection limits for analysis of Cl^-, SO_4^{2-}, NO_3^- and F^- are 0.007, 0.018, 0.016, and 0.006 mg/L. The testing precision the cation and anion analysis is 0.1-5.0%. ~~The ion~~ Charge balance errors ~~of the chemical results~~ were ~~are~~ less than 8%. ~~The hydrochemical and physical data are shown in Table 1. The s~~Stable isotopes ($\delta^{18}O$ and δ^2H) of water samples were measured ~~by~~ using a Finnigan MAT 253 mass spectrometer after on-line pyrolysis with a Thermo Finnigan TC/EA in the Stable Isotope~~s~~ Laboratory of the IGSNRR, CAS. The results are expressed in ‰ relative to international standards (V-SMOW (Vienna Standard Mean Ocean Water)) and ~~of~~ resulting $\delta^{18}O$ and δ^2H values are shown in Table 1~~. were expressed in ‰ relative to international standards (V-SMOW (Vienna Standard Mean Ocean Water))~~. The analytical precision for δ^2H is ±2‰ and for $\delta^{18}O$ is ±0.5‰. All hydrochemical, physico-chemical and isotope data are reported in Table 1.

~~Saturation indices for common minerals (i.e. calcite, dolomite, and gypsum) were calculated using PHREEQC version 2.8 (Parkhurst and Appelo, 1999) to understand the saturation status of these minerals in the aquifer. Ionic delta values were calculated to further investigate the hydrogeochemical behavior that take place in the aquifer and modify groundwater hydrochemistry. The ionic delta values express enrichment or depletion of each ion's concentration relative to its theoretical concentration~~Mixing calculations were also conducted on the basis of ~~calculated from the~~ Cl^- concentrations of the samples under ~~for~~ a conservative freshwater-seawater mixing system (Fidelibus et al., 1993; Appelo, 1994). ~~The delta values have been used as effective indicators of coastal groundwater undergoing freshening or salinizing processes, accompanied by related water-rock interaction (prevailingly cation exchange). Cl⁻ can be regarded as a conservative tracer for the calculations mentioned below.~~ The seawater contribution for each sample ~~can be~~is expressed ~~by~~ as a fraction of seawater (f_{sw}), ~~which can be calculated~~ using (Appelo and Postma, 2005):

$$f_{sw} = \frac{C_{Cl,sam} - C_{Cl,f}}{C_{Cl,sw} - C_{Cl,f}} \qquad (1)$$

where $C_{Cl,sam}$, $C_{Cl,f}$, and $C_{Cl,sw}$ refer to the Cl^- concentration in the sample, freshwater, and seawater, respectively. ~~Based on the f_{sw} value, the theoretical concentration ($C_{i,mix}$) of each ion in a water sample can be calculated by:~~

$$\cancel{C_{i,mix} = f_{sw} \cdot C_{i,sw} + (1 - f_{sw}) \cdot C_{i,f}} \qquad \cancel{(2)}$$

~~$C_{i,sw}$, and $C_{i,f}$ refer to the measured concentration of the ion i in the seawater and freshwater, respectively. The ionic delta value (ΔC_i) of ion i can be obtained by:~~

$$\cancel{\Delta C_i = C_{i,sam} - C_{i,mix}} \qquad \cancel{(3)}$$

~~$C_{i,sam}$ – the measured concentration of the ion i in the water sample.~~

4. Results

~~4.1 Groundwater dynamics~~

~~Due to the different groundwater pumping rate and patterns, the variation trend of groundwater level has been different in the east and west areas of the Yang-Dai River coastal plain. In the east part, owing to the intensive exploitation in the Zaoyuan well field, the groundwater level was gradually declined to be lower than the sea level during the 1980s. The center of groundwater level depression was located in Zaoyuan-Jiangying region, with the groundwater level lower than -3 m.a.s.l. The local government commenced to reduce the exploitation after 1992. The groundwater level decreased slowly after 1995, even started to recovery in some wells as a result of pumping reduction. During the extreme drought year (1999), the consequential increased water demand made the groundwater level declined again in the east region. In the late 1980s, the groundwater level at the west region was still more than 0 m.a.s.l. But in the late 1990s, due to the fast development of the local paper mills as the big water consumers, the groundwater level dropped year by year and had big falling amplitude after 2000, resulting in the overall transfer of groundwater depression center to the western region (Liushouying-Fangezhuang). The groundwater level in this center was up to -14 m.a.s.l. in May 2002.~~

~~Based on the data from the three monitoring wells, the seasonal variation of groundwater level in this area can be seen from Figure 3. After 2000, the groundwater level in the east of the Yang-Dai River coastal plain was mainly affected by the groundwater pumping for agricultural and domestic water use. During March and June of each year, the shallow groundwater pumping as the major water source for irrigation has resulted in the fast dropped water level occurred between April and June, down to the lowest level of water throughout the year. As the rainy season started in July, groundwater pumping began to decrease. Groundwater level rise rapidly with the infiltration of irrigation return-flow and rainfall, lateral subsurface runoff from the surrounding aquifers. After the end of the rainy season (July to September), the water level continues to rise gently and reach the annual maximum water level during January and February. With the~~

~~amount of recharge is reduced along with the increase of domestic water pumping, water level circularly slow down to the next agricultural peak. In addition to groundwater over-exploitation, climate change-induced recharge reduction in recent three decades has been also part of the cause of groundwater level declining, resulting in the seawater intrusion. The annual average rainfall varied from 639.7 mm (1954 - 1979) to 594.2 mm (1980-2010). It obviously finds that there is a significant decrease in rainfall over the last 30 years (Zhang, 2012). In general, the groundwater runoff intensity gradually decreases from the piedmont to the coastal region.~~

4.~~2~~ 1 Water stable isotopes (δ^2H and $\delta^{18}O$)

The local meteoric water line (LMWL, δ^2H=6.6 $\delta^{18}O$+0.3, n=64, r^2=0.88) is based on δ^2H and $\delta^{18}O$ mean monthly rainfall values between 1985 and 2003 from Tianjin station some 120 km SW of Qinhuangdao City (IAEA/WMO, 2006). Due to similar climate and position relative to the coast, this can be regarded as representative of the study area. ~~19 w~~Surface water samples collected from Yang River and Dai River (n = 19) have $\delta^{18}O$ and δ^2H values ranging from -10.1 to -0.6‰ (mean= -5.4‰) and ~~from~~ -71 to -11‰ (mean = -43‰), respectively. ~~It seems that the s~~Stable isotope~~s~~ compositions for surface water appear to exhibit~~have~~ significant seasonal variation (Fig. S3);~~.~~ f~~F~~or Yang River~~, 3 surface water~~ samples from~~d in~~ the relatively dry season (June 2008, n = 3) ~~were characterized by~~had mean $\delta^{18}O$ and δ^2H values ~~ranging from -5.5 to -1.1‰ (mean=~~of -3.0‰~~)~~ ~~and from -49~-15‰ (mean =~~ -31‰~~)~~, respectively; ~~. Whereas 6 water samples s~~sample~~d~~s ~~in~~ from the wet season (August 2009 and September 2010, n = 6) had mean~~ve~~ $\delta^{18}O$ and δ^2H values ~~ranging from -10.1 to -2.4‰ (mean=~~of -6.6‰~~)~~ ~~and from -71~-21‰ (mean =~~ -48~~‰),~~ ‰, respectively. ~~As to~~ Dai River~~,~~ samples showed similar results; the dry season mean ~~in dry season, 3 surface water samples are characterized by~~ $\delta^{18}O$ and δ^2H values (n = 3) ~~ranging from -3.9 to -0.6‰ (mean=~~were -2.6‰~~)~~ and ~~from -44~-11‰ (mean =~~ -32‰~~)~~, respectively; ~~and in~~ wet season samples (n = 7), ~~7 surface water samples have~~ had mean $\delta^{18}O$ and δ^2H values ~~ranging from -9.7 to -1.2‰ (mean=~~of -6.6‰~~)~~ and ~~from -69~-12‰ (mean =~~ -49‰~~)~~, respectively (Fig. ~~4~~3).

~~The water samples collected from Yang River and Dai River have similar stable isotopes composition.~~

The 56 groundwater samples ~~are~~ were characterized by $\delta^{18}O$ and δ^2H values ranging from -11.0 to -4.2‰ (mean= -6.5‰) and ~~from~~ -76 to -39‰ (mean = -50‰), respectively. Among ~~them~~these, shallow and deep groundwater samples showed similar mean values, although deep groundwater samples (n = 13) showed relatively narrow overall ranges (~~43 shallow groundwater samples have $\delta^{18}O$ and δ^2H values~~

~~ranging from -11.0 to -4.2‰ (mean = -6.6‰) and from -76~-39‰ (mean = -50‰), respectively; 13 deep groundwaters have δ^{18}O and δ^{2}H values ranging from~~ -7.8 to -5.1‰ and (mean = -6.3‰ ~~)~~for δ^{18}O; ~~and from~~ -58 to -43‰ and (mean = -50‰ for δ^{2}H; Fig. 43~~), respectively~~). Slight seasonal variation was evident in the groundwater isotope compositions; ~~For the~~ shallow groundwater from~~, during~~ the dry season (n = ~~,~~12) ~~water samples have~~showed δ^{18}O and δ^{2}H values ~~ranging~~ from -7.2 to -4.2‰ (mean = -5.7‰) and δ^{2}H values from ~~from~~ -56 to -39‰ (mean = -48‰)~~, respectively~~; while during the wet season (n =~~,~~ 31) ~~water samples are featured by~~ δ^{18}O and δ^{2}H values ranged~~with a range of~~ from -11.0 ~ -5.3‰ (mean = -6.9‰) and -76 ~ -43‰ (mean = -51‰), respectively. Some variability was also evident in deep groundwater compositions, although only three deep samples were collected during the dry season.~~For the deep groundwater, during the dry season, 3 water samples have δ^{18}O and δ^{2}H values ranging from -5.3 to -5.1‰ (mean = -5.2‰) and from -47~-45‰ (mean = -46‰), respectively; during the wet season, 10 water samples are featured by δ^{18}O and δ^{2}H values with a range of -7.8 ~ -5.2‰ (mean = -6.6‰) and -58 ~ -43‰ (mean = -51‰), respectively.~~

~~The local meteoric water line (LMWL, δ^{2}H=6.6 δ^{18}O+0.3, n=64, r^2=0.88) is based on δ^{2}H and δ^{18}O mean values of the monthly rainfall between 1985 and 2003 at Tianjin station some 120 km SW of Qinhuangdao City. The data were obtained from International Atomic Energy Agency/World Meteorological Organization (IAEA/WMO, 2006). Due to the similar climatic and coastal conditions between Tianjin and Qinhuangdao, this meteoric water line can be regarded as the local meteoric water line (LMWL) in this study.~~ From Figure 43, it can be seen that surface water ~~have~~ exhibits a much ~~more~~ wider range of δ^{18}O and δ^{2}H values relative to groundwater, with shallow groundwater in turn more spatially variable than deep groundwater. Water samples collected in the wet season ~~have~~ showed ~~more~~ wider ranges of δ^{18}O and δ^{2}H values relative to ~~water sampled in~~the dry season. Most ~~of~~ water ~~samples~~ samples of all types plot to the right of (below) the LMWL, with some surface water samples showing similar compositions to the local seawater (Fig. 43). T~~.~~he local s~~S~~eawater plots below (more negative) than typically assumed values (e.g. VSMOW = 0‰) for both δ^{2}H and δ^{18}O, and this water appears to represent~~s~~ an~~n~~ end-member involved in mixing with meteoric-derived waters in both ground and surface water (Fig. 43)~~ enriched in isotopes and plots far below the LMWL~~.

4.~~3~~ 2 Water salinity and ~~major~~ dissolved ions

TDS (total dissolved solids) concentrations of ~~the~~ surface water samples from Dai River ~~have a~~ range from ~~of~~ 0.3g/L~31.4g/L with ~~22-78%~~ Na$^+$ and~~,~~ Ca^{2+} comprising 22-78% and 4-56~~-4~~% ~~Ca^{2+}~~ of total cations and ~~36-91%~~ Cl$^-$ comprising 36-91% of total anions. The composition changes from~~,~~ Ca•Na•Mg-Cl•HCO$_3$ to Na-Cl water type from ~~the~~ upstream ~~-~~to ~~-the~~ downstream locations along with increasing salinity; Cl$^-$ concentrations vary from approximately 70 mg/L upstream to 16700 mg/L near the coastline, due to marine influence. ~~The Cl$^-$ concentrations varied from about 70 mg/L in the upstream to 16700 mg/L near the coastline.~~ Similar variation occurs along the ~~For~~ Yang River, ~~the collected water~~where samples ha~~v~~de TDS concentrations ~~of~~ between 0.3-26.1 g/L with increasing ~~percentages~~ concentrations and proportions ~~(33-91%)~~ of Cl$^-$ ~~concentrations~~ (63.2-14953.5 mg/L) from ~~the~~ up~~-reach~~ stream to ~~the~~ down~~-reach~~stream locations~~, with water types changed from Ca•Na-HCO$_3$•Cl•SO$_4$, Ca•Mg-Cl•SO$_4$•HCO$_3$ to Na-Cl~~. ~~The n~~Nitrate ~~contents~~ concentrations also range from 2.8 to 65.2 mg/L in the surface water samples, increasing downstream.

~~Groundwater hydrochemistry can be modified the comprehensive effects from geological, climatic, hydrogeological processes and anthropogenic activities.~~ In the early 1960s, groundwater pumped from the Zaoyuan well field ~~was featured by the~~exhibited Ca-HCO$_3$ water type and chloride concentrations of 90-130 mg/L; this was followed by rapid salinization since the 1980s (see section 2.3). ~~In the early 1970s, individual wells appear slightly salinized. It has been deteriorated rapidly since the early 1980s. The chloride concentration of groundwater from water supply wells was 90mg/L in 1963, 218 mg/L in 1975, 385 mg/L in 1984, 456.3 mg/L in 1986, 459.5 mg/L in 1995, 928.3 mg/L in 2000, 1367 mg/L in 2002, and 1290.4 mg/L in 2005 (Zang et al., 2010).~~ In this study, ~~the~~ shallow groundwater is characterized by TDS concentrations of 0.4-4.8 g/L with ~~the percentage of~~ Cl$^-$ (34-77%), Na$^+$ (12-85%) and~~,~~ Ca^{2+} (5-69%) being the predominant major anion and cations, respectively. ~~and water~~Groundwater hydrochemical types ~~varied~~ vary from Ca-HCO$_3$•Cl, Ca•Na-Cl, Na•Ca-Cl to Na-Cl~~, which can been seen from Piper plot~~ (Figure ~~5~~4). ~~The d~~Deep groundwater ~~is featured by~~has TDS concentrations ~~of~~ between 0.3-2.8g/L, ~~which is~~ dominated by Ca (up to 77% of major cations) in the upstream area and Na (up to 85% or major cations) near the coast, with water type ~~distributed in series of~~evolving from Ca-Cl•HCO$_3$ to~~,~~ Ca•Na-Cl and Na•Mg-Cl (Figure ~~5~~4). At present, t~~T~~he TDS of groundwater from the well field reaches 3.31 g/L with Na-Cl water type ~~in the~~(see well G15). ~~The relative high fracture~~The highest observed~~-~~ mixing proportions of seawater occur~~s~~ in ~~the~~ shallow well G10 and deep well G2, respectively, with calculated *fsw* values (according to equation 1) of 12.95% and 5.35%, respectively.

Hydrochemical features of thermal water from the Danihe-Luwangzhuang area (Fig. 1A) are distinct from the normal/low temperature groundwater. Previous work by Zeng (1991) and Hui (2009) identified geothermal water with high TDS in the fractures of deep metamorphic rock. The geothermal water was characterized by TDS values between 6.2-10.6 g/L and Ca•Na-Cl water type, while Cl^- concentrations ranged from 5.4 to 6.5 g/L and Sr concentrations from 6.73 to 89.8 mg/L. Some normal/low temperature groundwater samples collected in this study from wells G8, G19, and G9 featured by Ca•Na-Cl water type with relative high TDS ranges (0.8-1.4 g/L, 1.3-1.6 g/L, and1.5-2.8 g/L, respectively) and strontium concentrations (1.1-1.9 mg/L, 4.9-7.1 mg/L, and 7.3-11.6 mg/L, respectively), showing similarity with the geothermal system. Low temperature groundwater sampled in this study had Sr/Cl mass ratios ranging from 2.4 ×~~x~~ 10^{-4} to 1.6 ×~~x~~ 10^{-2}, with higher ratios in deep groundwater (range: 9.4 ×~~x~~ 10^{-4} to 1.3 ×~~x~~ 10^{-2}, median: 3.7 ×~~x~~ 10^{-3}) compared to shallow groundwater (median: 3.1 ×~~x~~ 10^{-3}), and groundwater generally higher than seawater/saline surface water (range: 3.7 ~~x~~× 10^{-4} to 5.8 ×~~x~~ 10^{-4}, median: 3.9 ×~~x~~ 10^{-4}; Table S1).

~~The nitrate~~Nitrate ~~contents~~ concentrations in groundwater ~~have a~~ range ~~of~~ from 2.0-178.5 mg/L (mean 90.1 mg/L) for shallow groundwater, and 2.0-952.1 mg/L (mean 232.1 mg/L) for the deep groundwater, respectively, with most ~~of which~~samples ~~seriously~~ exceedings the WHO drinking water standard (50 mg/L).

~~There is a geothermal field around Danihe-Luwangzhuang area (Fig. 1). Hydrochemical features of thermal water Aare very distinct from cold water. The previous investigation has identified the buried geothermal water with high TDS in the fracture/fissure of deep metamorphic rock (Zeng, 1991). Due to the pumping wells for pumping thermal water were protected and not permitted to be sampled, we have to collect some data associated this geothermal field from the previous research. The geothermal field is controlled by the fault distribution under confined state. The thermal water flows along the fault zone and enters the Quaternary aquifer, forming hot salt water distributed around the spill point and expanded towards downstream. It can result in the similar hydrochemical characteristics between Quaternary salt groundwater and deep original thermal waters from bedrocks. The geothermal water is characterized by Ca•Na-Cl water type, 6.2-10.6 g/L of TDS and 7.4-8.7 of pH values.~~ ~~Cl^- concentrations range from 5.4 to 6.5 g/L, Na^+ from 1.7 to 2.0 g/L, Ca^{2+} from 1.6 to 1.9 g/L, F^- from 3.0 to 3.6 mg/L, Sr from 6.73 to 89.8 mg/L, Li from 0.43 to 1.58 mg/L, and SiO_2 from 44.0 to 48.3 mg/L (Hui, 2009). The groundwater samples, collected from the wells G8, G19, and G9 with different depths, are featured by Ca•Na-Cl water type with relative high TDS ranges (0.8-1.4 g/L, 1.3-1.6 g/L, and1.5-2.8 g/L, respectively) and Sr contents (1.1-1.9 mg/L, 4.9-7.1 mg/L, and 7.3-11.6 mg/L, respectively).~~

5. Discussion~~s~~

5.1 Groundwater ~~flow system~~isotopes and ~~hydrochemical features~~hydrochemistry as indicators of mixing processes

~~Generally,~~The Quaternary groundwater system in the Yang-Dai River coastal plain ~~is~~ may be recharged by precipitation, irrigation return flow, river infiltration and lateral subsurface runoff (e.g. from mountain-front regions). ~~Due to the natural geological function and human pumping activities, there have been interactions between groundwater and geothermal waters around Danihe area or between groundwater and seawater in the coastal area. The g~~Groundwater geochemical ~~features~~ characteristics are then controlled by ~~the complex~~ hydrogeological conditions and ~~these hydrological~~mixing processes, including mixing induced by extensive groundwater pumping, as well as natural mixing and water-rock interaction. It is evident from the geochemistry that mixing has occurred between groundwater and seawater in the coastal areas, as well as between normal/low temperature groundwater and geothermal water in the inland areas (e.g. near the Danihe geothermal field). ~~The d~~Different sources of water ~~bodies~~ are generally characterized by somewhat distinctive~~different~~ ~~of~~ stable isotopic and hydrochemical compositions~~,~~, allowing mixing calculations to aid understanding of ~~determining~~ the groundwater salinization and mixing processes, as discussed below~~ in this area~~.

~~The s~~Stable isotopes of O and H in groundwater and surface water ~~can be used to describe the groundwater origin and to identify the mixing processes between different water bodies. The~~fall on a best-fit regression line ~~slope of the best-fit regression line for collected groundwater samples~~ (dashed line in Fig. ~~4~~3) ~~given as~~ with slope of $\delta^2H=4.4\times\delta^{18}O-21.7$, ~~which is~~ significantly lower than either the local or global meteoric water lines. Three processes are likely responsible for the observed range of isotopic compositions: 1. Mixing between saline surface water (e.g. seawater or saline river water affected by tidal ingress) and fresher, meteoric-derived groundwater or surface water; 2. Mixing between fresh meteoric-derived groundwater and saline thermal water; 3. Evaporative enrichment of surface water and/or irrigation return-flow, which may ~~The deviation of groundwater and surface water lines from the LMWL has evidenced evaporative processes occurred during water~~ infiltrate~~ion~~ groundwater in some areas~~ and surface runoff~~. A sub-group of surface water samples (e.g., S1 to S3, S7 and S12; termed 'brackish surface water') show marine-like stable isotopic compositions and major ion compositions (Fig. ~~4~~3 and Fig. 5). The 'fresh' surface water samples (e.g. EC values <1500 µS/cm) exhibit meteoric-like stable isotope compositions, with some samples (such as S9 and S10) showing clear evidence of evaporative enrichment in the form of higher δ^2H and particularly, $\delta^{18}O$ values (Fig. ~~4~~3).

Fresh groundwater has depleted $\delta^{18}O$ and δ^2H values relative to seawater and show a clear meteoric origin, albeit with modification due to mixing. Theoretically, the mixing of meteoric-derived fresh groundwater and marine water should result in a straight mixing line connecting the two end members; however this is also complicated in the study area by the possible mixing with geothermal water. The thermal groundwater has distinctive stable isotopic and major ion composition (Han, 1988; Zeng, 1991), allowing these mixing processes to be partly delineated. Stable isotopes of thermal groundwater are more depleted than low-temperature groundwater (e.g. $\delta^{18}O$ values of approximately -8‰, Fig. 8), indicating this likely originates in the mountainous areas to the north; Zeng (1991) estimated the elevation of the recharge area for the geothermal field to be from 1200 to 1500 m.a.s.l. Based on a bivariate plot of $\delta^{18}O$ vs. Cl^- with mixing lines and defined fresh and saline end-members, Fig. ~~6~~5 shows the estimated degree of mixing between fresh groundwater including shallow (G4) and deep (G25) groundwater end-members, and saline water, including seawater and geothermal end-members.

The two fresh end-members were selected to represent a range of different groundwater compositions/recharge sources, from shallow water that is impacted by infiltration of partially evaporated recharge (fresh but with enriched $\delta^{18}O$) to deeper groundwater unaffected by such enrichment (fresh and with relatively depleted $\delta^{18}O$). The narrower range and relatively enriched stable isotopes in shallow groundwater samples collected during the dry season compared with the wet season indicate some influence of seasonal recharge by either rainfall (fresh, with relatively depleted stable isotopes) or irrigation water subject to evaporative enrichment (more saline, with enriched stable isotopes and high nitrate concentrations; Currell et al., 2010) and/or surface water leakage. While there is overlap in the isotopic and hydrochemical compositions of shallow and deep groundwater (Fig. 3 & Fig. 4), this effect appears to only affect the shallow aquifer.~~34~~

Based on Fig. 5, the shallow groundwater samples (e.g. G15, G10, G11, G14) collected from or around the Zaoyuan well field appear to be characterized by mixing between fresh meteoric water and seawater (plotting in the upper part of Fig. ~~6~~5); while some deeper groundwater samples (e.g. G13, G2, G16, G14) collected from the coastal zone also appearing to indicate mixing with seawater. Groundwater sampled relatively close to the geothermal field (e.g. G9, G19) shows compositions consistent with mixing between low-temperature fresh water and saline thermal water (lower part of Fig. 5). This is more evident in deep groundwater than shallow groundwater, which is consistent with mixing from below, as expected for the deep-source geothermal water. Other samples impacted by salinization show more ambiguous compositions between the various mixing lines, which may arise due to mixing with either seawater, geothermal water or a combination of both (e.g., G29).

The estimated mixing fraction (f_{sw}) of marine water for the shallow brackish groundwater ranges from 1.2~13.0% and 2.6~6.0% for the deep brackish groundwater. The highest fraction of 13% was recorded in G10, located in the northerm part of the Zaoyuan well field, which is located near a tidally-impacted tributary of the Yang River (Fig 1). Relatively higher fractions of marine water in relatively shallow samples (including those from the well field) compared to deeper samples may indicate a more 'top down' salinization process, related to leakage of saline surface water through the riverbed, rather than 'classic' lateral sea water intrusion, which typically causes salinization at deeper levels due to migration of a salt water 'wedge' (e.g. Werner et al., 2013); this is consistent with results of resistivity surveys conducted in the region (Fig. 6). –The profile of chloride concentrations vs. depth indicates that salinization affects shallow and deep samples alike, with the most saline samples being relatively shallow wells in the Zaoy~~y~~uan well-field (Fig. ~~7~~7). ~~The composition of stable isotopes in groundwater samples collected in the relatively dry season has been narrower and enricher than that collected in the wet season. It could be resulted from evaporation processes during the infiltration of local irrigation return-flows in the dry season.~~

~~The composition of stable isotopes for thermal groundwater could be originated from precipitation, however, its ^{14}C age dating between 3.4-12.8ka with tritium content of less than 2 TU (Zeng, 1991), indicating thermal waters might be formed under cooler climate condition than present climate. The composition of stable isotopes of thermal groundwater are more depleted than that of cold groundwater, even lower than the cold groundwater from mountain-front area, indicating the thermal groundwater could be mainly originated from NW mountain area, where has higher elevation. The elevation range of recharge area for Danihe geothermal field is from 1200 to 1500 m.a.s.l obtained by Zeng (1991).~~

In general, brackish and fresh groundwater samples show distinctive major ion compositions, with the more saline water typically showing higher proportions of Na and Cl (Fig. ~~5~~4). This contrasts with historic data collected from the Zaoyuan well field, which showed Ca-HCO_3 type water with Cl concentrations ranging from 130 to 170 mg/L. This provides additional evidence that the salinization in this area is largely due to marine water mixing. More Ca-dominated compositions are evident in the region near the geothermal well field further in-land (e.g., G5, G8, G19, G29, and G24); consistent with a component of salinization that is unrelated to marine water intrusion. Plots of ionic ratios of Na/Cl and Mg/Ca vs. Cl also reveal a sub-set of relatively saline deep groundwater samples which appear to evolve towards the geothermal-type signatures with increasing salinity (Fig. ~~8~~8).

Stronger evidence of mixing of the geothermal water in the Quaternary aquifers (particularly deep groundwater) is provided by examining strontium concentrations in conjunction with chloride (Fig. ~~9~~9). The geothermal water from Danihe geothermal field has much higher Sr concentrations (up to 89.8 mg/L) than seawater (5.4-6.5 mg/L in this study), due to Sr-bearing minerals (i.e., celestite, strontianite) with Sr contents of 300-2000 mg/kg present in the bedrock (Hebei Geology Survey, 1987). Groundwater sampled from near the geothermal field in this study has the highest Sr concentrations e.g., G9 with Sr concentrations ranging from 7.4 to 11.6 mg/L, and G19 from 4.9 to 7.1 mg/L.

The plot of chloride versus strontium concentrations (Fig. ~~9~~9) shows that these samples and others (e.g., G16, G20, G27, G29) plot close to a mixing line between fresh low-temperature and saline thermal-groundwater. Mass ratios of Sr/Cl in these samples are also elevated relative to seawater by an order of magnitude or more (e.g. Sr/Cl >5.0 ×~~x~~ 10^{-3}, compared to 3.9 ×~~x~~ 10^{-4} in seawater, Table S1). Other samples from closer to the coast (e.g. G4) also approach the thermal-low temperature mixing line, indicating probable input of thermal water. Samples collected from the Zaoyuan well field generally plot closer to the Sr/Cl seawater mixing line (consistent with salinization largely due to marine water – Fig. ~~8~~9); however, samples mostly plot slightly above the mixing line with additional Sr, which may indicate more widespread (but volumetrically minor) mixing with the thermal water in addition to seawater.

5.2 Anthropogenic pollution of groundwater

The occurrence of high nitrate (and possibly also sulfate) concentrations in groundwater in both coastal and in-land areas also indicates that anthropogenic pollution is an important process impacting groundwater quality and salinity (Fig. ~~10~~10; Table 1). ~~Fresh groundwater has depleted δ^{18}O and δ^{2}H values relative to seawater. Theoretically, the mixing of fresh groundwater and seawater should show a straight line connecting the two end members. Obviously, some surface water samples (e.g. S1, S2, S3, S7, S12) are the mixture with seawater. In this study area, there are three end members (namely, fresh groundwater, thermal groundwater and seawater), which has been evidenced by the previous studies (Han, 1988; Zeng, 1991). Thus, the diagram of δ^{18}O vs. Cl^- (Fig. 6) can be used to identify the mixing pattern among three end members. Fig. 6 shows the mixing lines between shallow fresh groundwater (G4) and seawater, between deep fresh groundwater (G25) and seawater, between shallow fresh groundwater and thermal water, and~~

~~between deep fresh groundwater and thermal water. The shallow groundwater samples (e.g. G15, G10, G11, G14) collected from or around the Zaoyuan well field are characterized by mixing with seawater. The deep groundwater samples (e.g. G13, G2, G16, G14') collected from the coastal zone are also resulted from mixing with seawater. The sampling site of deep groundwater sample G29 is located between thermal field and the coastline and obviously affected by both of mixing processes. The groundwaters (e.g. G9, G19), sampled from the area affected by geothermal field are mixture between fresh cold groundwater with thermal waters. The mixing fraction (f_{sw}) of seawater has a range of 1.2~13.0% for the shallow brackish groundwater, and 2.6~6.0% for the deep brackish groundwater. f_{sw} reaches the highest percentage of 13% in the well G10, which is located in the north part of the well field.~~

~~At the late 1950s, groundwater pumped from the Zaoyuan well field was characterized by Ca-HCO_3 type water with Cl concentrations ranging from 130 to 170 mg/L. The hydrochemical data investigated in 1986 (Han, 1986) showed that there were mainly five water types in this study area, including Ca-HCO_3 type with TDS less than 0.5g/L distributed in the mountain-front area, Ca•Na-Cl•SO_4, Ca•Na•Mg-SO_4•Cl, or Na•Ca-Cl•SO_4 type water with TDS 0.4-0.7g/L distributed around the Zaoyuan well field and Wanggezhuang, Ca•Na-Cl type water with TDS 0.4-1.8g/L distributed around the geothermal field (Luwangzhuang) and Duzhai, Na-HCO_3 or Na-HCO_3•Cl type water with TDS 0.5-0.9g/L distributed the SW area close to the coastal zone, and Cl-Na type water with TDS 0.4-2.4g/L distributed in the coastal zone. Due to the disturbance of human activities, the current groundwater hydrochemitry has become more complex than that before. Compared salty water distributed 2 km away from coastline in the late 1950s, the distance has increased to about 7 km away from coastline. The Cl-Ca•Na or Cl-Ca type water type mainly distributed in the area affected by geothermal field, such as G5, G8, G19, G29, and G24, indicating the salinizing process during the mixing between cold groundwater and the thermal waters. In the upstream area, the groundwater samples (e.g. G7, G23, G25) have feature of Ca•Mg•Na-Cl•SO_4, Ca-Cl•SO_4, and Ca-Cl•HCO_3 type, not the Ca-HCO_3 type in the 1980s. It suggests that the salinized composition has resulted from the anthropogenic pollution. The groundwater samples (e.g. G10, G11, G15, G26) collected from the well field show the feature of Cl-Na• (Ca) type water with TDS 1.2-4.8 g/L. The samples (e.g. G1, G2, G3, G4, G12, G22, G14, G14') collected from the coastal zone show the water type of Na-Cl or Na•Ca-Cl•SO_4 or Ca•Na•Mg-Cl•SO_4, indicating that, apart from seawater intrusion, the anthropogenic pollution also plays important role on modifying the groundwater chemistry.~~

~~The s~~Seawater from Bohai Sea ~~has~~ is heavily affected by nutrient contamination, showing ~~relatively~~

~~higher~~ NO_3^- concentrations of ~~(~~810 mg/L in this study, and up to 1092 mg/L in ~~the coastal~~ seawater further north of the bay near ~~of~~ Dalian (~~,~~Han et al., 2015~~5~~), primarily due to wastewater discharge into the sea. The historic sampled NO_3^- concentration of groundwater in the well field increased from 5.4 mg/L in May 1985 to 146.8~339.4 mg/L in Aug 2010, while the concentration ~~of~~ in seawater ~~in this area~~ changed from 57.4 mg/L in May1985 to 810.1 mg/L in Aug 2010. ~~The diagram~~A bivariate plot ~~(Fig. 7)~~ of Cl^- vs. NO_3^- concentrations ~~of~~ in groundwater (Fig. ~~10~~10) can thus –be used to identify nitrate sources and ~~the different~~ mixing trends ~~in this study area~~, including ~~the mixing process with~~infiltration with contaminated seawater, ~~and~~ and other on-land ~~the~~ anthropogenic NO_3-sources (e.g. domestic/industrial wastewater discharge and/or~~,~~ NO_3^--bearing fertilizer input through ~~precipitation infiltration and the~~ irrigation return-flow)~~ in the inland area~~.

~~It can be seen f~~From ~~Fig. 7~~this plot (Fig. ~~9~~10) it appears that ~~that~~ the major source of NO_3^- in groundwater is ~~from~~ on-land anthropogenic inputs rather than mixing with seawater, which would result in relatively large increases in Cl along with NO_3. ~~, with the exception of~~Samples G10 and G15 (from the well field) are exceptions to this trend, ~~mixing~~ showing clear mixing with nitrate-contaminated seawater ~~in the well field~~. ~~The d~~Deep groundwater (e.g. G9, G14~~'~~) is also extensively contaminated ~~by~~ with high~~er~~ NO_3^- concentrations; ~~,~~ this ~~which~~ is likely associated with leakage from the surface via~~the~~ poorly constructed or abandoned wells - a problem of growing significance in China (see Han et al., 2016b; Currell and Han, 2017). According to one investigation by Zang et al.(2010), 14 of 21 pumping wells in the Zaoyuan well field have been abandoned due to ~~the salinized~~poor water quality, and 307 pumping irrigation wells (occupied 2/3 of total pumping wells for irrigation) in the region have also been abandoned. ~~However, the l~~Local ~~department~~ authorities have~~s~~ however not ~~made any~~implemented measures to deal with ~~those~~ abandoned wells, meaning they are a future legacy contamination risk – e.g. by allowing surface runoff impacted by nitrate contamination to infiltrate down well annuli.

5.~~2~~ 3 ~~Groundwater salinization processes~~Hydrochemical evolution during salinization

A hydrogeochemical facies evolution diagram (HFE-D) proposed by Giménez-Forcada (2010), was used to analyze the geochemical evolution of groundwater during seawater intrusion and/or freshening phases (Fig. 1~~1~~1). In the coastal zone, the river water shows an obvious mixing trend between fresh and saline end members. Some shallow groundwaters (e.g., G2, G4, G10, G13, G15) are also close to the mixing line between the surface-water end-members on this figure, indicating mixing with seawater without significant additional modification by typical water-rock interaction processes (e.g. ion exchange). Most brackish groundwaters (e.g., G11, G16, G17, G20, G25, G28, G29) have evolved in the series Ca-HCO_3 → Ca-Cl→ Na-Cl, according to classic seawater intrusion. A relative depletion in Na (shown in lower than marine Na/Cl ratios) and enrichment in Ca (shown as enriched Ca/SO_4 ratios) is evident in groundwater with intermediate salinities (e.g. Fig. ~~8~~8; Fig. 1~~0~~1), indicating classic base-exchange between Na and Ca during salinization (Appelo and Postma, 2005). Locally, certain brackish water samples (e.g., G1, G12, G26) appear to plot in the 'freshening' part of the HFE diagram (potentially indicating slowing or reversal of salinisation due to reduce~~d~~ in groundwater use), although these do not follow a conclusive trajectory. Water samples from the geothermal field (G5, G8, G9, and G19) plot in a particular corner of the HFE diagram away from other samples (being particularly Ca-rich); a result of their distinctive geochemical evolution during deep transport through the basement rocks at high temperatures.~~–~~

~~***5.2.1 Development of seawater intrusion and associated hydrochemical behavior***~~

~~The intensively pumping groundwater from the Quaternary aquifer of Yang-Dai River coastal plain has resulted in the development of groundwater depression cones from Zaoyuan well field to Fangezhuang, with the aggravation of seawater intrusion in this region. In the 1950s, the seawater intrusion in the study area was only occurred within 2 km distance from the coastline, and it expanded to over 5 km distance in the 1980s. In 1986, the groundwater depression cone centered in the Zaoyuan well field was characterized by 6 meters depths below the sea level, with the water level -3 m.a.s.l. The enclosed area by 0 m.a.s.l water level contours covered 10 km^2. The original Ca-HCO_3 type water changed to Ca•Na-Cl type. Apart from the intensive exploitation fresh groundwater from coastal aquifer, the successive drought (1976-1989) also played important roles on controlling the groundwater recharge and exacerbating seawater intrusion in the coastal area of north China (Wilhite, 1993; Han et al., 2015). In this study area, the annual mean precipitation was 668.7 mm during 1954-1995, the Cl concentrations was ranging from 130 to 170 mg/L in the Zaoyuan well field. Whereas the annual mean precipitation reduced to 559.7 mm during 1996-2011, resulting in Cl concentration in the well field up to 550 mg/L in May 1986, and 812 mg/L in July 2006. It has seriously threatened the safety of water supply in this region. The seawater intrusion in the coastal aquifer shows the wedge-shaped body and has vertically characterized by freshwater in the upper part and salt water in the lower part of shallow aquifer. Since 2002, with the establishment of anti-tide dam in the Yang River estuary area, it has good effect on preventing the horizontal pouring seawater into riverway.~~

~~Thus, the seawater intrusion is mainly caused by lateral inflow of seawater in the aquifer.~~

~~According to the guidelines of drinking water standards from China Environmental Protection Authority (GB 5749-2006) or US EPA or WHO, the guideline of chloride concentration for drinking water is 250 mg/L. Most groundwater distributed in the seawater intrusion area cannot be used for irrigation, the source of drinking water and industrial utilization. It has enhanced the scarcity of fresh water resources in this region by vicious cycle of groundwater level decline → seawater intrusion → groundwater salinization → groundwater level decline again. This will also influence the surface water runoff. How to judge the criterion of seawater intrusion? Generally, 250 mg Cl/L can be regarded as the intruded standard, and more than 1000 mg Cl/L as the serious intrusion (Jiang and Li, 1997; Zhuang et al., 1999). Some studies took the TDS (>1000 mg/L) as the intruded standard (e.g., Xue et al., 1997; Zhang and Peng, 1998). Water type can also be used as the intruded standard, such as Ca-Cl type water occurs during seawater intrusion into freshwater aquifers, and Na-HCO_3 type water displays during flushing of the mixing zone by freshwater (Appleo and Postma, 1993). Additionally, the multi-hydrochemical ionic ratios can also provide important confirmation of hydrogeochemical processes modifying groundwater chemistry during seawater intrusion (Vengosh et al., 1997; Jones et al., 1999). However, the frequent anthropogenic activities modified coastal hydrologic dynamics and hydrogeochemical characteristics to great extent. For instance, with except of modern seawater, the sources of chloride in groundwater system could be derived from paleoseawater relics in aquifers, infiltration of agricultural return flow with fertilizer solutions, and discharge of industrial and domestic wastewater.~~

~~Hydrogeochemical facies evolution diagram (HFE-D) proposed by Giménez-Forcada (2010) can be used to analyze the phase of seawater intrusion or freshening and its dynamics. From Fig. 8, it can be seen that most brackish groundwaters (e.g., G11, G16, G17, G20, G25, G28, G29) have evolved in the series of Ca-HCO_3 → Ca-Cl → Na-Cl facies under the intrusion period. Locally, several water samples (e.g., G1, G12, G26) collected from the interfluve area have been characterized by freshening process. Deep groundwater G11 sampled from the well field shows being under salinizing period in the relatively dry season, and under freshening period in the relatively wet season. In the coastal zone, the river water has obvious mixing trend between end members. Some shallow groundwaters (e.g., G2, G4, G10, G13, G15) are close to the mixing line between end members on this figure, indicating significant mixing with seawater. The groundwaters (G10, G11, G15, G26) collected from the productive wells of the Zaoyuan well field display the different processes occurring in salinizing or freshening stages, indicating that the~~

~~heterogeneous hydrogeological conditions could be responsible for this distinguished patterns.~~

~~The calculated results of saturated indices (Fig. 9) show that that SI_{cal} and SI_{dol} have some deviation from equilibrium (-0.4 to +0.5 for SI_{cal}, and -0.5 to +0.5 for SI_{dol}). The distribution of SI_{cal} and SI_{dol} is related to the sampling period. In the wet season, most of water samples are characterized by SI_{cal} <0 and SI_{dol} <0, suggesting they are under unsaturated for these minerals, while in the dry season, most of water samples are under saturated with respect to these minerals. In contrast, all sampled groundwater had negative saturation indices with respect to gypsum (SI_{gyp}<0), indicating that these water samples are under-saturated with respect to gypsum. The plots (Fig. 10 a-f) of ionic molar ratios (Na/Cl, SO_4/Cl, Mg/Ca, Ca/(SO_4+HCO_3), Ca/SO_4, and (Ca+Mg)/Cl) can be used to further reveal the groundwater salinized processes and dominated hydrochemical behavior. The brackish groundwaters in this study area have an enriched Ca^{2+} (i.e., the ratio of Ca/(HCO_3+SO_4)>1 with low ratios of Na/Cl and SO_4/Cl as the seawater proportion in the mixture increases. As shown in Fig. 10a, Na/Cl ratios of brackish groundwater affected by seawater intrusion are usually lower than the ratio (0.86) of modern seawater. The high Na/Cl ratios (>1) could be typical of anthropogenic sources (i.e., domestic waste waters). When seawater intrudes into coastal freshwater aquifers, Ca^{2+} on the clay-bearing sediments can be replaced by Na^+:~~

$$\cancel{2Na^{+} + Ca\text{-}X_2 \rightarrow 2Na\text{-}X + Ca^{2+}}$$

~~This process can decrease the Na/Cl ratios and increase the (Ca+Mg)/Cl ratios. The dolomitization process can be described by the transformation reaction (Appelo and Postma, 2005):~~

$$\cancel{2CaCO_3 + Mg^{2+} = CaMg(CO_3)_2 + Ca^{2+}}$$

~~It can result in Ca-enrichment over Mg in solution and that Mg/Ca ratios decreases. This process may also be characterized by Ca-Cl water type.~~

~~To explain the enrichment in Ca^{2+} relative to SO_4^{2-} concentrations, observed in most water samples (Fig. 10e), gypsum dissolution (SI_{gyp}<0) can be coupled by cation exchange reactions under the interaction with clay stratum and calcite precipitation with incongruent dissolution of dolomite and gypsum. Additionally, due to the ORP values ranging from 3 to 74 mV for 18 of 22 water samples collected in August 2010, the sulfate reduction under anaerobic conditions may be responsible for relatively high Ca/SO_4 and low SO_4/Cl ratios. Generally, low Na/Cl, SO_4/Cl and high Ca/(HCO_3+SO_4) (>1) ratios are further indicator of the arrival of seawater intrusion.~~

~~ΔNa is negative in most samples of this area (Fig. 11a and Fig. 12a). The depletion of Na^+ could be caused by the inverse cation exchange taken place with the clay sediments. This exchange produces Ca~~

~~release to the solution during the seawater intrusion. The positive ΔCa and ΔMg may be due to the dissolution of calcite, dolomite and gypsum present in the aquifer strata. Water flushing during aquifer recharge can result in positive ΔNa and negative ΔCa and/or ΔMg (Fig. 11a). For some water samples, the Ca enrichment is not accompanied by Na depletion, which could be caused by dolomitization (Ca enrichment with Mg depletion) (Fig. 12b). The excess of SO_4 compared to conservative mixing (Fig. 11d) can be explained by redissolution of the precipitated gypsum along the mixing front.~~

~~*5.2.2 Mixing between thermal and cold groundwater*~~

~~Sea level rose by about 100 m since the end of the last glacial period (18,000 years, 18 ka BP) and stabilized around 5 ka BP in the eastern China (Yang, 1996). The marine sediments could not be found in the geothermal field, indicating the transgression in the geologic history did not occur around Danihe area (Zeng, 1991). However, the fracture and structural fissure developed well in this study area became the major subsurface pathway of seawater intrusion. The previous studies have revealed that the geothermal waters in this area are characterized by the features of residual seawater and modern precipitation (Zeng, 1991; Hui, 2009). The results of ^{14}C age dating for the geothermal waters in this area are ranging from 3.4 ka to 12.8 ka with lower tritium contents (less than 2TU) (Zeng, 1991). The Piper plot (Fig. 5) shows CaNa-Cl type water for the geothermal waters. It is noteworthy that the geothermal water from Danihe geothermal field has higher Sr concentrations (up to 89.8 mg/L) relative to that in seawater (5.4-6.5 mg/L in this study), due to the Sr-bearing minerals (i.e., celestite, strontianite) with Sr contents of 300-2000 mg/kg present in the bedrock (Hebei Geology Survey, 1987). The mixture waters sampled from the geothermal field in this study also have the higher Sr concentrations relative to seawater, i.e., G9 with Sr concentrations ranging from 7.4 to 11.6 mg/L, and G19 from 4.9 to 7.1 mg/L. The diagram of chloride versus strontium concentrations of different water samples (Fig. 13) shows that the groundwater samples (e.g., G9, G19) collected from the geothermal field have obviously been characterized by closing to mixing line between fresh cold- and thermal-groundwater. Some waters (G16, G20, G29) sampled from the downstream area also close to this mixing line, indicating the thermal water overflows into the coastal aquifers in different depths. The water samples collected from the well field are located between two mixing lines (Fig. 13), suggesting the groundwater in the well field simultaneously suffered from the mixing with thermal water and obvious seawater intrusion. Additionally, the points of water samples (G5, G8, G9, and G19), collected from the geothermal field, mainly occurs on the HFE-D (Fig. 8) in the *12* (MixCa-Cl) and *16* (Ca-Cl) facies zones, indicating these waters have been modified by the reverse base-exchange reactions.~~

~~As both Cl and Br are not affected by water-rock interactions and usually behave conservatively, the Cl/Br ratio can be used as a reliable tracer to study the processes of evaporation and salinization of water (Edmunds, 1996; Jones et al., 1999). Standard seawater (Cl/Br molar ratio=650.8) may be distinguished from relics of evaporated seawater (normally less than 669.3), input of evaporite dissolution (more than 2256) and anthropogenic pollution (e.g., sewage effluents, Cl/Br ratios up to 1805; Vengosh and Pankratov, 1998) or agricultural return-flows with low Cl/Br ratios (Jones et al., 1999). It can be seen from Fig. 14 that the points of the thermal waters lie lower than the ratio line of standard seawater, indicating that they are affected by mixing with relics of evaporated seawater. The points of cold groundwaters (G9, G19) sampled from the geothermal field display between the seawater and the thermal waters, indicating these cold waters are mixture between cold groundwater and the thermal water, which has relics of evaporated seawater. However, it cannot exclude adding the Br inputs into groundwater system through the pesticides application of the pronounced agricultural activity (Davis et al., 1998), this effect could lower the Cl/Br ratios of the groundwaters. The groundwater sample G10 in the well field shows the feature of high Cl/Br ratio in Fig. 14, indicating obvious anthropogenic inputs (e.g., discharge domestic wastewater) occurring in the shallow aquifers around the well field.~~

~~***5.2.3 Interaction between surface- and ground-water***~~

~~Coastal zones encompass the complex interaction among different waters (i.e., river water, seawater, groundwater, rainfall water). The interaction between surface- and ground-water in the Yang-Dai River coastal plain is usually ignored by the previous studies. However, understanding how surface water interacts with the groundwater is essential for managing freshwater resources. Groundwater depression cone below the sea level has formed in the early 1980s. Due to the irrigation supported by transfer of surface water from the upper and middle stream of Yang-Dai River, the amount of surface water discharged into the Bohai Sea declined to great extent. Under the tide effects, seawater can be poured into the estuary of the downstream section of the rivers, resulting in the river bed filled with saltwater, which can cause mixing between river water and seawater. The results of water chemistry analysis from two river sections show that the distribution of salt water reached more than 10 km above the estuary of the Yang River, and about 4 km above the estuary of the Dai River (Han, 1988). It leaded to that the seawater simultaneously intruded into the coastal aquifers through not only the lateral subsurface flow from coastline to the inland but also vertical infiltration from the riverbed to both sides of the river. The hazard caused by the latter pattern had been more serious than the former pattern, before the establishment of anti-tide dam at the~~

~~estuary of Yang River. Currently, the seawater-intruded distance towards inland has been controlled within 4 km away from the coastline.~~

~~The stable isotope compositions of different water samples (Fig. 4) display that the points of most surface water samples are deviated from the LMWL to the right, indicating that these waters are likely to be subject to evaporation to different degrees. The points of surface water samples (S1, S2, S3, and S7) in Fig.4 close to the compositions of local seawater, indicating the pronounced mixing process with seawater for these surface waters. However, the samples S2, S6, S8, and S9 have the depleted compositions of stable isotopes, probably resulting from the exchange between them and local groundwater. S12, located at the estuary area, has variable compositions due to the sampling seasons. HFE-D shows that most of surface water samples are close to the mixing line between end members (freshwater and seawater). S9 is significantly characterized by salinization process probably due to the interaction with ambient groundwater. It can be seen from the relationship between ionic delta values and seawater proportions for the water samples (Fig. 11) that G1, G11, G12, G14', G26, G29, due to these wells close to the river or located at the flat interfluve, may be dominated by the obvious freshening process. While G2, G3, and G16 under the salinizing process could be subject to the vertical infiltration of saltwater in the river. The points of surface waters (S1, S2, S3, and S7) on Fig. 4 and Fig. 8 are distributed along the mixing line between fresh- and sea-water end members. It is due to the direct mixture occurs in the riverway. S12 sampled from the Dai River estuary may be contaminated by the wastewater discharge with higher Sr concentration relative to seawater. By contrast, surface water from the Dai River have higher seawater proportions compared with that from Yang River, owing to that the local government did not establish anti-tide dam in the Dai River estuary. G1, G2, G3, G10 and G13 collected from coastal zone are obviously mixed with seawater with closing to the mixing line between seawater and freshwater in Fig. 13.~~

5.~~3~~4 Conceptual model of ~~groundwater flow patterns~~salinization and management implications

~~Generally, groundwater in this study area is mainly originated from precipitation, river infiltration, lateral subsurface runoff, upflow of geothermal waters and seawater intrusion in the coastal area. The associated hydrological processes driven by the natural (hydrologic, geologic, climatic) changes and anthropogenic activities have resulted in groundwater salinization processes, along with the complex hydrogeochemical characteristics of groundwater system. Groundwater changes from Ca-HCO_3 type water in the piedmont area to the Na-Cl type water in the coastal area.~~

Coastal zones encompass the complex interaction among different water bodies (i.e., river water, seawater and groundwater). The interactions between surface- and ground-water in the Yang-Dai River coastal plain have generally been ignored in previous studies. However, the surface water chemistry data show that the distribution of salt water has historically reached more than 10 km inland along the estuary of the Yang River, and approximately 4 km inland in the Dai River (Han, 1988). The relatively higher proportion of seawater-intrusion derived salinity in shallow samples in this study, along with the evidence from resistivity surveys (Fig. ~~X~~6; Zuo, 2006) indicate that intrusion by vertical leakage from these estuaries is therefore an important process. The hazard associated with this pathway in recent times has been reduced by the construction of a tidal dam, which now restricts seawater ingress along the Yang estuary to within 4 km of the coastline. This may alleviate salinization to an extent in future in the shallow aquifer by removing one of the salinization pathways, however, as described, there are multiple other salinization processes impacting the groundwater in the Quaternary aquifers of the region.

A conceptual model of the groundwater flow system in the Yang-Dai River coastal plain ~~can be~~is summarized in Fig. ~~15~~1~~2~~2. This model presents an advance on the previous understanding of the study area, by delineating f~~F~~our ~~subsurface~~ major processes responsible for groundwater salinization in this area. These are: 1. ~~, including s~~Seawater intrusion by lateral sub-surface flow; 2. Interaction between saline surface water and groundwater (e.g. vertical leakage of saline water from the river estuaries); 3. ~~, return-flow of agricultural irrigation, m~~Mixing ~~with~~ between low-temperature groundwater and deep geothermal water; and, 4. Irrigation return-flow and associated anthropogenic contamination ~~interaction between surface water and groundwater/seawater, could be responsible for the groundwater salinization in this area~~. Both the lateral and vertical intrusion of saline water are driven by the long-term over-pumping of groundwater from fresh aquifers in the region. The ~~Two aspects of seawater intrusion, identified by depleted ΔNa and enriched ΔCa with Ca-Cl type water and Ca/(HCO_3+SO_4)>1 and lower Na/Cl and SO_4/Cl relative to these ratios of seawater, can be delineated, namely vertical infiltration of saltwater inflow towards the inland estuary and lateral inflow of seawater driven by over-pumping groundwater from fresh aquifers. i~~Irrigation return-flow from local ~~groundwater~~ agriculture ~~can~~ results from over-irrigation of crops, and is responsible for ~~cause groundwater~~extensive nitrate pollution (up to 340 mg/L NO_3^- in groundwater of this area) ~~due to the infiltration and~~ probably due to dissolution of fertilizers during infiltration. The somewhat enriched stable isotopes in shallow groundwater (more pronounced in the dry season) also indicate that such return-flow may recharge water impacted by evaporative salinization into the aquifer. The ge~~Ge~~othermal water, with distinctive chemical composition (e.g. depleted stable isotopes, high TDS, Ca~~, F,~~ and Sr concentrations), is also demonstrated in this study to be a significant contributor to groundwater salinization, via upward mixing. The study area is therefore in a situation of unusual vulnerability, in the sense that it faces salinization threats simultaneously from lateral, downward and upward migration of saline water bodies.

According to drinking water standards and guidelines from China Environmental Protection Authority (GB 5749-2006) and/or US EPA and WHO, chloride concentration in drinking water should not exceed 250 mg/L. At the salinity levels observed in this study - many samples impacted by salinization contain >500mg/L of chloride (Table 1) - a large amount of groundwater is now or will soon be unsuitable for domestic usage, as well as irrigation or industrial utilization. So far, this has enhanced the scarcity of fresh water resources in this region, leading to a cycle of groundwater level decline → seawater intrusion → loss of available freshwater → increased pumping of remaining fresh water. If this cycle continues, it is likely to further degrade groundwater quality and restrict its usage in the future. Such a situation is typical of the coastal water resources 'squeeze' highlighted by Michael et al., (2017). Alternative management strategies, such as restricting water usage in particular high-use sectors, such as agriculture, industry or tourism, that are based on a comprehensive assessment of the social, economic and environmental benefits and costs of these activities, warrants urgent and careful consideration.

~~flows into the Quaternary aquifers, mixing with cold groundwater, and transports to the downstream area of Yang River Basin. Additionally, the interaction between surface- and ground-water can cause seasonal flushing local groundwater in the upstream interfluve or lead to saltwater infiltration affected by tide/surge along the riverbed at the estuary.~~

6. Conclusions

~~It has been recognized that g~~Groundwater in the Quaternary aquifers of the Yang-Dai River coastal plain is ~~the~~ an important water resource for agricultural irrigation, ~~urban and~~domestic use (including for tourism) ~~tourism development~~ and industrial ~~utilization~~activity. ~~Natural climate change (e.g., continuous drought, overflow of geothermal water) and~~ Extensive groundwater utilization ~~human activities have~~has made the problem of groundwater salinization in this area increasingly prominent, ~~even~~ resulting in the closure of ~~the Zaoyuan well field~~wells in the area. Based on the analysis of hydrochemical and stable isotopic compositions of different water bodies, ~~including surface water, cold groundwater, geothermal water, and seawater,~~ we delineated the key ~~groundwater flow system and~~ groundwater salinization processes. Seawater intrusion is the main ~~aspect~~ process responsible for ~~the groundwater~~ salinization in the coastal ~~zone,~~zone; however this likely includes~~ing the~~ vertical saltwater infiltration along the riverbed into aquifers~~, which is affected by the tide/surge process, and~~ as well as ~~the~~ lateral seawater intrusion caused by pumping for fresh groundwater at the Zaoyuan wellfield. The ~~overflow~~ upward mixing of ~~the~~ highly mineralized thermal water into the Quaternary aquifers ~~along the fault zone mixes with the cold groundwater and makes it salinized~~is also evident, particularly through the use of stable isotope, chloride and strontium end-member mixing analysis. Additionally, significant ~~The thermal water has characterized by lower Cl/Br ratios and higher Sr concentrations relative to seawater. It cannot be ignored that the salinization or~~ nitrate pollution from the anthropogenic activities (e.g., agricultural irrigation return-flow with dissolution of fertilizers) and locally, intrusion of heavily polluted seawater, are also evident. ~~Additionally, the interaction between surface- and ground-water can also affect the groundwater salinization in this area. Different approaches of hydrochemical analysis, such as Piper plot, HFE-D, major ionic ratios (Na/Cl, SO_4/Cl, Ca/SO_4, (Ca+Mg)/Cl, Ca/(SO_4+HCO_3), Cl/Br) and Sr, were used in this study to identify the different hydrogeochemical reactions and freshening or salinizing processes in the Quaternary aquifers.~~

Groundwater salinization has become a prominent water environment problem in the coastal areas of northern China (Han et al., 2014; Han et al., 2015; Han et al., 2016a), ~~which has caused the~~and threatens to create further paucity of fresh water resources, which may prove a significant impediment to further social and economic ~~and has become the bottleneck of urban~~ development in these regions ~~to a certain extent~~. Since the 1990s, the local government has begun to pay attention to the ~~development~~ problem of seawater intrusion, and ~~the~~ irrational exploitation of groundwater has been restricted in some cases. The Zaoyuan well field ~~has~~ ceased to pump groundwater since 2007, while an~~. The~~ anti-tide dam (designed to protect against tidal surge events) ~~has been~~ established in the Yang River estuary ~~area in 2002,~~may also reduce saline intrusion ~~effectively intercepting the seawater pouring into riverway during the tide/surge period~~in future. However, due to the significant lag-time associated with groundwater systems, a response in terms of water quality may take time to emerge, and in the meantime the other salinization and pollution impacts documented here may continue to threaten water quality~~ These actions have made the rate of intrusion slowed down~~. ~~The joint use of surface water and groundwater with reasonable exploitation program is essential and economical for the local water resources management.~~In this regard, we recommend ~~However,~~

~~the quantitative understanding to the vertical and lateral saltwater intrusion into fresh aquifers~~continued monitoring of groundwater quality and levels, and active programs to reduce input of anthropogenic contaminants such as nitrate from fertilizers, and appropriate well-construction and decommissioning protocols to prevent contamination through preferential pathways.

~~should be obtained from further continuous groundwater monitoring and numerical groundwater flow and transport modeling. This study would be benefit the local agricultural development and groundwater resources management.~~

Acknowledgement

This research was supported by Zhu Kezhen Outstanding Young Scholars Program in the Institute of Geographic Sciences and Natural Resources Research, Chinese Academy of Sciences (CAS) (grant number 2015RC102), and Outstanding member program of the Youth Innovation Promotion Association, CAS (grant number 2012040). The authors appreciate the helpful field work and data collection made by Mr Yang Jilong from Tianjin Institute of Geology and Mineral Resources, Dr. Wang Peng and Dr Liu Xin from Chinese Academy of Sciences.

References

An T.D., Tsujimura M., Phu V.L., Kawachi A., Ha D.T., 2014. Chemical Characteristics of Surface Water and Groundwater in Coastal Watershed, Mekong Delta, Vietnam. The 4th International Conference on Sustainable Future for Human Security, SustaiN 2013. Procedia Environmental Sciences. 20:712-721.

Andersen, M.S., Jakobsen, V.N.R., Postma, D. 2005. Geochemical processes and solute transport at the seawater/freshwater interface of a sandy aquifer. Geochimica et Cosmochimica Acta. 69(16): 3979-3994.

Appelo C. A. J., Postma D., 1993. Geochemistry, Groundwater and Pollution, first edition. A. A. Balkema, Brookfield, Vt.

Appelo C.A.J., 1994. Cation and proton exchange, pH variations, and carbonate reactions in a freshening aquifer. Water Resour. Res., 30, 2793-2805.

Appelo C.A.J., Postma D., 2005. Geochemistry, Groundwater and Pollution, second edition. Taylor & Francis Group.

Bao J., 2005. Two-dimensional numerical modeling of seawater intrusion in Qinhuangdao Region. Master's Thesis. Tongji University, Shanghai, China. (Chinese with English abstract)

Barbecot F., Marlin C., Gibert E., Dever L., 2000. Hydrochemical and isotopic characterisation of the Bathonian and Bajocian coastal aquifer of the Caen area (northern France). Applied Geochemistry. 15:791-805.

Bobba A.G., 2002. Numerical modelling of salt-water intrusion due to human activities and sea-level change in the Godavari Delta, India. Hydrological Sciences. 47(S), S67-S80.

Bobba A.G., 2002. Numerical modelling of salt-water intrusion due to human activities and sea-level change in the Godavari Delta, India. Hydrological Sciences. 47(S), S67-S80.

Bouchaou L., Michelot J.L., Vengosh A., Hsissou Y., Qurtobi M., Gaye C.B., Bullen T.D., Zuppi G.M., 2008. Application of multiple isotopic and geochemical tracers for investigation of recharge, salinization, and residence time of water in the Souss–Massa aquifer, southwest of Morocco. Journal of Hydrology. 352: 267-287.

Brockway R., Bowers D., Hoguane A., Dove V., Vassele V., 2006. A note on salt intrusion in funnel-shaped estuaries: Application to the Incomati estuary, Mozambique. Estuarine, Coastal and Shelf Science. 66:1-5.

Cary L., Petelet-Giraud E., Bertrand G., Kloppmann W., Aquilina L., Martins V., Hirata R., Montenegro S., Pauwels H., Chatton E., Franzen M., Aurouet A., the Team. Origins and processes of groundwater salinization in the urban coastal aquifers of Recife (Pernambuco, Brazil): A multi-isotope approach. Science of the Total Environment. 530-531:411-429.

Chen M., Ma F., 2002. Groundwater resources and the environment in China. Seismological Press. Beijing. pp255-281. (in Chinese)

Craig, H., 1961. Standard for reporting concentration of deuterium and oxygen-18 in natural water. Science 133, 1833–1834.

Creel L., 2003. Ripple effects: Population and coastal regions. Population Reference Bureau. pp1-7.< http://www.prb.org/Publications/Reports/2003/RippleEffectsPopulationandCoastalRegions.aspx>

Currell M.J., Cartwright, I., Bradley, D.C., Han, D.M., 2010. Recharge history and controls on groundwater quality in the Yuncheng Basin, north China. Journal of Hydrology. 385: 216-229.

Currell M.J., Dahlhaus P.D., Ii H. 2015. Stable isotopes as indicators of water and salinity sources in a southeast Australian coastal wetland: identifying relict marine water, and implications for future change. Hydrogeology Journal. 23: 235-248.

Currell M.J., Han D. 2017. The Global Drain: Why China's water pollution problems should matter to the rest of the world. Environment: Science and Policy for Sustainable Development. 59(1): 16-29.

de Montety V., Radakovitch O., Vallet-Coulomb C., Blavoux B., Hermitte D., Valles V., 2008. Origin of groundwater salinity and hydrogeochemical processes in a confined coastal aquifer: Case of the Rhône delta (Southern France). Applied Geochemistry. 23: 2337-2349.

Edmunds W. M., 1996. Bromine geochemistry of British groundwaters. Mineral. Mag., 60, 275–284.

El Yaouti F., El Mandour A., Khattach D., Benavente J., Kaufmann O., 2009. Salinization processes in the unconfined aquifer of Bou-Areg (NE Morocco): A geostatistical, geochemical, and tomographic study. Applied Geochemistry. 24:16-31.

Ferguson G., Gleeson T., 2012. Vulnerability of coastal aquifers to groundwater use and climate change. Nature Climate Change. 2, 342-345.

Fidelibus M.D., Giménez E., Morell I., Tulipano L., 1993. Salinization processes in the Castellon Plain aquifer (Spain). In: Custodio, E., Galofré, A. (Eds.), Study and Modelling of Saltwater Intrusion into Aquifers. Centro Internacional de Métodos Numéricos en Ingeniería, Barcelona, pp267-283.

Garing C., Luquot L., Pezard P.A., Gouze P., 2013. Geochemical investigations of saltwater intrusion into the coastal carbonate aquifer of Mallorca, Spain. Applied Geochemistry. 39:1-10.

Ghassemi F., Chen T.H., Jakeman A.J., Jacobson G., 1993. Two and three-dimensional simulation of seawater intrusion: performances of the "SUTRA" and "HST3D" models. AGSO J. Aust.Geol.Geophys. 14(2-3):219-226.

Ghiglieri G., Carletti A., Pittalis D., 2012. Analysis of salinization processes in the coastal carbonate aquifer of Porto Torres (NW Sardinia, Italy). Journal of Hydrology. 432-433:43-51.

Giambastiani B.M.S., Antonellini M., Oude Essink G.H.P., Stuurman R.J., 2007. Saltwater intrusion in the unconfined coastal aquifer of Ravenna (Italy): A numerical model. Journal of Hydrology. 340:91-104.

Giménez-Forcada E., 2010. Dynamic of sea water interface using hydrochemical facies evolution diagram, Ground Water. 48, 212-216.

Gingerich S., Voss C., 2002. Three-dimensional variable-density flow simulation of a coastal aquifer in southern Oahu, Hawaii, USA, in Proceedings SWIM17 Delft 2002, edited by R. Boekelman, pp.93-103, Delft Univ. of Technol., Delft, Netherlands.

Han D.M., Kohfahl C., Song X.F., Xiao G.Q., Yang J.L., 2011. Geochemical and isotopic evidence for palaeo-seawater intrusion into the south coast aquifer of Laizhou Bay, China. Applied Geochemistry, 26(5):863-883.

Han D.M., Song, X.F., Currell, M.J., Yang, J.L., Xiao G.Q. 2014. Chemical and isotopic constraints on the evolution of groundwater salinization in the coastal plain aquifer of Laizhou Bay, China. Journal of Hydrology 508: 12-27.

Han D., Post V.E.A., Song X., 2015. Groundwater salinization processes and reversibility of seawater intrusion in coastal carbonate aquifers. Journal of Hydrology. 531:1067-1080.

Han, D., Song, X., Currell, M. 2016a Identification of anthropogenic and natural inputs of sulfate into a karstic coastal groundwater system in northeast China: evidence from major ions, $\delta^{13}C_{DIC}$ and $\delta^{34}S_{SO4}$. Hydrology and Earth System Sciences 20(5): 1983-1999.

Han, D., Currell, M.J., Cao, G. 2016b. Deep challenges for China's war on water pollution. Environmental Pollution. 218: 1222-1233.

Han Z., 1988. Seawater intrusion into coastal porous aquifer- a case study of the alluvial plain of Yang River and Dai River in Qinhuangdao City. China University of Geosciences, Beijing, China. (Chinese with English abstract)

Han Z., 1990. Controlling and harnessing of the seawater intrusion the alluvial plain of Yang River and Dai River in Qinhuangdao.Geoscience (Journal of Graduate School, China University of Geosciences). 4(2):140-151. (Chinese with English abstract)

Hebei Geology Survey, 1987. Report of regional geological and tetonic background in Hebei Province. Internal materials.

Hui G., 2009. Characteristics and formation mechanism of hydrochemistry of geothermal water in Danihe, Funing District of Qinhuangdao region. Science & Technology Informaion. 9:762-763. (in Chinese)

IAEA/WMO, 2006. Global Network of Isotopes in Precipitation. The GNIP Database, Vienna. <http://www-naweb.iaea.org/napc/ih/IHS_resources_gnip.html>.

IPCC, Climate Change 2007: The Physical Science Basis, Contribution of Working Group I to the Fourth Assessment Report of the Intergovernmental Panel on Climate Change, S. Solomon et al., Eds. (Cambridge Univ. Press, Cambridge, 2007).

Jiang A., Li D., 1997. Characteristics of shallow groundwater hydrochemistry modified by saltwater intrusion in the south coast plain of Laizhou Bay. Acta Oceanologica Sinica.19(4):142-147. (in Chinese)

Jones B.F., Vengosh A., Rosenthal E. Yechieli Y., 1999. Geochemical investigations. In: Bear et al. (eds) Seawater Intrusion in Coastal Aquifers - Concepts, Methods and Practices, pp51-72.

Langevin C.D., Zygnerski M.R., White J.T., Hughes J.D., 2010. Effect of sea-level rise on future coastal groundwater resources in southern Florida, USA. SWIM21-21st Salt Water Intrusion Meeting. Azores, Portugal., June 21-26, 2010. Pp125-128.

Larsen, F., Tran, L.V., Hoang, H.V., Tran, L.T., Chistiansen, A.V., Pham, N.Q., 2017. Groundwater salinity influenced by Holocene seawater trapped in the incised valleys in the Red River delta plain. Nature Geoscience 10: 376-382.

Lee, S., Currell, M., Cendon, D.I., 2016. Marine water from mid-Holocene sea level highstand trapped in a coastal aquifer: Evidence from groundwater isotopes, and environmental significance. Science of the Total Environment. 544: 995-1007

Masterson J.P., 2004. Simulated interaction between freshwater and saltwater and effects of ground-water pumping and sea-level change, Lower Cape Cod aquifer system, Massachusetts: U.S. Geological Survey Scientific Investigations Report 2004-5014, 72 p.

Mazi, K., Koussis, A.D., Destouni, G., 2014. Intensively exploited Mediterranean aquifers: proximity to tipping points and control criteria for sea intrusion. Hydrol. Earth Syst. Sci. 18, 1663-1677.

Meng F., 2004. Rational development of groundwater resources on the coastal zone of Qinhuangdao area. Marine Geology Letters. 20(12):22-25. (Chinese with English abstract)

Michael H.A., Post V.E.A., Wilson A.M., Werner A.D. 2017. Science, society and the coastal groundwater squeeze. Water Resources Research. 53. 2610-2617.

Mondal N.C., Singh V.P., Singh V.S., Saxena V.K., 2010. Determining the interaction between groundwater and saline water through groundwater major ions chemistry. Journal of Hydrology. 388:100-111.

Montenegro S.M.G., de A. Montenegro A.A., Cabral J.J.S.P., Cavalcanti G., 2006. Intensive exploitation and groundwater salinity in Recife coastal plain (Brazil): monitoring and management perspectives. Proceedings 1st SWIM-SWICA Joint Saltwater Intrusion Conference, Cagliari-Chia Laguna, Italy - September 24-29, 2006. pp79-85.

Moore W.S., 1996. Large groundwater inputs to coastal waters revealed by 226Ra enrichments. Nature 380,612-214.

Narayan K.A., Schleeberger C., Bristow K.L., 2007. Modelling seawater intrusion in the Burdekin Delta Irrigation Area, North Queensland, Australia. Agricultural Water Management. 89:217-228.

Pan G., Yang Y., Zhang L., 1990. Survey report of geothermal water in Qinhuangdao city of Hebei Province. Team of mineral hydrological and engineering geology from the Bureau of Geology and mineral Resources of Hebei Province, China. (in Chinese)

Parkhurst D.L., Appelo C.A.J., 1999. User's Guide to PHREEQC – A Computer Program for Speciation, Reaction-Path, 1D-Transport, and Inverse Geochemical Calculation. US Geol. Surv. Water-Resour. Invest. Rep. 99-4259.

Post V.E.A., 2005. Fresh and saline groundwater interaction in coastal aquifers: Is our technology ready for the problems ahead? Hydrogeology Journal. 13:120-123.

Price R.M., Herman J.S., 1991. Geochemical investigation of salt-water intrusion into a coastal carbonate aquifer: Mallorca, Spain. Geological Society of America Bulletin. 103:1270-1279.

Pulido-Leboeuf P., 2004. Seawater intrusion and associated processes in a small coastal complex aquifer (Castell de Ferro, Spain). Applied Geochemistry. 19:1517-1527.

Radhakrishna I., 2001. Saline fresh water interface structure in Mahanadi delta region, Orissa, India. Environmental Geology. 40(3):369-380.

Rahmawati N., Vuillaume J., Purnama I.L.S., 2013. Salt intrusion in Coastal and Lowland areas of Semarang City. Journal of Hydrology. 494:146-159.

Robinson M.A., Gallagher D.L., Reay W.G., 1998. Field observations of tidal and seasonal variations in ground water discharge to estuarine surface waters. Ground Water Monitoring and Remediation. 18 (1): 83-92.

Shen Z., Zhu Y., Zhong Z., 1993. Theoretical basis of hydrogeochemistry. Geological Publishing House. Beijing, China. (in Chinese)

Sherif M.M., Singh V.P., 1999. Effect of climate change on sea water intrusion in coastal aquifers. Hydrological Processes 13, 8:1277-1287.

Shi M.Q., 2012. Spatial distribution of population in the low elevation coastal zone and assessment on vulnerability of natural disaster in the coastal area of China. Master thesis of Shanghai Normal University, 24–32.(Chinese with English abstract)

Simpson, M.J., Clement, T.P., 2004. Improving the worthiness of the Henry problem as a benchmark for density-dependent groundwater flow models. Water Resources Research 40 (1), W01504 doi:10.1029/2003WR002199.

Sivan O., Yechieli Y., Herut B., Lazar B., 2005. Geochemical evolution and timescale of seawater intrusion into the coastal aquifer of Israel. Geochimica et Cosmochimica Acta. 69(3):579-592.

Smith A.J., Turner J.V., 2001. Density-dependent surface water-groundwater interaction and nutrient discharge in the Swan-Canning Estuary. Hydrolological Processes. 15:2595-2616.

SOA (State Oceanic Administration of the People's Republic of China), 2015. China's Marine Environment Bulletin: 2014. Released 11th March, (in Chinese).

Sophocleus M., 2002. Interactions between groundwater and surface water: the state of science. Hydrogeology Journal. 10:52-67.

Sun J., Yang Y., 2007. Seawater intrusion characteristics in Qinhuangdao. Journal of Environmental Management College of China. 17(2):51-54. (Chinese with English abstract)

UN Atlas, 2010. UN Atlas: 44 Percent of us Live in Coastal Areas. <http://coastalchallenges.com/2010/01/31/un-atlas-60-of-us-live-in-the-coastal-areas/>.

Vengosh A., Gill J., Reyes A., Thoresberg K., 1997. A multi-isotope investigation of the origin of ground water salinity in Salinas Valley, California. American Geophysical Union, San Francisco, California.

Vengosh A., Pankratov I., 1998. Chloride/bromide and chloride/fluoride ratios of domestic sewage effluents and associated contaminated ground water. Ground Waer. 36(5):815-824.

Vengosh A., Spivack A.J., Artzi Y., Ayalon A. 1999. Geochemical and boron, strontium, and oxygen isotopic constraints on the origin of the salinity in groundwater from the Mediterranean coast of Isreal. Water Resources Research. 35(6): 1877-1894.

Walraevens, K., Cardenal-Escarcena, J., Van Camp, M., 2007. Reaction transport modelling of a freshening aquifer (Tertiary Ledo-Paniselian Aquifer, Flanders-Belgium). Applied Geochemistry. 22: 289-305.

Wang, J., Yao, P., Bianchi, T.S., Li, D., Zhao, B., Cui, X., Pan, H., Zhang, T., Yu, Z., 2015. The effect of particle density on the sources, distribution, and degradation of sedimentary organic carbon in the Changjiang Estuary and adjacent shelf. Chemical Geology. 402:52-67.

Weber, K., Stewart, M., 2004. A critical analysis of the cumulative rainfall departure concept. Ground Water 42 (6), 935–938.

Werner, A.D., 2010. A review of seawater intrusion and its management in Australia. Hydrogeology Journal. 18(1):281-285.

Werner A.D., Bakker M., Post V.E.A., Vandenbohede A., Lu C., Ataie-Ashtiani B., Simmons C.T., Barry D.A., 2013a. Seawater intrusion processes, investigation and management: Recent advances and future challenges. Advances in Water Resources.51:3-26.

Werner A.D., Simmons C.T., 2009. Impact of sea-level rise on seawater intrusion in coastal aquifers. Ground Water. 47:197-204.

Westbrook S.J., Rayner J.L., Davis G.B., Clement T.P., Bjerg P.L., Fisher S.J., 2005. Interaction between shallow groundwater, saline surface water and contaminant discharge at a seasonally and tidally forced estuarine boundary. Journal of Hydrology, 302:255-269.

Wilhite D.A., 1993.Drought Assessment, Management, and Planning: Theory and Case Studies. Springer U S. p628.

Xu G., 1986. Analysis of seawater intruding into aquifer system in Beidaihe Region.Hydrogeology & Engineering Geology. 2:7-10. (in Chinese)

Xue Y., Wu J., Xie C., Zhang Y., 1997. Study of seawater and saltwater intrusion in the coast plain of Laizhou Bay. Chinese Science Bulletin. 42(22):2360-2367. (in Chinese)

Xue Y.Q., Wu J.C., Ye S.J., Zhang Y.X., 2000. Hydrogeological and hydrogeochemical studies for salt water intrusion on the South Coast of Laizhou Bay, China. Ground Water. 38, 38-45.

Yang H., 1996. Sea-level changes in east China over the past 20000 years. in Study of Environmental Change. Hohai University Press. Nanjing, China. pp390-395.

Yang L., 2011. Formation mechanism of bedrock fracture type-geothermal water in Qinhuangdao area. West-china Exploration Engineering. Urumchi, China. 10:151-152. (in Chinese)

Yang Y., Gao S., Xie Y., 2008. Assessment and control countermeasures of seawater intrusion hazard on Qinhuangdao Region. The Chinese Journal of Geological Hazard and Control. 19(3):139-143. (Chinese with English abstract)

Yang Y., He Q., Xie Y., Cao C., 1994. Grey model prediction of seawater intrusion of Qinhuangdao. The Chinese Journal of Geological Hazard and Control. 5(sup.):181-183. (Chinese with English abstract)

Yechieli Y., Kafri U., Sivan O., 2009. The inter-relationship between coastal sub-aquifers and the Mediterranean Sea, deduced from radioactive isotopes analysis. Hydrogeology Journal. 17:265-274.

Zang W., Liu W., Guo J., Zhang X., 2010. Geological hazards of seawater intrusion and its control measures in Qinhuangdao City, Hebei Province. The Chinese Journal of Geological Hazard and Control. 21(4):120-125. (Chinese with English abstract)

Zeng J., 1991. Geochemistry of geothermal water in Qinhuangdao area, Hebei Province. Bull. Institute of Hydrogeology and Engineering Geology, Chinese Academy of Geological Sciences. 7:111-127.

Zhang B., 2012. Mechanism of Seawater Intrusion Using Hydrochemistry and Environmental Isotopes in Qinhuangdao Yang Dai River Plain. Master's Thesis. Xiamen University, Fujian, China. (Chinese with English abstract)

Zhang Q., Volker R.E., Lockington D.A., 2004. Numerical investigation of seawater intrusion at Gooburrum, Bundaberg, Queensland, Australia. Hydrogeol. J. 12 (6), 674-687.

Zhang Z., Peng L., 1998. Groundwater hydrochemical characteristics on seawater intrusion in eastern and southern coasts of Laizhou Bay. China Environmental Science. 18(2):121-125.

Zhuang Z., Liu D., Yang M., Li H., Qiu H., Ning P., Song W., Xu Z., 1999. The role of anthropogenic activities in the evolution of saline water intrusion processes. Journal of Ocean University of Qingdao. 29(1):141-147. (Chinese with English abstract)

Zuo W., 2006. Survey and Research on Seawater Intrusion in the Yandaihe Plain of Qinhuangdao City. Doctoral Thesis. China University of Geosciences, Beijing, China. (Chinese with English abstract)

Zuo W., Yang Y., Dong Y., Liang M., 2009. The numerical study for seawater intrusion in Yanghe and Daihe coastal plain of Qinhuangdao City. Journal of Natural Resources. 24(12):2087-2095. (Chinese with English abstract)

Appendix for the paper titled "Delineating multiple salinization processes in a coastal plain aquifer, northern China: hydrochemical and isotopic evidence" by Han and Currell

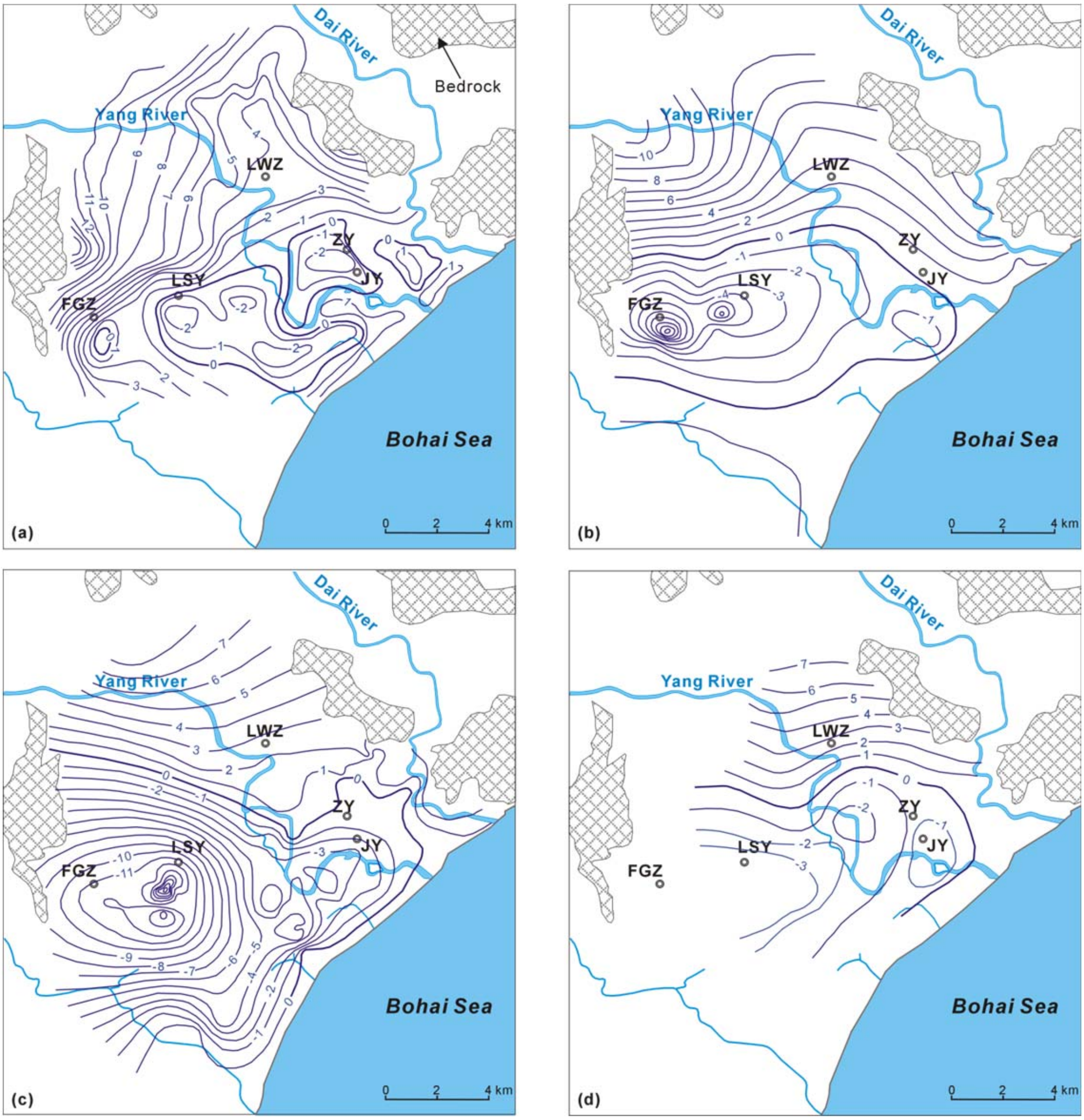

Fig. S1 Maps showing the distribution of groundwater level contours in shallow aquifer (a) in 1986 (from Han, 1988), (b) in 1998 (from Zuo, 2006), (c) in 2004 (from Zuo, 2006), and (d) in 2010 (this study). The depression area refers to the area enclosed by 0 m.a.s.l. contour line of groundwater levels.

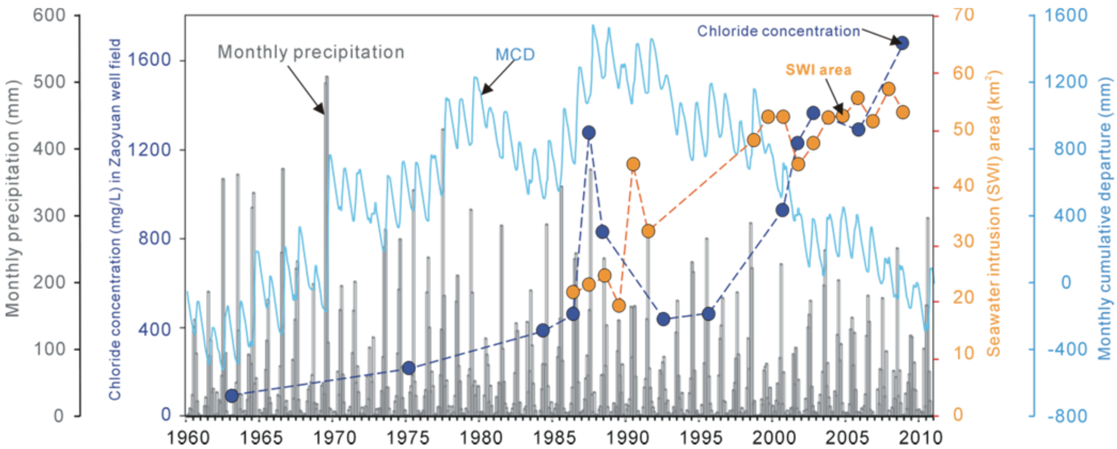

Fig. S2 Graph showing the temporal variation of monthly cumulative rainfall departure (CRD, Weber and Stewart, 2004), monthly precipitation, average concentration of chloride in groundwater (dark blue) and surface area with >250 mg Cl/L (yellow) between 1963 and 2008 (data from Zang et al., 2010).

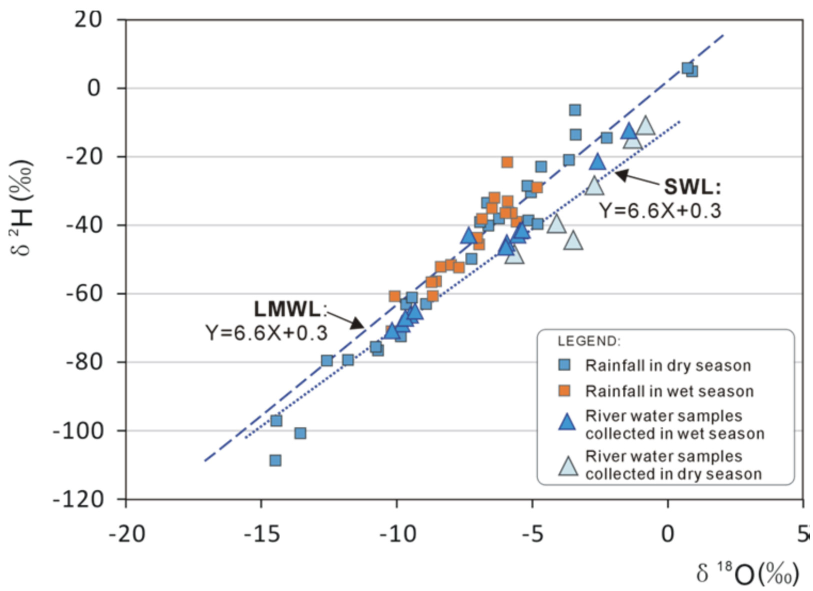

Fig. S3 Graph showing δ^2H vs. $\delta^{18}O$ of water samples in rainfall and river water. Dry season- July to October; wet season- November to June.

Table S1. NO_3/Cl and Sr/Cl ratios in water samples

WaterType	ID	Sampling Time	Cl mg/L	NO_3 mg/L	Sr mg/L	NO_3/Cl	Sr/Cl ($\times10^{-3}$)
Shallow groundwater samples:							
Fresh Groundwater	G4	Aug.2010	124.3	92.6	0.67	0.745	5.41
	G27	Aug.2010	177.5	163.0	1.22	0.918	6.88
	G12	Aug.2010	276.9	31.9	0.25	0.115	0.90
	G17	Aug.2010	88.8	39.5	0.33	0.445	3.68
	G18	Aug.2010	124.3	137.8	0.71	1.109	5.71
	G1	Sep.2009	220.1	2.0	0.66	0.009	3.00
	G4	Sep.2009	124.3	178.5	0.85	1.437	6.83
	G5	Sep.2009	303.4	162.3	1.14	0.535	3.74
	G23	Sep.2009	88.8	163.4	0.55	1.841	6.17
	G7	Sep.2009	81.7	41.2	0.41	0.505	5.01
	G8	Sep.2009	334.6	85.4	1.19	0.255	3.57
	G11	Sep.2009	222.9	74.5	0.84	0.334	3.75
	G12	Sep.2009	174.0	46.0	0.53	0.264	3.06
	G28	Sep.2009	127.8	22.5	0.58	0.176	4.54
	G18	Sep.2009	110.1	152.9	0.65	1.389	5.94
	G20	Sep.2009	246.9	107.1	3.94	0.434	15.94
	G17	Sep.2009	243.5	126.4	0.71	0.519	2.91
	G3	Jun.2008	315.0		0.46		1.47
	G4	Jun.2008	74.6	75.8	0.47	1.017	6.29
	G5	Jun.2008	310.9	119.5	1.43	0.384	4.61
	G8	Jun.2008	349.7	55.9	1.08	0.160	3.07
	G12	Jun.2008	281.0	29.8	0.19	0.106	0.68
	G17	Jun.2008	227.9	92.6	0.57	0.406	2.50
	G18	Jun.2008	115.5	144.2	0.41	1.249	3.55
	G20	Jun.2008	234.3	18.2	2.10	0.078	8.95
Brackish Groundwater	G1	Aug.2010	312.4	120.0	0.54	0.384	1.71
	G3	Aug.2010	654.3	106.0	0.97	0.162	1.49
	G15	Aug.2010	435.7	181.3	1.60	0.416	3.67
	G26	Aug.2010	784.6	339.4	1.20	0.433	1.53
	G11	Aug.2010	646.1	414.1	1.51	0.641	2.34
	G20	Aug.2010	596.4	177.9	3.95	0.298	6.62
	G5	Aug.2010	447.3	253.3	0.78	0.566	1.74
	G8	Aug.2010	596.4	141.4	1.87	0.237	3.13
	G7	Aug.2010	299.6	338.3	0.66	1.129	2.20
	G19	Aug.2010	600.0	211.9	7.10	0.353	11.84
	G24	Aug.2010	646.1	952.1	2.44	1.474	3.78
	G22	Sep.2009	408.3	2.0	0.70	0.005	1.72
	G10	Sep.2009	2563.1	27.7	1.92	0.011	0.75
	G14	Sep.2009	291.1	109.8	0.82	0.377	2.81
	G24	Sep.2009	454.4	441.5	0.93	0.972	2.05
	G19	Sep.2009	622.0	91.5	4.87	0.147	7.83
	G1	Jun.2008	717.1	87.7	0.17	0.122	0.24
	G11	Jun.2008	451.2		1.00		2.21
	G14	Jun.2008	372.8	267.3	0.93	0.717	2.48
	G15	Jun.2008	1675.6	146.8	2.17	0.088	1.29

Deep Groundwater samples:							
Fresh Groundwater	G25	Aug.2010	68.1	71.0	0.25	1.042	3.66
	G16	Sep.2009	214.4		2.68		12.51
	G29	Sep.2009	255.6	26.3	0.20	0.103	0.77
Brackish Groundwater	G29	Aug.2010	803.4	143.0	6.95	0.178	8.65
	G16	Aug.2010	766.8	5.5	4.00	0.007	5.21
	G9	Jun.2008	823.6	47.4	7.40	0.058	8.98
	G9	Sep.2009	917.4	65.8	8.02	0.072	8.74
	G9	Aug.2010	1228.3	337.4	11.59	0.275	9.44
	G14'	Aug.2010	553.8	433.7	1.06	0.783	1.91
	G13	Aug.2010	908.8	210.6	0.26	0.232	0.29
	G13	Jun.2008	945.4		0.55		0.58
	G13	Sep.2009	882.0		0.35		0.39
	G2	Jun.2008	1093.4		1.03		0.94
River water samples:							
Fresh water samples							
Dai River	S9	Aug.2010	80.3	65.2	0.34	0.813	4.20
Dai River	S12	Aug.2010	71.3	41.9	0.30	0.588	4.14
Dai River	S8	Aug.2010	68.6	54.9	0.32	0.801	4.67
Yang River	S6	Aug.2010	66.0	51.9	0.30	0.786	4.53
Yang River	S2	Aug.2010	63.2	40.2	0.26	0.636	4.10
Yang River	S5	Sep.2009	85.2	12.9	0.36	0.152	4.27
Yang River	S4	Sep.2009	733.1	6.6		0.009	
Yang River	S6	Sep.2009	99.4	6.6	0.30	0.067	3.04
Dai River	S9	Sep.2009	88.8	6.8	0.36	0.077	4.03
Dai River	S8	Sep.2009	174.0	6.4	0.55	0.037	3.17
Yang River	S6	Jun.2008	81.7	12.6	0.31	0.154	3.82
Dai River	S10	Jun.2008	208.9	23.1	0.57	0.111	2.72
Dai River	S9	Jun.2008	92.3	7.5	0.35	0.081	3.81
Brackish and salt water samples							
Yang River	S3	Sep.2009	11289.4		4.29		0.38
Dai River	S12	Sep.2009	16766.3		7.64		0.46
Dai River	S11	Sep.2009	1601.5	2.8	0.93	0.002	0.58
Yang River	S1	Jun.2008	14953.5		5.55		0.37
Yang River	S2	Jun.2008	8328.3		3.37		0.40
Dai River	S7	Jun.2008	16677.1		6.36		0.38
Seawater:	SW1	Aug.2010	14768.3	810.1	5.79	0.055	0.39
	SW1	Sep.2009	16568.0		6.45		0.39
	SW2	Sep.2009	14484.8		5.43		0.37

Note: NO_3/Cl and Sr/Cl – mass ratios